

**Fritz-Haber-Institut der  
Max-Planck-Gesellschaft  
Berlin**

**17th Meeting of the Fachbeirat**

**Berlin, 12th - 14th February 2014**



**Poster Abstracts**







**Fritz-Haber-Institut der  
Max-Planck-Gesellschaft  
Berlin**

**17th Meeting of the Fachbeirat  
Berlin, 12th – 14th February 2014**

**Poster Abstracts**

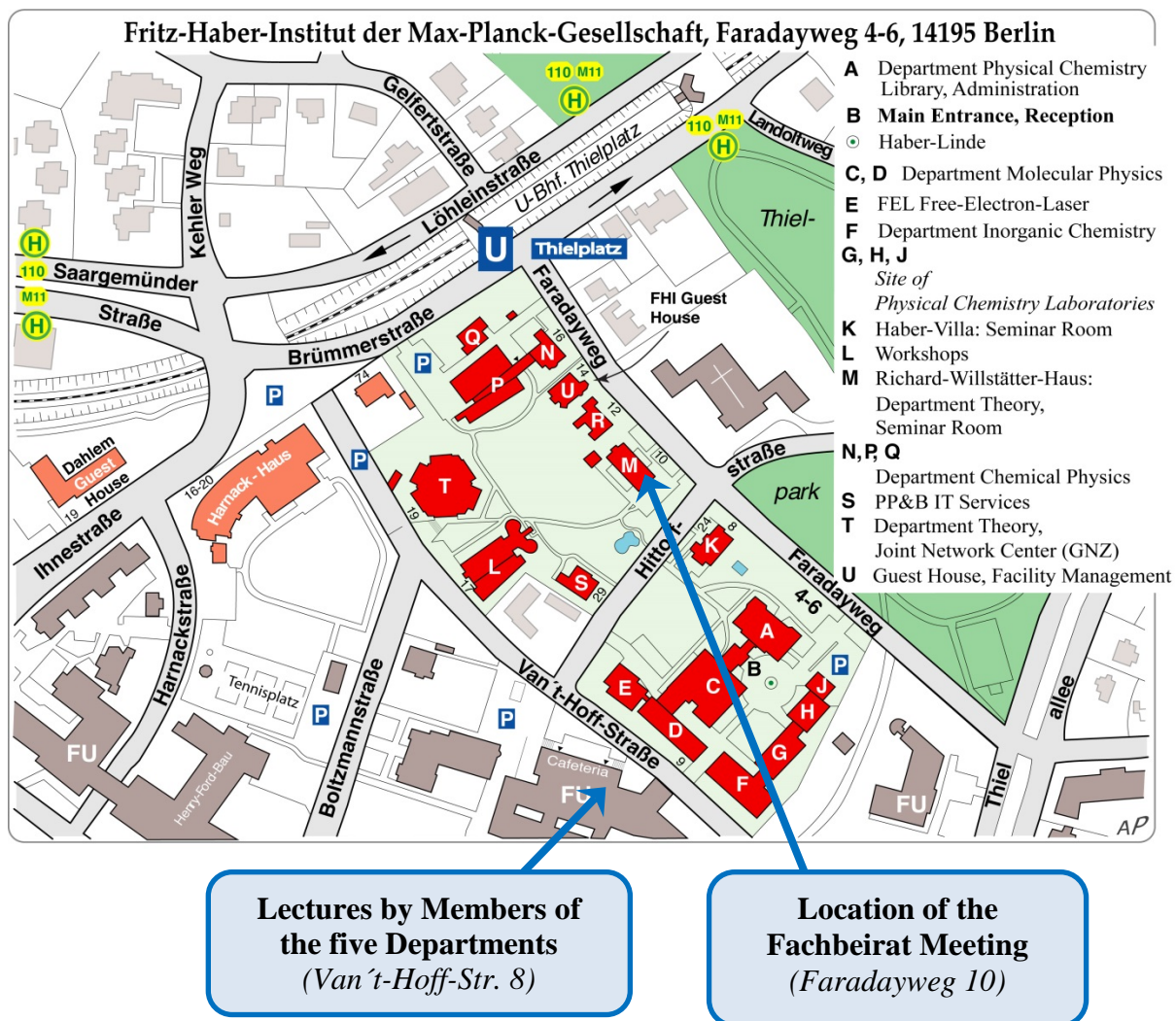


**The posters can be found in the following buildings:**

	<b>Building</b>
<b>Department of Inorganic Chemistry</b>	<b>F</b>
<b>Department of Chemical Physics</b>	<b>P</b>
<b>Department of Molecular Physics</b>	<b>C, D</b>
<b>Department of Physical Chemistry</b>	<b>A</b>
<b>Theory Department</b>	<b>T</b>



# Local Map





## **Contents**

	<b>Page</b>
<b>Department of Inorganic Chemistry (AC)</b>	
Poster List	<b>1</b>
Poster Abstracts	<b>5</b>
<b>Department of Chemical Physics (CP)</b>	
Poster List	<b>33</b>
Poster Abstracts	<b>35</b>
<b>Department of Molecular Physics (MP)</b>	
Poster List	<b>55</b>
Poster Abstracts	<b>57</b>
<b>Department of Physical Chemistry (PC)</b>	
Poster List	<b>75</b>
Poster Abstracts	<b>79</b>
<b>Theory Department (TH)</b>	
Poster List	<b>103</b>
Poster Abstracts	<b>107</b>
<b>Notes</b>	<b>125</b>







## Department of Inorganic Chemistry

### Poster List

- AC 1.0 Cu-Based Catalysts for Methanol Synthesis**
- AC 1.1 Cu,Zn Catalysts for Methanol Synthesis: The Mechanisms of Calcination and Reduction**  
A. Tarasov, J. Schumann, M. Behrens, and R. Schlögl
- AC 1.2 The Hydrogenation of CO<sub>x</sub> to Methanol on Cu-Based Catalysts**  
J. Schumann, S. Zander, N. Thomas, A. Tarasov, T. Lunkenbein, S. Wrabetz, J. Kröhnert, D. Teschner, F. Studt, J. Nørskov, M. Behrens, and R. Schlögl
- AC 2.0 Catalysts for the Oxygen Evolution Reaction**
- AC 2.1 Dynamics and Stability of the Active Phase and the Support of Electro-Catalysts for OER**  
R. Arrigo, Y. Yi, J. Tornow, M. Hävecker, M.E. Schuster, A. Knop-Gericke, and R.Schlögl
- AC 2.2 Manganese Oxide Materials as Oxygen Evolution Catalysts**  
C. Massué, K. Mette, N. Thomas, C. Ranjan, M. Lerch, P. Strasser, M. Behrens, and R. Schlögl
- AC 3.0 Metals in Oxidation Reactions**
- AC 3.1 Ethylene Epoxidation over Ag: Unraveling the Active Oxygen Species**  
T.C.R. Rocha, T. Jones, P. Kristiansen, L. Duda, S. Piccinin, A. Knop-Gericke, and R. Schlögl
- AC 3.2 Active Oxygen Surface Species on Gold and Copper Catalysts in Oxidation Reactions**  
M. Greiner, A. Kluyshin, B. Johnson, T.C.R. Rocha, M. Hävecker, A. Knop-Gericke, and R. Schlögl
- AC 4.0 EMIL: The Energy Materials In-Situ Laboratory Berlin**  
M. Hävecker, G. Reichardt, F. Schäfers, S. Hendel, R. Follath, J. Bahrtdt, M. Scheer, E. Stotz, R. Arrigo, A. Knop-Gericke, K. Lips, and R. Schlögl

**AC 5.0 Carbon in Catalysis and Material Sciences**

**AC 5.1 Single Layer Graphene Growth on Transition Metal Surfaces**

R. Blume, R.S. Weatherup, P. Kidambi, Z.-J. Wang, A. Knop-Gericke, M.G. Willinger, and R. Schlögl

**AC 5.2 CNT-Supported Transition Metals and Carbides in Catalysis**

B. Frank, Z.-L. Xie, K. Friedel, F. Girgsdies, G. Wowsnick, R. Arrigo, M.E. Schuster, Y. Yi, M. Hävecker, A. Knop-Gericke, R. Schlögl, and A. Trunschke

**AC 6.0 Nanostructured Catalysts in Activation of Light Alkanes**

**AC 6.1 MoV(Te,Nb)O<sub>x</sub> Catalysts for Propane Oxidation: Hydrothermal Synthesis and Functional Properties**

J. Noack, M. Jastak, M. Sanchez-Sanchez, P. Kube, R. Naumann d'Alnoncourt, T. Lunkenbein, F. Girgsdies, F. Rosowski, R. Schlögl, and A. Trunschke

**AC 6.2 The Catalytically Active Surface Between Bulk and Gas Phase: Investigating Interfacial Charge Transport Under Working Conditions**

C. Heine, M. Heenemann, A. Trunschke, R. Schlögl, and M. Eichelbaum

**AC 6.3 Structural Analysis of Silica-Supported Transition Metal Oxide Catalysts by X-ray Absorption: Combined Theoretical and Experimental Studies**

C.S. Guo, L.L. Sun, K. Hermann, T. Wolfram, K. Amakawa, P.K. Nielsen, P. Kube, M. Hävecker, A. Trunschke, and R. Schlögl

**AC 7.0 Reversible Charge Storage Mechanism in Lithium Ion Batteries**

**AC 7.1 Silicon Anodes for Lithium Ion Batteries**

B. Davaasuren, M. Pradel, N. Gilliard, M.E. Schuster, M.G. Willinger, J. Tornow, and R. Schlögl

**AC 8.0 Methodological Developments of the Electron Microscopy Group**

**AC 8.1 In-Situ Investigations of Surface Dynamics by Environmental Scanning Electron Microscopy**

Z.-J. Wang, G. Weinberg, M.G. Willinger, and R. Schlögl

- AC 8.2**    **Micro-Reactors for the Investigation of Dynamic Processes by Transmission Electron Microscopy**  
T. Lunkenbein, M.E. Schuster, M.G. Willinger, and R. Schlögl
- AC 8.3**    **Theory of Periodic Overlayers and Interference Lattices: Moirons at Work**  
K. Hermann
- AC 9.0**    **Oxidative Coupling of Methane**
- AC 9.1**    **Fuel-Rich Methane Oxidation in a High-Pressure Tubular Reactor Studied by Optical-Fiber-Laser-Induced Fluorescence, Spatially Resolved Multi-Species Axial Reactor Profile Measurements, and Microkinetic Simulations**  
H. Schwarz, O. Korup, M. Geske, C.F. Goldsmith, R. Schlögl, and R. Horn
- AC 9.2**    **Oxidative Activation of Methane over Au-Fe/MgO Model Catalysts**  
P. Schwach, M.G. Willinger, A. Trunschke, and R. Schlögl



## Cu-Based Catalysts for Methanol Synthesis

The synthesis of methanol is one of the major syngas routes in the modern chemical industry. Additionally, the CO<sub>2</sub> hydrogenation reaction ( $\text{CO}_2 + 3 \text{H}_2 \rightarrow \text{CH}_3\text{OH} + \text{H}_2\text{O}$ ) is a preferred way for the utilization of carbon dioxide in the context of clean and sustainable fuel production. Cu-based catalysts are applied in the existing industrial methanol synthesis, in particular Cu/ZnO composite systems, and are also the most promising starting point and benchmark for novel CO<sub>2</sub> utilization processes.

Despite the long experience with the application of these materials, there are still a number of unanswered questions regarding the mode of operation of this catalyst. A true catalyst design for an optimization of the established process as well as for application in new dynamic CO<sub>2</sub> conversion reactions requires deeper knowledge of the nature of the active sites, the reaction mechanism of methanol synthesis, the nature and function of the synergetic Cu-ZnO interaction and the role of the promoter.

Our research strategy in this project aims at understanding the materials chemistry of the industrial benchmark system to identify the relevant properties for high catalytic activity and to learn to control the responsible structural features through preparation. Thus, much emphasis is put on controlled catalyst synthesis to generate a materials library of well-characterized and uniform catalysts as the key to structure-function-relationships. Here, the thermal decomposition and reduction of the catalyst precursor, i.e. the solid state chemistry of the actual genesis of the active phase, is a new object of research that is based on the insights obtained in the previous detailed study of precursor synthesis. This is documented on the poster AC 1.1.

In addition to diffraction, spectroscopic and thermal methods routinely applied to monitor the success of the catalyst syntheses, a careful functional characterization of our materials is performed in close collaboration with the methodologically oriented working groups of the Department, in particular using TEM, XPS and microcalorimetry.

Next to controlled synthesis and careful structural characterization, a thorough catalytic testing has moved more into the focus of the project in the last years. Contrary to the catalyst screening approach taken earlier to successfully decipher the industrial catalyst synthesis recipe, our current test protocols routinely also involve the change of reaction parameters such as space velocity and feed gas composition and also include isotope labelling studies. The potential of this systemic approach is demonstrated on poster AC 1.2, which shows how relevant new mechanistic insights can be deduced from experimental evidence obtained on high-performance materials.

Within the Cu project fruitful collaboration exist with the MPI for Chemical Energy Conversion (M. Bukhtiyarova), Stanford University (J. Nørskov), Ruhr-University Bochum (M. Muhler), Technical University Munich (O. Hinrichsen), Technical Universität Berlin (T. Ressler), Clariant Produkte GmbH (terminated in June 2013) and others. Financial support was given by the Bayerisches Staatministerium für Wissenschaft (NW-0810-0002).

## Cu,Zn Catalysts for Methanol Synthesis: The Mechanisms of Calcination and Reduction

A. Tarasov, J. Schumann, M. Behrens, and R. Schlögl

Cu/ZnO/(Al<sub>2</sub>O<sub>3</sub>) catalysts for methanol synthesis are prepared by a multi-step preparation comprised of co-precipitation, ageing, washing and drying, calcination and reduction<sup>1</sup>. After having extensively studied the influence of the first preparation step, namely the co-precipitation, and the role of the resulting different precursor phases for the activity in methanol synthesis<sup>2-3</sup>, we have now investigated the following synthesis steps, i.e. the decomposition during calcination and the reduction during catalyst activation. Given that a precursor material of high phase purity is used, such investigations can provide a mechanistic understanding of the solid state chemistry during the genesis of the actual active form of the catalyst. Long-term goal is the linking of synthesis parameters with the relevant structural properties of the resulting catalyst.

We have performed a detailed thermokinetic study<sup>4</sup> of the calcination process of suitable Cu,Zn-hydroxyl carbonate precursors by coupled TG, DSC and MS techniques. Two main decomposition steps were observed. The first step (300-400°C) is usually accompanied by simultaneous evolution of CO<sub>2</sub> and H<sub>2</sub>O, while the high temperature step (400-500°C) is exclusively due to release of CO<sub>2</sub>. This second step is ascribed to decomposition of the “high-temperature carbonate (HT-CO<sub>3</sub>)” also known as anion-modified metal oxide, which forms in the first step and decomposes to metal oxide afterwards. TG investigations revealed that the amount of formed high-temperature carbonate is strongly depended on water transfer conditions. Presence of water vapor in the reaction atmosphere crucially influences the reaction kinetics by promoting the decomposition of the HT-CO<sub>3</sub> and favouring CuO and ZnO crystallisation.

With this knowledge, catalysts with different amounts of HT-CO<sub>3</sub> were prepared from the same precursor by systematic variation of the heating rate. Despite the distinct trends of the calcined samples regarding crystallinity and HT-CO<sub>3</sub> content, only small differences in activities were observed. Thus, no direct correlation of the HT-CO<sub>3</sub> amount and the catalytic performance could be established. However, a possible general effect of the presence of HT-CO<sub>3</sub> on the formation of the active Cu phase was indicated by the thermal analysis of the reduction. A two-step mechanism was found for HT-CO<sub>3</sub>-containing CuO/ZnAl<sub>2</sub>O<sub>4</sub> pre-catalysts<sup>5</sup>. The intermediate formation of Cu(I) was confirmed by *in situ* NEXAFS analysis. The kinetic analysis allowed not only the prediction of the phase composition at given reduction conditions, but also revealed that the rate of the final reaction step Cu(I)→Cu(0) was controlled by the HT-CO<sub>3</sub>-decomposition. It thus seems likely that HT-CO<sub>3</sub> contributes to the “chemical memory” of the resulting catalyst by steering the kinetics of the crystallization of the active metal, potentially favoring the incorporation of lattice defects through a hindered reduction.

### References

1. M. Behrens, and R. Schlögl, *Z. Anorg. Allg. Chem.*, DOI: 10.1002/zaac.201300356.
2. M. Behrens, S. Zander, P. Kurr *et al.*, *J. Am. Chem. Soc.* **135**, 6061 (2013).
3. S. Zander, B. Seidlhofer, and M. Behrens, *Dalton Trans.* **41**, 13413 (2012).
4. A. Tarasov *et al.*, *Non-Isothermal Kinetic Methods*, Edition Open Access (2013).
5. A. Tarasov, S. Kühl, J. Schumann *et al.*, *High Temp.-High Press.* **42**, 377 (2013).

## The Hydrogenation of CO<sub>x</sub> to Methanol on Cu-Based Catalysts

J. Schumann, S. Zander, N. Thomas, A. Tarasov, T. Lunkenbein, S. Wrabetz, J. Kröhnert, D. Teschner, F. Studt\*, J. Nørskov\*, M. Behrens, and R. Schlögl

We have recently reported on the structural properties of the active site ensembles responsible for the methanol synthesis reaction<sup>1</sup> and found that Zn(O<sub>x</sub>)-decorated stepped Cu surfaces are suitable models for the complex industrial catalyst. However, there are still open questions regarding the mechanism of methanol synthesis. In particular the carbon source, CO or CO<sub>2</sub>, and the role of the “Cu-ZnO synergy” on the reaction pathway are controversial for high performance catalysts.

New insights into these questions were obtained in a comparative study of Cu particles in interfacial contact with reducible ZnO and irreducible MgO nanoparticles. Both composite materials were synthesized according to the industrial protocol through mixed precursor compounds (cf. Poster AC 1.1), but in case of Cu/MgO with the complete substitution of Zn<sup>2+</sup> by Mg<sup>2+</sup> cations<sup>2</sup>. While the Cu microstructure of the two catalysts was similar, the catalytic performance was dramatically different. Cu/ZnO was the expected good methanol synthesis catalyst in CO<sub>2</sub>-containing syngas, while Cu/MgO showed high performance only in pure CO/H<sub>2</sub>.

Both catalysts were comprehensively characterized by, among other techniques, TEM, XPS, *in situ* TGA, microcalorimetry and vibrational spectroscopy of adsorbed CO. As a major result, oxide coverage of the metal surface was observed only for Cu/ZnO. The overgrowth of ZnO<sub>x</sub> is related to strong metal support interaction. The combination of different TEM techniques revealed that a layered “graphitic” phase of ZnO<sub>x</sub> is involved in the supply of ZnO<sub>x</sub> entities to the Cu surface. CO adsorption experiments indicated that the adsorptive properties of the catalyst are affected by the presence of ZnO<sub>x</sub>.

Catalytic studies with <sup>13</sup>CO<sub>2</sub>-labeled syngas clearly showed that CO<sub>2</sub> is the dominant precursor for methanol on both ZnO-containing and ZnO-free catalysts. The high CO hydrogenation activity of Cu/MgO was quenched in the presence of CO<sub>2</sub>; an effect that was accompanied by a reversible increase in the weight of the working catalyst likely due to formation of a heavier adsorbate layer. DFT calculations<sup>3</sup> using Cu(211) and CuZn(211) with Zn atoms residing in the surface steps as model sites for Cu/MgO and Cu/ZnO revealed that formate adsorbs on both surfaces in the presence of CO<sub>2</sub>. It acts as a poison for CO hydrogenation and allows fast formation of methanol only on CuZn(211), where the Zn atoms strengthen the binding to the O-bound intermediates like formate and accelerate their hydrogenation. Conversely, interaction of intermediates binding through C-atoms like formyl is weakened.

Based on the experimental and theoretical evidence, a comprehensive picture of CO<sub>x</sub> hydrogenation on Cu emerges: Both pathways to methanol through CO and CO<sub>2</sub> are possible on Cu, but in the industrial process the presence of CO<sub>2</sub> and ZnO<sub>x</sub> is required for high performance and directs the reaction toward CO<sub>2</sub> hydrogenation.

### References

1. M. Behrens, F. Studt, I. Kasatkin, S. Kühl *et al.*, *Science* **336**, 893 (2012).
2. S. Zander, E.L. Kunkes *et al.*, *Angew. Chem. Int. Edit.* **52**, 6536 (2013).
3. F. Studt, F. Abild-Pedersen, J.B. Varley, and J.K. Nørskov, *Catal. Lett.* **143**, 71 (2013).

\* Department of Chemical Engineering, Stanford University, CA, USA

## Catalysts for the Oxygen Evolution Reaction

Water splitting into hydrogen and oxygen is a key reaction for the conversion of renewable energy to chemical energy in form of fuels. While the desired product is hydrogen, which can be used directly or as a reactant in downstream conversion into other synthetic fuels (Poster AC 1.0), the limiting catalytic processes are related to the oxygen evolution reaction (OER). The long-term research goal of this project is to combine expertise from electrochemistry, materials science and catalysis to provide a better mechanistic understanding of OER and of the dynamic changes of the electrode under working conditions. We aim to use this knowledge for a rational catalyst development and optimization.

As a first step, direct access to the surface chemistry of working electrodes during OER was enabled by *in situ*-Near Ambient Pressure X-ray Photoelectron Spectroscopy (NAPXPS) and this technique was coupled to electrochemical characterization and online product analysis for gas-phase water electrolysis on model systems (Poster AC 2.1). In order to investigate the relevant interface between liquid water and the electrode under conditions of the oxygen evolution reaction a hard X-ray beamline will be implemented at BESSY (EMIL project Poster 4.0). The application of hard X-ray NAPXPS will allow increasing the mean free path of the emitted photoelectrons and thereby the electrons will pass the liquid water film (a few nm thick) on top of the working electrode, which will be key experiment for this project.

Regarding materials development, we address the stabilization of the electrode integrity in the (electro-)chemical stress of the working environment and the replacement of rare and expensive active phases like  $\text{IrO}_2$  and  $\text{RuO}_2$  with more abundant materials. Our efforts regarding novel catalysts are focused on Manganese oxide phases (Poster AC 2.2). Various synthesis methods of  $\text{MnO}_x$ -based OER catalysts have been tested and characterized and their performance was compared to benchmark materials to study the effect of the Mn oxidation state, the  $\text{MnO}_x$  polymorph and of particle size, shape and dispersion. Among these catalysts are  $\text{MnO}_x/\text{CNT}$  composites (CNT: carbon nanotubes). Carbon materials are attractive support materials due to their high electric conductivity and specific surface area, but can suffer from oxidative corrosion under OER conditions (Poster AC 2.1). We have performed degradation studies on different nanostructured carbon materials to understand the mechanism of the electro-oxidation of carbon and to evaluate its potential as support in long-life electrodes.

The different synthesis and characterization methods that are developed and have been established so far within this new project provide the toolbox that will allow complementary insights into the chemistry of OER catalysts in the near future.

Within the water splitting project fruitful collaborations exist with the MPI for Chemical Energy Conversion, Mülheim/Ruhr (S. Buller, C. Ranjan), the Technical University of Berlin (P. Strasser, M. Lerch) and the Helmholtz-Zentrum Berlin. Financial support was given by the Federal Ministry of Economics and Technology (P.S.STRC625) and the German Science Foundation (DFG, Priority Program SPP-1613).

## Dynamics and Stability of the Active Phase and the Support of Electrocatalysts for OER

R. Arrigo, Y. Yi, J. Tornow, M. Hävecker\*, M.E. Schuster, A. Knop-Gericke, and R. Schlögl

The (electro-)chemically induced changes of electrocatalysts under working conditions are of fundamental interest as they will directly affect the catalytically active surface and the reaction mechanism and can provide a guide to catalyst optimization. Such changes involve reversible redox chemistry at the surface of the active phase as well as irreversible corrosion of the conductive support material, which are of paramount importance for water electrolysis technology. Both aspects have been studied under anodic potentials relevant for the oxygen evolution reaction (OER).

We have used *in situ* Near Ambient Pressure X-ray Photoelectron Spectroscopy (NAPXPS) to observe the reacting interface during gas-phase water electrolysis on a Pt model system<sup>1</sup>. This technique allowed investigation of the O1s, C1s and Pt4f core levels of the active catalyst and was combined with electrochemical techniques such as cyclic voltammetry (CV) and chrono-amperometry (CA) under relevant polarization. The electrocatalytic function was furthermore verified by continuous online analysis of the gas phase composition. It was possible to distinguish the transient active state of the electrode from a more stable, oxidic state that represents a deactivated state. The impact of the voltage on the OER indicates that the reaction kinetics are enhanced by the manipulation of the electrode Fermi level: stronger Pt–O bonds in stable oxidic phase induce overpotential. The results suggest that the prevention of unnecessary oxide overlayers during OER is a way to stabilize the integrity of the active surface.

Furthermore, we have investigated the stability of different carbonaceous materials as support for electrocatalysts (Poster AC 2.2). Emphasis is placed on the carbon electrochemical degradation under OER potential as function of different carbon nanostructures and different pre-treatments with the aim to correlated structural features with electrochemical stability. The electrochemical studies are corroborated by various characterization methods including electron microscopy and vibrational spectroscopy. During corrosion of carbon nanotubes (CNTs), different regimes have been identified in the CA plots and assigned to different stages of oxidative attack finalizing in the formation of a stable passivating surface oxide, which prevents the CNTs from further corrosion. In contrast the CNTs fully decomposed in our thermal oxidation experiments. Hence electrochemically, the thermodynamically favored decomposition of graphitic carbon to CO and CO<sub>2</sub> is blocked by the surface oxide. The drawback of the carbons stability is the impeded charge transfer through the surface oxide, which will probably also affect the electron transport to the attached electrocatalyst. The formation of the surface oxide was observed for all investigated carbon materials but differed in kinetics. The kinetics also increased with increasing acidity of the aqueous electrolyte.

### References

1. R. Arrigo, M. Hävecker, M.E. Schuster, C. Ranjan, E. Stotz, A. Knop-Gericke, and R. Schlögl, *Angew. Chem. Int. Edit.*, DOI: 10.1002/anie.201304765.

\* Helmholtz-Zentrum Berlin für Materialien und Energie GmbH, Elektronenspeicherring BESSY II, Albert-Einstein-Str. 15, 12489 Berlin, Germany

## Manganese Oxide Materials as Oxygen Evolution Catalysts

C. Massué, K. Mette, N. Thomas, C. Ranjan\*, M. Lerch\*\*, P. Strasser\*\*,  
M. Behrens, and R. Schlögl

Active oxygen evolution reaction (OER) catalysts based on  $\text{MnO}_x$  have been reported in many different configurations ranging from bio-inspired complexes over mineral phases to electrodeposited films. There are still many open questions regarding, e.g., the nature of the active sites for OER, the role of the Mn oxidation state and of the  $\text{MnO}_x$  polymorph as well the effect of  $\text{MnO}_x$  particle size, shape and dispersion. From a more applied point of view, supported  $\text{MnO}_x$ -based materials need to be developed, which fulfil different requirements depending on the targeted mode of water splitting – photocatalytic or electrolytic in alkaline or acidic media. In addition to the fundamental understanding of the OER catalysis, stability of  $\text{MnO}_x$ -phases and integrity of the assembled electrodes under working conditions are major challenges. To account for this variety, we have taken different approaches to solid  $\text{MnO}_x$ -based OER catalysts in the last years with the long-term goal of finding generic patterns in structure-functions relationships over various materials and conditions.

For instance, nanostructured  $\text{MnO}_x$  can be dispersed on commercial carbon nanotubes (CNTs, cf. Poster AC 2.1) by incipient wetness impregnation and deposition symproportionation precipitation<sup>1</sup>. A strong influence of the preparation history on the electrocatalytic performance was observed. Various characterization techniques revealed distinct differences in the as-prepared samples as a result of the two different preparation methods. The average initial oxidation state was higher for the symproportionated  $\text{MnO}_x$ , but in both cases an easy adjustability of the oxidation state of Mn by post-treatment of the catalysts was observed as a function of oxygen partial pressure and temperature.

To study the role of oxide supports,  $\alpha\text{-MnO}_2/\text{SnO}_2$  composite catalysts were synthesized by a modified co-precipitation technique. Their performance and stability in acidic media was measured using a sacrificial agent screening test. The results confirm an activating and stabilizing effect of  $\text{SnO}_2$  that depends on the Mn:Sn ratio and the calcination temperature.

For application in photocatalytic OER,  $\text{MnO}_x$  was deposited on TaON semiconductor particles that absorb visible light using a wet impregnation technique followed by calcination. The Mn loading was systematically varied and TEM and activity tests show the existence of an optimal loading of 5 wt.% Mn/TaON leading to a uniform and nanostructured coverage with high specific activity.

In summary, synthesis, characterization and testing techniques have been established for  $\text{MnO}_x$  to yield a broad materials basis for studying the various aspects of OER catalysts.

### References

1. K. Mette, A. Bergmann, J.-P. Tessonnier, M. Hävecker, L. Yao, T. Ressler, R. Schlögl, P. Strasser, and M. Behrens, *ChemCatChem* **4**, 851 (2012).

\* Max-Planck-Institute for Chemical Energy Conversion, Stiftstrasse 34-36, Mülheim/Ruhr, Germany

\*\* Technical University Berlin, Straße des 17. Juni 124, 10623 Berlin, Germany

## Metals in Oxidation Reactions

The main activities in the project “Metals in Heterogeneous Catalytic Oxidation Reactions” were focused on Ag-, Au- and Cu catalysts within the last two years. Therefore, the poster AC 3.1 is dedicated to the research on Ag in ethylene epoxidation, in particular, the promotion of Ag with Cl in the ethylene epoxidation reaction has been considered. The poster AC 3.2 summarizes the results obtained in the field of oxidation reactions on Au and Cu.

The promotion effect of chlorine on silver catalysts in the ethylene epoxidation reaction was studied. The addition of chlorinated hydrocarbon to the reaction feed is a standard industrial practice to promote selectivity to the epoxide. However, the chemical foundations of this technological procedure are still not comprehensively understood, which limits the further development of improved catalysts. To shed new light into this question we used near ambient pressure X-ray photoelectron spectroscopy (NAP-XPS) to correlate the modification at the silver catalyst surface—induced by chlorine promotion—with the catalytic performance measured at the same time. In addition, a more bulk-sensitive technique—resonant inelastic X-ray scattering (RIXS)—was applied to identify oxygen species under reaction conditions. Reference measurements performed on Ag single crystal surfaces were compared to DFT calculations of core-level shifts for Ag-O structural models.

The catalytic activity of Au was studied. In other more-reactive metals—such as Ag, Cu, Ru—the activity and selectivity in heterogeneous catalytic oxidation reactions is controlled by the formation of subsurface oxygen species. In order to form active oxygen species in Au, extended Au foils were exposed to ozone atmospheres. NAP-XPS investigations have shown, that a metastable surface oxide is formed during the ozone exposure, which decomposes in vacuum.

Cu was characterized under conditions of the ethylene epoxidation. The two stoichiometric oxides  $\text{Cu}_2\text{O}$  and  $\text{CuO}$  were formed under reaction conditions. NAP-XPS measurements revealed that temperature programmed reduction (TPR) of  $\text{CuO}$  to  $\text{Cu}_2\text{O}$  in ethylene generates ethylene epoxide.

The correlation between the abundance of different oxygen species on metal surfaces during the ethylene epoxidation reaction and the catalytic performance will be discussed.

## Ethylene Epoxidation over Ag: Unraveling the Active Oxygen Species

T.C.R. Rocha, T. Jones\*, P. Kristiansen\*\*, L. Duda\*\*, S. Piccinin\*, A. Knop-Gericke, and R. Schlögl

For many decades, Ag-based catalysts have been used to produce ethylene oxide at large scales by the chemical industry. Nevertheless, the mechanism of this selective oxidation is still controversial, and consequently the development of new catalysts is limited. In one of the proposed mechanisms, different forms of oxygen on the Ag surface play a central role in controlling the selectivity to the epoxide<sup>1</sup>. In the present work we combine state-of-the-art X-ray spectroscopic techniques and DFT calculations to address the challenging task of identification and assignment of distinct oxygen species on the Ag catalyst surface and further correlation with catalytic performance.

Ag powders with typically 100 nm average particle size were used as catalysts. Initially, we used the NAP-XPS end-station at HZB/BESSY to characterize the oxygen species on Ag catalysts at mbar range under O<sub>2</sub> atmosphere and classify them as nucleophilic (Onucl) or electrophilic (Oelec), based on the oxygen specie's electronic and reactivity characteristics<sup>2</sup>. Next, we considered the dynamics of a non-promoted catalyst under ethylene epoxidation to establish a spectroscopic surface descriptor based on the distribution of oxygen species on the Ag catalyst that capture trends in selectivity (Oelec/Onucl). Afterwards, we exploited this parameter to study the promotion effect of Cl on the epoxidation, by quantitatively correlating the increase in selectivity induced by Cl to changes in the distribution of O species. We show that the Cl promoter renders a more selective Ag catalyst as a result of changes in the balance between electrophilic and nucleophilic oxygen species, which are proposed active species in the epoxidation reaction. Furthermore, the possible role of bulk-dissolved oxygen species was investigated using an innovative reaction cell developed for ambient pressure RIXS measurements performed at ALS and HZB/BESSY.

We have also performed extensive DFT calculations of surface energetics, electronic structure and core-level shifts for several Ag-O structural models, which are compared with reference measurements on Ag single crystals. The combination of theory with reference experiments has helped us to improve the assignments and the interpretation of the spectral fingerprints. Using this approach, we hope to convert the wealth of spectroscopic features into structural information that might bring new insights to the reaction mechanism of epoxidation over Ag.

### References

1. V.I. Bukhtiyarov, and A. Knop-Gericke, Ethylene Epoxidation over Silver Catalysts, in Nanostructured Catalysts, Royal Society of Chemistry, Cambridge (2011).
2. T.C.R. Rocha, A. Oestereich, D. Demidov, M. Hävecker, V.I. Bukhtiyarov, A.Knop-Gericke, and R. Schlögl, Phys. Chem. Chem. Phys. **14**, 4554 (2012).

\* Uppsala University, Ångström Laboratory, Uppsala, Sweden

\*\* Scuola Internazionale Superiore di Studi Avanzati, Trieste, Italy

## Active Oxygen Surface Species on Gold and Copper Catalysts in Oxidation Reactions

M. Greiner, A. Klyushin, B. Johnson, T.C.R. Rocha, M. Hävecker\*, A. Knop-Gericke, and R. Schlögl

It was recently found—using Near-Ambient-Pressure X-ray Photoemission spectroscopy (NAP-XPS)—that a multitude of oxygen surface and sub-surface species exist on silver catalysts during the partial oxidation of ethylene<sup>1</sup>. The population distribution of these oxygen species was found to be correlated with the catalytic selectivity for ethylene epoxide.

To further investigate the importance of oxygen surface species in partial-oxidation reactions, we have investigated alternative metal catalysts—having similar electronic structures as silver, i.e. gold and copper—*in-situ* during oxidation and partial-oxidation reactions, using NAP-XPS.

As gold is very difficult to oxidize, we utilize the highly oxidizing species O<sub>3</sub> to form oxygen surface species on the gold surface<sup>2</sup>. The resulting meta-stable surface oxide phase generates sites for CO adsorption and provides reactive atomic oxygen species upon decomposition.

Copper is much more oxidizable than both gold and silver. It can form two stoichiometric oxides—Cu<sub>2</sub>O and CuO. We find that, under conditions for ethylene epoxidation, both oxides can be formed; however, the higher-oxidation-state oxide, CuO, is found to be more active in ethylene epoxidation than the lower-oxidation-state oxide, Cu<sub>2</sub>O. By performing temperature-programmed reduction reactions of Cu<sub>2</sub>O and CuO powders in ethylene, and simultaneously monitoring the NEXAFS spectra, we find that ethylene reduces CuO to Cu<sub>2</sub>O. Surprisingly, during this reaction, ethylene epoxide is produced. In contrast, when Cu<sub>2</sub>O is reduced by ethylene, only total-oxidation products are produced. This observation suggests that lattice oxygen may play an important role in ethylene epoxidation on copper oxides.

These results provide insight into the various surface oxide species that are involved in oxidation and partial oxidation reactions, and contribute to the general understanding of such catalysts.

### References

1. T.C.R. Rocha, A. Oestereich, D. Demidov, M. Hävecker, V.I. Bukhtiyarov, A. Knop-Gericke, and R. Schlögl, *Phys. Chem. Chem. Phys.* **14**, 4554 (2012).
2. A. Klyushin, T.C.R. Rocha, M. Hävecker, A. Knop-Gericke, and R. Schlögl, PCCP submitted.

\* Helmholtz-Zentrum Berlin / BESSY II, Albert-Einstein-Str. 15, 12489 Berlin, Germany

## EMIL: The Energy Materials In-Situ Laboratory Berlin

M. Hävecker\*, G. Reichardt\*, F. Schäfers\*, S. Hendel\*, R. Follath\*\*\*, J. Bahrtdt\*,  
M. Scheer\*, E. Stotz, R. Arrigo\*\*\*, A. Knop-Gericke, K. Lips\*, and R. Schlögl

The Helmholtz-Zentrum Berlin (HZB) and the Fritz-Haber-Institut der Max-Planck Gesellschaft (MPG) have established a research alliance to implement EMIL, the *Energy Material In-situ Laboratory Berlin* at the BESSY II synchrotron light source. The EMIL-facility is dedicated to in-situ and in-system X-ray based analysis of materials and devices for photovoltaic applications/processes and catalytic materials for sustainable energy supply and storage. EMIL is subdivided into SISSY@EMIL focusing on investigations in photovoltaics and photocatalysis and CAT@EMIL for near ambient pressure spectroscopies on catalysts. Furthermore, at PINK@EMIL a high photon flux with moderate spectral resolution in the tender and hard X-ray regime 2 keV – 10 keV will be available. The X-ray light source for these stations will consist of two canted insertion devices<sup>1</sup>, a variably polarizing APPLE II undulator for soft X-rays (80 eV- 2.2 keV), and a planar cryogenic undulator for hard X-rays up to 10 keV. The end stations can either be operated with both beams simultaneously focused into one spot or use alternatively either the soft- or the hard X-ray radiation<sup>2</sup>, thus enabling X-ray based investigation of sample structures with information depths ranging from the sub-nanometer up to the micron scale. Details of the beamline optical layout will be presented.

Recently, a prototype of a near ambient pressure - high kinetic energy XPS end station (NAP-HE-XPS; extending the general design of 2<sup>nd</sup> generation NAP-XPS systems<sup>3</sup>) to be operated at the EMIL@CAT beamlines has been developed and put into operation at the ISSS beamline at BESSY II. This spectrometer covers a wide kinetic energy range of photoelectrons ( $E_{kin} \leq 7000$  eV) while maintaining a huge acceptance angle ( $\pm 22^\circ$ ) and in-situ capability (up to 25 mbar gas/vapor pressure). The modular structure of this instrument and thus the highly flexible sample environment concept will be discussed.

Finally, reaction cell designs that allow one to study electro-catalytic modifications of electrode materials like Pt under the presence of liquid and gaseous water will be shown and first results will be discussed<sup>4</sup>.

### References

1. P. Schmid, J. Bahrtdt, T. Birke, R. Follath, P. Kuske, D. Simmering, and G. Wüstefeld, Proceedings of IPAC 2012, New Orleans, Louisiana, USA.
2. R. Follath, M. Hävecker, G. Reichardt, K. Lips, J. Bahrtdt, F. Schäfers, and P. Schmid, *J. Phys.*, Conf. Ser. **425**, 212003 (2013).
3. D.E. Starr, Z. Liu, M. Hävecker, A. Knop-Gericke, and H. Bluhm, *Chem. Soc. Rev.* **42**, 5833 (2013).
4. R. Arrigo, M. Hävecker, M.E. Schuster, C. Ranjan, E. Stotz, A. Knop-Gericke, and R. Schlögl, *Angew. Chem. Int. Ed.*, DOI: 10.1002/anie.201304765.

\* Helmholtz-Zentrum Berlin / BESSY II, Albert-Einstein-Str. 15, 12489 Berlin, Germany

\*\* Paul Scherrer Institut, Villingen PSI, Switzerland

\*\*\* MPG for Chemical Energy Conversion (CEC), Stiftstr. 34-36, 45470 Mülheim a.d. Ruhr, Germany

## Carbon in Catalysis and Material Sciences

The key aspects of our work concerning nanostructured carbon materials are related to the growth of Single Layer Graphene (SLG) on transition metal surfaces and the modification and investigation of nanostructured carbon materials as catalyst or support in acid-base, hydrogenation, and oxidation reactions.

Chemical vapour deposition has been used to growth SLG on transition metal surfaces such as Ni and Cu. To gain insight into the formation mechanism of the graphene layer, X-ray photoelectron spectroscopy, X-ray absorption spectroscopy, and electron microscopy have been applied (AC 5.1).

Multiwalled carbon nanotubes (CNTs) were modified to use them as support in heterogeneous catalysis. Acidic and/or basic functionalities have been introduced, *i.e.*, by anchoring of sulfonic acid units via a radical-based strategy or by defect-mediated generation of nitrogen functionalities via ammonia treatment, respectively. Before metal loading, isopropanol decomposition was applied as the probe reaction to characterize the modified CNT-based supports in terms of their acid-base properties (AC 5.2).

Metal nanoparticles supported on N-containing carbon nanotubes (N-CNTs) exhibit improved catalytic performance in many catalytic applications (*e.g.*, liquid phase selective oxidation, H<sub>2</sub>O<sub>2</sub> direct synthesis, CO hydrogenation) compared to the N-free counterpart. The beneficial effect of the N species on nanocarbons arises from the peculiar metal-support interaction enabling the stabilization of very small nanoparticles against agglomeration. Our work aims to identify the electronic interaction of each type of N species present on the carbon surface with Pd, Rh and Mo<sub>x</sub>C nanoparticles and their relevance for the catalytic behavior. The reactivity of the Pd/N-CNT catalysts was studied in electro-catalytic oxygen reduction and catalytic selective hydrogenation of phenyl-acetylene. Supported Rh and Mo<sub>x</sub>C nanoparticles were investigated in higher alcohol synthesis from syngas (AC 5.2).

Furthermore, the reactivity of quinone group decorated carbon clusters was investigated by DFT as a model for the ODH of propane and ethylbenzene (AC 6.0). It was found that the formation of carbon-centered radicals as the suggested intermediates for selective ODH strongly depends on the spin multiplicity state of the cluster, *i.e.*, only the highest stable spin state leads to their formation, whereas the reaction in lower states stops at relatively stable surface ethers. Moreover, barriers depend on edge geometry (armchair vs. zigzag) and curvature (planar model vs. single-wall CNT). The formation of radical intermediates could be confirmed experimentally. Using high gas velocities the short-lived radicals could be stabilized in a solution of 5,5-dimethyl-1-pyrroline N-oxide to form a stable adduct, which was identified by EPR spectroscopy.

## Single Layer Graphene Growth on Transition Metal Surfaces

R. Blume\*, R.S. Weatherup\*\*, P. Kidambi\*\*, Z.-J. Wang, A. Knop-Gericke, M.G. Willinger, and R. Schlögl

A single layer of  $sp^2$  bonded carbon is considered as a well suited component in next-generation electronic, optoelectronics and microsystems due to its unique electrical, mechanical, surface and thermal properties. However, controlled growth of this so-called Single Layer Graphene (SLG), with high quality, has been proven difficult to achieve. To understand the key atomistic mechanisms of SLG formation, several transition metal (TM) surfaces such as Ni and Cu were probed ex- and in-situ, during defined chemical vapour deposition (CVD)<sup>1</sup>, as well as during carbon diffusion through TM films<sup>2</sup>, by X-ray photoelectron spectroscopy (XPS), near edge X-ray absorption fine structure spectroscopy (NEXAFS), scanning tunneling microscopy (STM) and (environmental) scanning electron microscopy ((E)SEM).

The results obtained in these studies revealed that for very high (Fe) and very low (Cu) carbon solubilities, SLG is formed via a single reaction path. In contrast, for intermediate solubilities, e.g. in Ni, several partially superimposing reaction paths were observed, including the formation of surface carbides and dissolved carbon atoms<sup>3</sup>. These paths have a strong impact on the resulting orientation of the SLG with respect to the substrate and its quality. Catalyst-SLG interaction and SLG corrosion resistance were examined by artificially aging SLG by repeated reduction/re-oxidation cycles. While on Ni, SLG proved to be mostly unaffected, on Cu originally strongly interacting as-grown graphene transforms to quasi-free-standing graphene upon air exposure by intercalating oxygen<sup>4</sup>. This transformation is reversible and, with regard to defect density and oxidation/corrosion resistance, strongly affects the stability and transferability of SLG.

### References

1. R.S. Weatherup, B.C. Bayer, R. Blume, C. Baetz, P.R. Kidambi, M. Fouquet, C.T. Wirth, R. Schlögl, and S. Hofmann, *Chem. Phys. Chem.* **13**, 2544 (2012).
2. R.S. Weatherup, C. Baetz, B. Dlubak, B. Bayer, P. Kidambi, R. Blume, R. Schlögl, and S. Hofmann, accepted by *Nanoletters*, (2013).
3. L.L. Patera, C. Africh, R.S. Weatherup, R. Blume, S. Bhardwaj, C. Castellarin-Cudia, A. Knop-Gericke, R. Schlögl, G. Comelli, S. Hofmann, and C. Cepek, *ACS Nano* **7**, 7901 (2013).
4. P. Kidambi, B. Bayer, R. Blume, Z.J. Wang, C. Baetz, R.S. Weatherup, M.G. Willinger, R. Schlögl, and S. Hofmann, accepted by *Nanoletters* (2013).

\* Helmholtz-Zentrum Berlin/ BESSYII, Albert-Einstein-Str. 15, 12489 Berlin, Germany

\*\* Department of Engineering, Univeristy of Cambridge, United Kindgom

## CNT-Supported Transition Metals and Carbides in Catalysis

B. Frank, Z.-L. Xie, K. Friedel, F. Girgsdies, G. Wowsnick, R. Arrigo, M.E. Schuster, Y. Yi, M. Hävecker\*, A. Knop-Gericke, R. Schlögl, and A. Trunschke

Transition metals and carbides supported on functionalized carbon nanotubes (CNTs) have been studied in various catalytic reactions to understand the influence of support properties on the product distribution. In particular, nitrogen-doped nanocarbons (N-CNTs) provide potentially interesting electronic properties and furthermore could improve the anchoring of metal nanoparticles.

Syngas conversion to higher alcohols offers an attractive way to produce chemicals and fuels based on renewable feedstock. The syntheses of 3 wt.% Rh on N-CNTs and N-free oCNTs as model catalysts resulted in highly dispersed and homogeneously distributed Rh particles that comprise an average particle size of  $< 3$  nm as determined by electron microscopy. Under high pressure reaction conditions<sup>1</sup> a space-time-yield of 3.3 mol (C<sub>2+</sub> alcohols)/mol(Rh)/h has been achieved for Rh/N-CNTs, whereas Rh/oCNTs are less active (0.6 mol/mol(Rh)/h). The effect of promoters will be addressed.

The less expensive group VI transition metal carbides show catalytic features similar to noble metals thus a related study focuses on the impact of synthesis conditions and carbon surface properties on the catalytic performance of MoC/CNT catalysts. Surface-oxidized CNTs were impregnated with ammonium heptamolybdate to achieve final Mo<sub>x</sub>C loadings of 5-30 wt% after carburization in 20 vol.% CH<sub>4</sub>/H<sub>2</sub> at 700 °C<sup>2</sup>. Other carbon supports such as N-doped CNTs, sulfonic acid functionalized CNTs, graphite, and activated carbon were treated in a similar way to generate a library of catalysts. For rapid screening, methanol steam reforming was chosen as a test reaction.

Palladium nanoparticles supported on N-containing carbon nanotubes show improved catalytic performance in liquid phase selective oxidation<sup>3</sup>, and H<sub>2</sub>O<sub>2</sub> direct synthesis<sup>4</sup>. The electronic interaction of Pd nanoparticles with different types of nitrogen-containing functional groups on the CNT surface has been studied by X-ray absorption spectroscopy. In particular, the nature of the N-Pd interaction for pyridine N and quaternary N species in N-CNTs was analysed by N K-edge NEXAFS. The electronic state of Pd coordinated to the N species has been studied by photoelectron spectroscopy. The relevance of the Pd-N interaction for the catalytic behaviour of Pd/N-CNTs in electro-catalytic oxygen reduction reactions and catalytic selective hydrogenation of phenyl-acetylene will be discussed.

### References

1. B. Frank *et al.*, Chem. Ing. Tech. **85**, 1290 (2013).
2. B. Frank *et al.*, ChemCatChem **5**, 2296 (2013).
3. R. Arrigo *et al.*, Phys. Chem. Chem. Phys. **14**, 10523 (2012).
4. R. Arrigo *et al.*, ChemSusChem, DOI 10.1002/cssc.201300616.

\* Helmholtz-Zentrum Berlin/BESSY II, Solar Energy Research Department, Albert-Einstein-Straße 15, 12489 Berlin, Germany

## Nanostructured Catalysts in Activation of Light Alkanes

Sustainable substitution of crude oil by natural gas or renewable resources requires catalysts that accomplish the activation of short chain alkanes with high selectivity. Mo- and V-based oxides have been widely investigated in direct oxidation of ethane and propane to olefins and oxygenates with limited success. In particular, desired products of propane oxidation, like propylene or  $\alpha$ - $\beta$ -unsaturated oxygenates are extensively subjected to consecutive reactions due to the high reactivity of allylic intermediates. Therefore, basic understanding of the catalytic activation of intermediates and the corresponding reaction networks is necessary beyond the first, rate-determining step of the reaction, which involves hydrogen abstraction and determines the activity. From the materials point of view bulk transition metal oxides, metal oxide monolayers, nanostructured carbon and carbides (AC 5.0) are included in the work.

Bulk mixed metal oxide catalysts have been prepared applying different techniques, which include precipitation, sol-gel, and hydrothermal synthesis. Hydrothermal routes give access to metastable phases and defective materials. The formation of MoVTeNb oxides has been screened by varying reaction time and temperature with the goal to identify optimal hydrothermal conditions. Insight into the chemistry inside the autoclave was provided by in-situ Raman spectroscopy. Based on the acquired knowledge, a new synthesis concept was developed that comprises the sequential addition of reactants under hydrothermal conditions. Continuously measured spectroscopic data indicate the appropriate addition time. This method allows the synthesis of materials with improved functionality in shorter times and with increased yield (AC 6.1).

Phase-pure catalysts have been studied in selective oxidation of ethane, propane, and butane. A broad field of reaction parameters was investigated in propane oxidation over MoVTeNb oxide composed of the orthorhombic M1 phase (ICSD no. 55097). The bulk structure of the catalyst and its catalytic performance are stable as long as strongly reducing conditions are avoided. A simplified reaction network is proposed in which the partial pressure of oxygen and steam are factors that determine activity and selectivity. Phase-pure catalysts (M1, vanadyl pyrophosphate) have also been investigated using complementary in-situ spectroscopic techniques including photoelectron spectroscopy and microwave conductivity measurements to reveal dynamic and reversible surface changes depending on the feed composition. The active phase turned out to be as a self-supported thin layer. Relations between chemical and electronic structure of this layer, the bulk of the catalyst, and selectivity are discussed (AC 6.2).

Monolayers of V and Mo oxides on the surface of mesostructured silica have been studied as model systems. In the case of silica-supported  $\text{MoO}_x$ , a steep increase in catalytic activity of the oxidative dehydrogenation of propane and metathesis of propene has been found at a Mo loading close to one monolayer. The structure of the Mo oxide surface species (two-fold anchored tetrahedral di-oxo  $(\text{Si}-\text{O}-)_2\text{Mo}(=\text{O})_2$  units), however, is affected little by the loading. The experimentally observed phenomenon is explained by formation of frustrated surface species where the availability of anchoring silanol species is limited by the high loading and by lateral interactions between the surface species. The concept, which seems to be applicable also to other metal oxides is supported by in-situ spectroscopy, in particular NEXAFS spectroscopy at the oxygen K-edge in combination with DFT calculations (AC 6.3).

## MoV(Te,Nb)O<sub>x</sub> Catalysts for Propane Oxidation: Hydrothermal Synthesis and Functional Properties

J. Noack\*, M. Jastak, M. Sanchez-Sanchez, P. Kube, R. Naumann d'Alnoncourt\*, T. Lunkenbein, F. Girgsdies, F. Rosowski\*\*, R. Schlögl, and A. Trunschke

Mixed metal oxides with complex crystal structure including transition metals, such as Mo and V are known to be good catalysts in the activation and selective oxidation of light alkanes. Complex MoVTenb oxides that crystallize in the so-called M1 structure are highly stable and selective in the direct oxidation of propane to acrylic acid<sup>1</sup>. In order to gain insight in the complex structure-property relationships of M1, the phase was prepared applying various techniques, which result in phase-pure M1 material of different chemical composition and with varying particle morphology<sup>2-4</sup>.

The preparation of quinary MoVTenb oxide was performed stepwise by consecutive addition of the reactants under hydrothermal conditions<sup>5</sup>. The formation of the desired species is monitored by Raman spectroscopy under reaction conditions. An aqueous solution of (NH<sub>4</sub>)<sub>6</sub>Mo<sub>7</sub>O<sub>24</sub> is reacted with NH<sub>4</sub>[NbO(C<sub>2</sub>O<sub>4</sub>)<sub>2</sub>] to form the first building block of the M1 structure in which Nb is the central atom of a pentagonal bipyramidal unit {(Mo<sub>5</sub>)Nb} surrounded by five MoO<sub>6</sub> octahedra. When a vanadyl sulphate solution is added at 175°C, these basic units are connected. Upon addition of telluric acid, the building blocks are converted to semi-crystalline M1, which is crystallized at 650°C in argon stream. The resulting M1 catalyst is characterized by high selectivity of acrylic acid in selective oxidation of propane leading to an increase in space-time yield by a factor of five.

A series of M1 structured catalysts including only Mo and V were prepared by hydrothermal synthesis and tested in propane oxidation where a feed composition of C<sub>3</sub>H<sub>8</sub>/O<sub>2</sub>/H<sub>2</sub>O/N<sub>2</sub> = 3/12/10/75 vol-% was applied. Depending on the hydrothermal synthesis conditions, catalysts with different degrees of crystallinity and porosity are obtained. While the highly crystalline catalyst shows the highest conversion, the selectivity to the products acrylic acid, acetic acid and CO<sub>x</sub> are almost the same independent of the particle morphology. Relations between catalysts performance, structural stability, and surface dynamics will be discussed.

### References

1. R. Naumann d'Alnoncourt *et al.*, J. Catal. submitted.
2. Y.V. Kolen'ko *et al.*, ChemCatChem **3**, 1597 (2011).
3. Y.V. Kolen'ko *et al.*, ChemCatChem **4**, 495 (2012).
4. K. Amakawa *et al.*, ACS Catalysis **3**, 1103 (2013).
5. M. Sanchez Sanchez *et al.*, Angew. Chem. Int. Ed. **51**, 7194 (2012).

\* BasCat, UniCat-BASF Joint Lab, Technische Universität Berlin, Sekr. BEL 6, Marchstraße 6, 10587 Berlin, Germany

\*\* BASF SE, Heterogeneous Catalysis, Process Research and Chemical Engineering, Carl-Bosch-Straße 38, 67056 Ludwigshafen, Germany

## The Catalytically Active Surface Between Bulk and Gas Phase: Investigating Interfacial Charge Transport Under Working Conditions

C. Heine, M. Heenemann, A. Trunschke, R. Schlögl, and M. Eichelbaum

Interfacial charge transport is playing a decisive role in the heterogeneously catalyzed oxidative activation of alkanes, often accompanied by the transfer of a large number of electrons and oxygen atoms across phase boundaries. Many recent investigations have demonstrated that under alkane oxidation conditions the active surface deviates significantly from the bulk in both chemical and electronic structure<sup>1-3</sup>. Hence, not only solid/gas but also solid/solid interfaces, described by semiconductor physics concepts, have to be taken into account to comprehend the working mode of an oxidation catalyst. Thus, the overall goal of our research is the investigation of kinetics and thermodynamics of charge transport at interfaces under reaction conditions and to understand their consequences on catalytic activity and selectivity.

In order to study charge transport in high performance powder catalysts under working conditions, we developed a method based on the microwave cavity perturbation technique (MCPT). This enables the investigation of (di)electric properties of catalysts inside fixed bed flow reactors in a contact-free and non-invasive manner. Thus, it avoids contact resistance and other electrode related difficulties<sup>4</sup>. Studies on the selective alkane oxidation catalysts vanadyl pyrophosphate<sup>2</sup>, MoVTeNbO<sub>x</sub> M1<sup>3</sup> and newly synthesized vanadium(IV) phosphates<sup>5</sup> show that the samples respond reversibly like semiconducting electrical gas sensors (chemiresistors) to the gas phase chemical potential. Moreover, complementary *in-situ* X-ray photoelectron spectroscopy indicates that the V<sup>4+</sup>/V<sup>5+</sup> ratio on the surface can be tuned by the applied gas phase and can pin the Fermi level of the catalyst to the corresponding surface state. This effect was shown by observing systematic changes of the work function, bending of the valence band and by shifts of core level energies<sup>3</sup>. The thus modulated charge carrier density in the subsurface depletion layer causes a response of the electrical conductivity as measured by MCPT. As a result, charge transport between bulk, surface and gas phase could be identified and explained by an extrinsic surface state semiconductor model.

Current research encompasses the development of a microwave Hall effect setup, which will allow the determination of charge carrier mobilities in catalysts under reaction conditions and, finally, the deduction of absolute charge carrier densities. Another goal is the extension of MCPT to a multi-frequency spectroscopic method. A frequency dependent conductivity measurement will permit the differentiation between interface and intrinsic electronic properties as well as between free and bound charge carriers.

### References

1. M. Hävecker *et al.*, J. Catal. **285**, 48 (2012).
2. M. Eichelbaum *et al.*, Angew. Chem. Int. Ed. **51**, 6246 (2012).
3. C. Heine *et al.*, J. Phys. Chem. C submitted.
4. M. Eichelbaum *et al.*, Phys. Chem. Chem. Phys. **14**, 1302 (2012).
5. M. Eichelbaum *et al.*, ChemCatChem **5**, 2318 (2013).

## Structural Analysis of Silica-Supported Transition Metal Oxide Catalysts by X-ray Absorption: Combined Theoretical and Experimental Studies

C.S. Guo\*, L.L. Sun, K. Hermann, T. Wolfram, K. Amakawa, P.K. Nielsen, P. Kube, M. Hävecker\*\*, A. Trunschke, and R. Schlögl

Modern theoretical methods applying density-functional theory (DFT) can be used to interpret experimental results from X-ray absorption (XAS/NEXAFS), and can provide an understanding of structure on a microscopic scale. Here we review recent theoretical and experimental work on electronic and structural properties of different supported vanadia-, molybdena-, and titania-silica particles which can form active centers in catalysts of industrial relevance.

Monolayers and sub-monolayers of V, V/Ti, Ti, and Mo have been grafted on the surface of meso-structured silica applying different techniques. The resulting catalysts reveal interesting catalytic properties in oxidative dehydrogenation of propane and metathesis of propene<sup>1,2</sup>.

DFT calculations, using the StoBe code, are performed on oxygen core excitations in different vanadia-, molybdena-, and titania-silica clusters. These results are compared with O K-edge NEXAFS measurements of corresponding catalysts on SBA-15 silica and can yield structural details of the nanoparticles. Differently binding oxygen, inside  $\text{MeO}_x$  (Me = V, Mo, Ti) and  $\text{SiO}_2$ , can be clearly distinguished in the theoretical spectra. A comparison with experimental NEXAFS spectra for different supported vanadia species provides clear evidence that polymeric  $\text{VO}_x$  exists at the catalyst surface and the exclusive presence of monomeric vanadia groups can be ruled out<sup>3</sup>. The comparison for supported molybdena species suggests that tetrahedral dioxo  $\text{MoO}_4$  units, binding by one or two Mo-O-Si bridges with the silica support, dominate the experimental spectrum for low Mo loading<sup>4</sup>. At higher Mo loadings the NEXAFS spectra can be explained by distorted  $\text{MoO}_4$  complexes where adjacent oxygen atoms in the complex start to interact<sup>5</sup>. The comparison for supported titania species suggests that with the present preparation monomeric titania species at low coverage on SBA-15 will form tetrahedral complexes where titanyl oxygen is saturated by hydrogen yielding OH groups at the Ti centers<sup>6</sup>.

### References

1. N. Hamilton *et al.*, Catal. Sci. & Technol. **2**, 1346 (2012).
2. K. Amakawa *et al.*, J. Am. Chem. Soc. **134**, 11462 (2012).
3. M. Cavalleri *et al.*, J. Catal. **262**, 215 (2009).
4. C.S. Guo *et al.*, J. Phys. Chem. C **115**, 15449 (2011).
5. K. Amakawa *et al.*, Angew. Chem. Int. Ed. DOI: anie.201306620 (2013).
6. C.S. Guo *et al.*, J. Phys. Chem. C **116**, 22449 (2012).

\* Southwest Jiaotong University, Supercond. and New Energy Center, Chengdu, Sichuan, 610031 China

\*\* Helmholtz-Zentrum Berlin/BESSY II, Solar Energy Research Department, Albert-Einstein-Strasse 15, 12489 Berlin, Germany

## Reversible Charge Storage Mechanism in Lithium Ion Batteries

Significantly improving the energy density of lithium ion batteries requires new electrode materials. But the currently known high energy electrode materials suffer from a severe degradation upon cycling. Our aim is to identify the mechanism for degradation and develop strategies to enhance the electrodes stability. Therefore we need to understand the charge storage mechanism and to identify the processes impeding it. This has an analogy to the deactivation mechanism of catalyst, especially since we expect the interface chemistry of the battery electrodes to play a major role for the battery degradation. Hence a similar analytical research strategy as used for catalysis research is required to investigate the electrodes stability. So the initial prerequisite is the preparation of well defined active electrode materials, which then are analyzed with sophisticated microscopical and spectroscopical analytical methods. For our research we focused on silicon as anode material and  $\text{LiFePO}_4$  as material for the cathode.

We developed a cold-wall-shower-head CVD reactor, which enables us to prepare well defined silicon thin film with variable morphologies and surface terminations. The reactor was designed to operate with a wide selection of gases including  $\text{N}_2$ , Ar,  $\text{H}_2$ ,  $\text{O}_2$ ,  $\text{SiH}_4$ ,  $\text{CH}_4$ , HCl and  $\text{NH}_3$ . In addition, for liquid precursors such as  $\text{SiHCl}_3/\text{SiCl}_4$  two parallel bubbler lines are installed. An inductive heating system is attached to the reactor and enables us to make local heating of the reactor zone. The reactor can be operated in a wide temperature range between  $350^\circ\text{C}$  to  $2500^\circ\text{C}$ , while the temperature's upper end side is used for premodifying carbon supports. The deposition process is automatized by controlling all electronics and valves via a home-written LabVIEW program, which allows great operational flexibility and avoids user dependent errors to ensure the safety and reproducibility of the samples. These manifold sides of our CVD reactor give a wide spectrum of possible applications besides the Si-deposition, including surface activation, passivation, termination and graphitization.

The batteries are prepared with carbonate based electrolytes, including variable additives, inside an argon filled glovebox and cycled with a multichannel potentiostat to the required cycle and state of charge. Disassembly of the batteries is carried out inside the glovebox and the electrodes are air tightly transported to the analytical tool. Several of these tools needed modifications to be operational without air contamination to the sample. Beside other modifications we therefore installed a transfer system to our SEM and put a FTIR spectrometer inside a glovebox. From the microscopic and spectroscopic analysis of the silicon based battery anodes we depict dissolution of silicon into the solid electrolyte interphase as one possible degradation mechanism of the electrode.

For the research on the cathode side we compared the chemical state of lithium inside  $\text{LiFePO}_4$  and  $\text{LiCoO}_2$  by electron energy loss spectroscopy and found indications for a charge transfer towards the lithium in  $\text{LiFePO}_4$ . Contrary the lithium is purely ionic in  $\text{LiCoO}_2$ , so no charge transfer is observed.

For the silicon based battery research we have a fruitful collaboration with the Volkswagen AG and with the group of Prof. Maier from Max Planck Institute of Solid State Research in Stuttgart. The group of Prof. Maier is also involved in the research on the  $\text{LiFePO}_4$  which is prepared in the group of Prof. Antonietti from the Max Planck Institute of Colloids and Interfaces in Potsdam.

## Silicon Anodes for Lithium Ion Batteries

B. Davaasuren, M. Pradel, N. Giliard, M.E. Schuster, M.G. Willinger, J. Tornow, and R. Schlögl

The theoretical gravimetric capacity of silicon as anode material in lithium ion batteries is with 3580 mAh/g about ten times higher compared to graphite (372 mAh/g), which is today's standard. This makes it extraordinarily attractive for the application in high energy batteries, but on the contrary its cycling stability still is far too low. We intend to figure out the parameters limiting the silicon stability and develop routes for impeding the degradation. We therefore use well defined silicon thin films, which we deposit by chemical vapor deposition (CVD). In contrast to the classical electrode preparation by mixing conductive additives and binders to form a paste, the CVD process allows us to investigate solely the properties of the silicon component. Since we expect the surface chemistry to have a severe influence on the electrode degradation, the possible modifications on the silicon surface by CVD is a useful further ability of this preparation method.

To analyze the silicon at specific states of charge, a CVD substrate without any lithium storage properties is required. We therefore used titanium instead of carbon. Titanium has several advantages for our use including, high melting point and immiscibility with lithium. But direct deposition of silicon on titanium results in the formation of titanium-silicide phases. Therefore,  $Ti_xN_y$  was deposited on the titanium substrate as blocking layer for silicon diffusion. The reaction conditions were tried to be optimized against the formation of a single TiN-phase using  $N_2$  as a nitrogen precursor. As a result we are ending up with a two phase region of different titanium-nitride phases including TiN,  $Ti_2N$ ,  $TiN_{0.3}$  and  $TiN_{0.9}$ . Further, optimization is necessary to ensure the formation of single phase TiN as a passivation layer. A promising attempt is to use  $NH_3$  as a nitrogen precursor.

In order to investigate the charge storage and transfer mechanism in a silicon anode, we proposed several sample design concepts. Samples with same surface areas but with various thicknesses of silicon were prepared and cycled against a lithium electrode. The results show that the charge storage capacity strongly depends on the film thickness. This clearly indicates that the charge is stored in the silicon's bulk instead of at the surface.

This information is quite important to analyze experiments with electrodes made in the classical way from a paste. Here we observed the formation of a solid electrolyte interphase (SEI) by scanning electron microscopy (SEM). A more detailed study with energy filtered transmission electron microscopy revealed that this SEI contained also silicon, which is obviously dissolved into it and hereby lowers the amount of bulk silicon. Since studies with SEM and impedance spectroscopy proofed a continuously growing SEI with cycling and the location of charge storage is inside the bulk silicon, this dissolution process is a possible degradation mechanism. We will determine the strength of this influence on the total electrode degradation in future studies.

This research is conducted by a fruitful collaboration with Volkswagen AG and further studies on the charge transport are performed in collaboration with the group of Prof. J. Maier from the MPI for solid state research in Stuttgart.

## Methodological Developments of the Electron Microscopy Group

Besides routine investigations of samples in terms of morphology, structure and elemental composition, which is provided as electron microscopy service for the members of the department, the electron microscopy group has concentrated on the full exploitation of the analytical power of the microscopes and further development of methods for chemical electron microscopy in catalysis.

Chemical electron microscopy means analytical electron microscopy with a strong focus on the chemical state of the investigated material by spectroscopic analysis and especially, under consideration of dynamic processes. The Electron Microscopy group is following different strategies for the study of reaction-induced surface and bulk modifications through ex- and in-situ observation.

On the mesoscale, a significant methodological development of in-situ environmental scanning electron microscopy (ESEM) could be achieved. A laser heating system was developed for drift and contamination free heating up to 1000°C, the gas feeding and vacuum system have been improved and a mass spectrometer for gas phase analysis has been implemented. The set-up is now versatile and allows a wide range of in-situ experiments under different atmospheres, pressures and temperatures as well as the application of electrochemical potentials (see Poster AC 8.1). In parallel to the experimental development, investigations on contrast mechanisms and the processes of signal generation in ESEM are conducted. In order to calibrate the sensitivity of the detected secondary electron signal to changes in the work-function at the surface of metal catalysts, we presently investigate the well calibrated CO oxidation on Pt. The results are promising and demonstrate the potential of the ESEM technique as surface-science tool.

On the atomic scale, we have developed high- and ambient-pressure micro-reactors for the investigation of microscopic amounts of catalysts by coupling ex-situ catalytic reaction to electron microscopic investigation via a sample transfer system. Using this approach we are able to investigate identical particles before and after exposure to catalytically relevant conditions in the transmission electron microscope (TEM). Hence, limitations of environmental TEM in terms of pressure, selection of gases and the catalytic relevance of experimental conditions can be avoided (see Poster AC 8.2). For in-situ investigations inside the TEM, we have further improved a home built TEM holder, which is designed to enable sample heating and simultaneous application of electric potential. Recent developments in commercial TEM sample holders for in-situ experiments are also followed. In cooperation with Protochips, a manufacturer of MEMS device based TEM holders, we are presently designing a gas feeding system for in-situ experiments in the microscope.

## In-Situ Investigation of Surface Dynamics by Environmental Scanning Electron Microscopy

Z.J. Wang, G. Weinberg, M.G. Willinger, and R. Schlögl

Advanced electron microscopy and catalysis are today mostly related through ultra-high resolution observations of atomistic details of periodic and aperiodic structures. The interest in such images is motivated by the desire to “see” active sites and to obtain a visual impression of the atomic details of nanostructures. ETEM is advocated as the ultimate solution to obtain the structure of active catalysts. Catalysis, however, is a multi-scale phenomenon that is related to its observable performance by a very large scaling factor of the dimension of Avogadro’s number ( $6 \times 10^{23}$ ). The minimum ensemble of active sites that we can observe by chemical analysis is of the order of  $10^{10}$  and thus never accessible with atomic resolution. Problem-oriented electron microscopy for catalysis should thus consider the mesoscopic unit of analysis with the same level of attention that it provides for the level of atomic resolution. We have thus modified a commercial environmental scanning electron microscope (ESEM) for in-situ experiments under conditions that are relevant for catalysis. The instrument is capable of covering the same pressure range as in high-pressure XPS experiments at BESSY (see Posters AC 3.1, 3.2 and 4.0.) and provides complementary visual information on reaction induced surface dynamics.

Two examples for the study of dynamics on metal surfaces by ESEM will be presented. The first is on the structural dynamics of silver in catalytic oxidation reactions, the second one on the dynamics of graphene formation and growth by ethylene decomposition on metal catalysts.

In the case of silver we observe oxygen induced surface dynamics under conditions of methanol oxidation. Surface modifications are initially characterized by abnormal grain growth and in later stages, by the formation of surface steps. The temporal behaviour thus demonstrates the relation between surface dynamics and the occurrence of different types of oxygen species as observed by in-situ XPS<sup>1</sup> (Poster AC 3.1).

In the case of graphene growth by catalytic chemical vapour deposition on metal films<sup>2</sup>, we are able to visually follow a complete CVD process involving substrate annealing, graphene nucleation and growth and finally, substrate cooling. It was found that graphene growth on copper above 850°C occurs on a pre-melted, highly mobile surface. We show that dynamics of growth are related with the degree of copper surface mobility and discuss its dependence on temperature, atmosphere and grain orientation.

### References

1. T.C.R. Rocha, A. Oestereich, D. Demidov, M. Hävecker, V.I. Bukhtiyarov, A. Knop-Gericke, R. Schlögl, *Phys. Chem. Chem. Phys.* **14**, 4554 (2012).
2. P.R. Kidambi, B.C. Bayer, R. Blume, Z.J. Wang, C. Baehtz, R.S. Weatherup, M.G. Willinger, R. Schlögl, and S. Hofmann, *Nano Lett.* **13**, 4769-4778 (2013).

## Micro-Reactors for the Investigation of Dynamic Processes by Transmission Electron Microscopy

T. Lunkenbein, M.E. Schuster, M.G. Willinger, and R. Schlögl

Modern transmission electron microscopes (TEMs) are capable of delivering structural, compositional and chemical information at the atomic level. For catalysis, the arrangement of the atoms in vacuum at thermodynamic equilibrium is certainly of interest, however, for the understanding of dynamic processes that occur in the interaction of the catalyst with its surrounding, the requirement of a good vacuum inside the TEM column is a serious limitation. E. Ruska has pioneered in-situ electron microscopy by exposing samples in the microscope to different gases at various pressures already in 1942<sup>1</sup>. Nowadays, environmental transmission electron microscopes are commercially available and used for the investigation of dynamic processes inside the microscope. This method, however, is restricted to a few non-corrosive gases and low pressures. Furthermore, the influences of the electron beam during the imaging process, the exact composition of the atmosphere inside the TEM column, as well as the temperature at the place of observation, remain unclear.

To overcome these limitations, two TEM-grid micro-reactors were developed for high and ambient pressure catalysis, respectively. The reactors allow a decoupling of the catalytic reaction from the imaging process. Imaging at identical location before and after experiments in the micro-reactor allows following morphological, structural and chemical changes of precursors and catalytically active materials. Transport of the sample between TEM and micro-reactor is enabled via vacuum transfer holders and glove box without contact to ambient environment. Hence, the restrictions with respect to pressure, atmosphere and electron beam are omitted. Experiments are carried out on microscopic amounts of catalyst supported on an inert TEM grid. The small amount of catalyst guarantees that all catalyst particles are exposed to the same conditions. Due to the small mass of catalyst, an ultra-high sensitive proton-transfer reaction mass spectrometer (PTR-MS) is used to follow the catalytic conversion and to guarantee that the investigated particles show relevant catalytic function.

First results obtained with the high pressure TEM Grid (HITEM) micro-reactor will be presented. Present investigations are focusing on the methanol synthesis over Cu/ZnO/Al<sub>2</sub>O<sub>3</sub> catalysts at 30 bars (see also Poster AC 1.2). We are able to follow the transformation from the precursor to the active catalyst and investigate reasons for deactivation through the observation of identical particles.

Furthermore, the ambient pressure TEM Grid (AMBITEM) micro reactor as well as a home built TEM holder for electrochemical experiments will be presented.

### References

1. E. Ruska, *Kolloid-Zeitschrift*, **100**, 212-219 (1942).

## Theory of Periodic Overlayers and Interference Lattices: Moirons at Work

K. Hermann

Rotated and/or scaled overlayers at regular single crystal surfaces, such as graphene on hexagonal Ru(0001)<sup>1,2</sup> or silver on Ni(111) substrate<sup>3</sup>, are found to exhibit, apart from their intrinsic 2-dimensional layer periodicity, additional long-range order expressed by approximate surface lattices with very large lattice constants. This collective effect can be described geometrically analogous to 2-dimensional (lateral) interference resulting in periodic moiré patterns characterized by 2-dimensional moiré lattices. The patterns, consisting of similar local surface regions (*moirons*), are accounted for mathematically by Fourier analysis and concepts of coincidence lattice theory<sup>4</sup>. The theoretical treatment yields simple algebraic expressions for all moiré lattice parameters defining the moiron arrangement in its dependence on rotation angle  $\alpha$  and scaling factors  $p_1, p_2$  for ideal  $(p_1 \times p_2)R\alpha$  overlayers on substrate surfaces described by general Bravais lattices. Well separated moirons are found to appear only for rotation angles below  $10^\circ$  and scaling factors  $p_i$  between 0.8 and 1.2.

For isotropically scaled overlayers without rotation, denoted as  $(p \times p)$ , the general formalism yields a singularity for  $p = 1$  which results in very large moiré lattices. This is observed for graphene layers on hexagonal metal surfaces<sup>1-3</sup> where the measured moiré lattice constants agree quantitatively with theory. For rotated overlayers without scaling, denoted as  $(1 \times 1)R\alpha$ , the general formalism yields a singularity for  $\alpha = 0^\circ$  which also leads to very large moiré lattices. This is observed for superimposed graphene layers where the measured moiré lattice constants agree exactly with the theoretical prediction. For general isotropically scaled and rotated overlayers, denoted as  $(p \times p)R\alpha$ , the formalism can also describe measured moiré lattices quantitatively as demonstrated for graphene layers on top of hexagonal BN layers. Further, the formalism can explain moiré lattice shifts resulting from overlayer shifting which occurs for graphene at stepped metal surfaces where giant moiron shifts are observed.

### References

1. D. Martoccia, P.R. Willmott, T. Brugger, M. Björck, S. Günther, C.M. Schlepütz, A. Cervellino, S.A. Pauli, B.D. Patterson, S. Marchini, J. Wintterlin, W. Moritz, and T. Greber, *Phys. Rev. Lett.* **101**, 126102 (2008).
2. M. Iannuzzi, I. Kalichava, H. Ma, S.J. Leake, H. Zhou, G. Li, Y. Zhang, O. Bunk, H. Gao, J. Hutter, P.R. Willmott, and T. Greber, *Phys. Rev. B* **88**, 125433 (2013).
3. C. Chambon, J. Creuze, A. Coati, M. Sauvage-Simkin, and Y. Garreau, *Phys. Rev. B* **79**, 125412 (2009).
4. K. Hermann, *J. Phys. Cond. Matter* **24**, 314210 (2012).

## Oxidative Coupling of Methane

The oxidative coupling of methane (OCM) to C<sub>2</sub> hydrocarbons was studied in a joint effort in the Berlin-centered Cluster of Excellence „Unifying Concepts in Catalysis” (UniCat).

It is known in literature that the OCM reaction can be catalyzed by a large number of different catalyst materials, although they do not share a common structural motive. The reaction mechanism is proposed to follow a heterogeneous/homogeneous reaction scheme. The proposed reaction mechanisms found in literature include an activation of methane on the catalyst surface followed by the release of methyl radicals into the gas phase, where ethane is formed by pairing of two methyl radicals in presence of a third body. It is worth to emphasize that the reaction occurs even without a catalyst, however with low C<sub>2</sub> selectivity.

UniCat devotes a research package to the homogeneous part of the OCM reaction aiming for a comprehensive kinetic description based upon observables or theoretically verified input data. Therefore, gas-phase OCM has been studied in our spatial profile reactor (AC 9.1). The reactor applies a capillary sampling technique that allows to measure micrometer resolution spatial reactor profiles of species concentrations and gas phase temperature along the centerline of a reactor tube of 18 mm inner diameter. The length of the free gas phase investigated in our experiments was up to 100 mm.

Reactor profiles measured at different reaction conditions by means of temperature and pressure have been compared with simulation done in the group. The most accurate mechanism from Dooley *et al.* has been adapted to simulate the homogeneous OCM reaction in our reactor using full Navier-Stokes microkinetic numerical simulations.

The profile reactor setup has been improved recently by the development of a novel fiber-optic laser-induced fluorescence (LIF) method, which is applied for *in-situ* detection of formaldehyde. Formaldehyde is an important intermediate in the oxidation process. The method extends the reactor setup to an additional spectroscopic method, which is planned to be applied for OH radical detection in the future.

Furthermore, the role of surface structure and defects in the oxidative coupling of methane was studied over magnesium oxide as a model catalyst. Pure MgO nanoparticles with varying primary particle size, shape and surface area were synthesized by sol-gel synthesis, oxidation of metallic magnesium, hydrothermal post treatment of ultra-pure MgO at normal pressure and in a microwave autoclave. Based on kinetic studies combined with comprehensive structural and surface characterization by electron microscopy, infrared and ESR spectroscopy, a mechanism for the oxidative coupling of methane on freshly dehydroxylated MgO is proposed. The abundance of monoatomic steps on the MgO surface is correlated with the consumption rate of methane and the formation rate of C<sub>2</sub> coupling products. The mechanism changes dynamically with time on stream, because water formed as by-product acts as catalyst poison that initiates the sintering of the MgO particles by preferential depletion of the highly active monoatomic steps. The function of defects as active sites under stationary conditions and the effectiveness of Au and Fe as promoters are discussed (AC 9.2).

## Fuel-Rich Methane Oxidation in a High-Pressure Tubular Reactor Studied by Optical-Fiber-Laser-Induced Fluorescence, Spatially Resolved Multi-Species Axial Reactor Profile Measurements, and Microkinetic Simulations

H. Schwarz, O. Korup\*, M. Geske\*\*, C.F. Goldsmith\*\*\*, R. Schlögl, and R. Horn\*

The predicted depletion of the conventional crude oil reserves set off a growing research interest in natural gas as chemical feedstock. Conventional approaches rely on indirect conversion pathways, where methane is first converted in synthesis gas, followed by a gas-to-liquid process (GTL) and cracking of the GTL products. These multi-step strategies are particularly capital intensive and alternative direct production routes for basic chemical building block such as ethylene would be of utmost economic interest.

Oxidative coupling of methane (OCM) could be such a desirable conversion route; in which methane is transformed into ethylene directly under fuel-rich feed compositions and temperatures around 1000 K. It has been suggested in literature, that the OCM reaction proceeds via a homogeneous/heterogeneous coupled mechanism<sup>1</sup> on a variety of catalyst materials<sup>2</sup>. Additionally, the importance of free radical reactions for OCM has long been recognized. Two gas-phase methyl radicals are proposed to combine in the gas phase to form ethane, which is subsequently dehydrogenated to ethylene.

To disentangle the complex reaction network between gas and surface reactions, microkinetic mechanisms for both domains are required. Presently, the microkinetic surface mechanisms on typical OCM catalysts such as MgO and Li/MgO are scarce and highly speculative, whereas the gas phase oxidation of methane has been studied for decades, and microkinetic mechanisms have been reported with varying complexity.

Gas-phase OCM has been studied in our spatial profile reactor<sup>3</sup>. The reactor allows the measurement of high-resolution axial species concentration and gas-phase temperature profiles along the centerline of the reactor tube of 18 mm inner diameter. A novel fiber-optic laser-induced fluorescence (LIF) method<sup>4</sup> has been developed recently, and is applied for in situ detection of formaldehyde, which is an important intermediate in the oxidation process. Optical access is provided by the novel fiber-optic LIF probe.

Additionally, Full Navier-Stokes microkinetic numerical simulations were performed and validated against the experimental dataset. It was found, that the selected mechanism gives qualitatively and quantitatively correct predictions for the main species profiles. However, the results show that predictive kinetic modeling of industrial processes is still challenging, as the evolution of C2 products was less accurate.

### References

1. D.J. Driscoll, *et al.*, J. Am. Chem. Soc. **107**, 58 (1985).
2. J.H. Lunsford, *Angew. Chem. Int. Edit.* **34**, 970 (1995).
3. E.V. Kondratenko, and M. Baerns, *Handbook of Heterogeneous Catalysis* **6**, 3010 (2008).
4. R. Horn *et al.*, *Rev. Sci. Instrum.* **81**, 064102 (2010).
5. H. Schwarz, R. Schlögl, R. Horn, *Appl. Phys. B* **109**, 19 (2012).

\* Institute of Chemical Reaction Engineering, Hamburg University of Technology, Eißendorfer Straße 38, 1073 Hamburg, Germany

\*\* BasCat, UniCat-BASF Joint Lab, Technische Universität Berlin, Sekr. BEL 6, Marchstraße 6, 10587 Berlin, Germany

\*\*\* Chemical Engineering, Brown University, Providence, USA

## Oxidative Activation of Methane over Au-Fe/MgO Model Catalysts

P. Schwach, M.G. Willinger, A. Trunschke, and R. Schlögl

Activation of methane over heterogeneous catalysts remains an attractive subject in view of the abundance of natural gas and renewable methane resources. In this context, oxidative coupling of methane (OCM) to ethane or ethene over alkaline earth oxides doped with alkali elements or transition metal ions received particular attention. Freund *et al.*<sup>1</sup> provide evidence that strongly bound  $\text{O}_2^-$  species as precursor of dissociatively adsorbed  $\text{O}_2$  are formed on highly ordered CaO films doped with  $\text{Mo}^{2+}$ . The results indicate that  $\text{O}_2$  activation on doped oxides does not require any structural surface defects. Accordingly, it is suggested that activation of methane on smooth surfaces of transition-metal-doped wide-gap oxides may involve such activated oxygen species.

To prove the applicability of the concept to powder catalysts, we introduced Fe as a dopant in ppm quantity into polycrystalline  $\text{MgO}^2$ . The presence of Fe atoms on the surface may introduce additional redox chemistry into the activation mechanism of methane, but, even in an ideal solid solution, terminating Fe atoms cannot be avoided. Therefore, the Fe-MgO catalyst was modified by subsequent adsorption of highly dispersed gold on the surface. An Au-MgO catalyst was included in the study for reference. The synthesis resulted in a high dispersion of the dopants as indicated by electron microscopy (HAADF STEM and HRTEM), temperature-programmed reduction-oxidation cycles, UV-vis, and EPR spectroscopy. Segregated phases can be basically excluded.

Gold seems to block the active sites on the surface of MgO since Au-MgO shows only negligible activity. This is ascribed to the propensity of gold to adsorb at step edges of the MgO and thus covering the active sites related to edges. Fe-MgO is more active and selective resulting in higher yield. Further increase in methane conversion and selectivity is achieved by co-doping with Fe and Au. After a formation period with increasing activity, Au-Fe-MgO shows stable activity at the time scale of the present experiment. This behaviour is surprising and novel for alkaline earth metal oxide-based catalysts.

Two types of gold were evidenced based on the catalytic results: In single doped Au-MgO only the step-decorating poisoning effect was found. Through the presence of sub-surface iron species in the co-doped system the edge decorating effect was massively overruled by a beneficial effect of creating structurally stable novel active sites at terraces of the MgO without introducing vacancies that may destabilize the system at longer time on stream. This second gold species apparently arises from a significant gold-support interaction achieved by the strain in the MgO due to iron doping that has been evidenced by electron microscopy. Electronic doping of MgO terraces is also achieved through iron dissolution only, but with significant lower effectiveness.

### References

1. Y. Cui *et al.*, *Angew. Chem. Int. Ed.* **52**, 11385 (2013).
2. P. Schwach *et al.*, *Angew. Chem. Int. Ed.* **52**, 11381 (2013).





## Department of Chemical Physics

### Poster List

- CP 1**      **IV-LEED Studies of  $V_2O_3(0001)$  and  $MoO_3$  on  $Au(111)$**   
F. Feiten, E. Primorac, H. Kuhlenbeck, and H.-J. Freund
- CP 2**      **CO Oxidation on Au Cluster on Biphase  $Fe_2O_3/Pt(111)$**   
H. Qiu, E. Bauer, V. Staemmler, H. Kuhlenbeck, and H.-J. Freund
- CP 3**      **CO Oxidation over Ultra-Thin Films of Transition Metal Oxides**  
Y. Martynova, B.H. Liu, Q. Pan, M. McBriarty, I.M.N. Groot,  
S. Shaikhutdinov, and H.-J. Freund
- CP 4**      **Towards Metal-Supported Ultrathin Films of Zeolites and Clays**  
J.A. Boscoboinik, X. Yu, B. Yang, E. Emmez, S. Shaikhutdinov,  
and H.-J. Freund
- CP 5**      **Resolving the Structure of Glass**  
C. Büchner, L. Lichtenstein, S. Stuckenholtz, M. Heyde, and  
H.-J. Freund
- CP 6**      **Doping 2D Silicates Towards Aluminosilicates**  
C. Büchner, L. Lichtenstein, S. Stuckenholtz, G. Thielsch, M. Heyde,  
and H.-J. Freund
- CP 7**      **Oxygen Activation on Mo-Doped CaO Films**  
Y. Cui, M. Baldofski, J. Sauer, N. Nilius, and H.-J. Freund
- CP 8**      **Ceria Thin Films: A Model System for Reducible Oxides**  
Y. Pan, J. Paier, C. Penschke, J. Sauer, N. Nilius, and H.-J. Freund
- CP 9**      **Impact of Molecular Adsorption on the Quantized Electronic Structure  
of Planar Au Clusters on MgO Thin Films**  
C. Stiehler, Y. Pan, W.-D. Schneider, P. Koskinen, H. Häkkinen, N. Nilius,  
and H.-J. Freund

- CP 10**     **A UHV Compatible W Band EPR Spectrometer for the Characterization of Paramagnetic Surface Species**  
D. Cornu, J. Rucker, W. Hänsel-Ziegler, T. Risse, and H.-J. Freund
- CP 11**     **Auger Parameter Analysis Applied to Oxide-Supported Metal Atoms and Particles**  
W.E. Kaden, Y. Fujimori, M. Sterrer, and H.-J. Freund
- CP 12**     **Surface Science Investigations into Catalyst Preparation**  
R.M. Dowler, F. Ringleb, M. Sterrer, and H.-J. Freund
- CP 13**     **Heats of Adsorption and Surface Reaction for CO and O<sub>2</sub> on Pd Nanoparticles by Single Crystal Adsorption Microcalorimetry**  
M. Peter, S. Adamovski, J. M. Flores-Camacho, J.-H. Fischer-Wolfarth, K.-H. Dostert, C.P. O'Brien, S. Schaueremann, and H.-J. Freund
- CP 14**     **Chemoselective Partial Hydrogenation of Multi-Unsaturated Hydrocarbons over Pd/Fe<sub>3</sub>O<sub>4</sub>/Pt(111) Model Catalysts**  
K.-H. Dostert, C.P. O'Brien, W. Ludwig, A. Savara, S. Schaueremann, and H.-J. Freund
- CP 15**     **Reverse Transformation of Fe<sub>3</sub>O<sub>4</sub> into Fe<sub>2</sub>O<sub>3</sub>**  
F. Genuzio, A. Sala, Th. Schmidt, and H.-J. Freund
- CP 16**     **SMART-II: An Aberration Corrected LEEM/PEEM with Space Charge Compensation and a New Type of Electrostatic Omega Filter**  
F. Genuzio, H. Marchetto, Th. Schmidt, and H.-J. Freund
- CP 17**     **The Control System at the FHI FEL**  
H. Junkes, W. Schöllkopf, and M. Wesemann

## IV-LEED Studies of $V_2O_3(0001)$ and $MoO_3$ on $Au(111)$

F. Feiten, E. Primorac, H. Kuhlenbeck, and H.-J. Freund

$V_2O_3(0001)$  can be grown on  $Au(111)$  and some other substrates. It has been the topic of a number of investigations including structural characterizations, adsorption studies and calculations. Based on vibrational spectroscopy and STM results it was assumed that the as-prepared surface is terminated by a layer of vanadyl groups. This was recently questioned by two studies employing ion scattering based methods<sup>1,2</sup>, which proposed that  $V_2O_3(0001)$  is terminated by the so-called  $O_3$  structure. IV-LEED studies were performed in order to provide additional evidence for one of the two terminations. Recently recorded IV-LEED curves could be fitted by calculated curves with a Pendry R-factor of 0.13, assuming that the surface is vanadyl-terminated, while for termination by the  $O_3$  structure a Pendry R-factor of 0.23 was obtained. These results strongly favour vanadyl termination. While the agreement between computed and experimental curves is good regarding the energies of the structures, it is less favourable regarding the intensities. Therefore the studies are still going on in order to improve the R-factor.

High-quality  $MoO_3$  layers can be grown on  $Au(111)$ . For thicknesses of more than two monolayers these layers assume the structure of  $\alpha-MoO_3(010)$  with a low density of defects. IV-LEED data were recorded for a monolayer which should have the structure of a single layer of  $\alpha-MoO_3(010)$  according to a DFT study<sup>3</sup>. The experimental data could be fitted by calculated curves with a very good Pendry R-factor of 0.05. The structure of the layer is indeed similar to that of a single layer of  $\alpha-MoO_3(010)$ , but the atomic positions are different from those proposed by the DFT study.

For the IV-LEED studies a modified version of the Barbieri/Van Hove Symmetrized Automated LEED package<sup>4</sup> was used, complemented by a search algorithm with a certain degree of global search capability (CMA-ES), which in the general case will enlarge the convergence space compared to the one of Tensor-LEED. The required LEED computations are performed in parallel. For the measurements a channel plate LEED system was employed in order to minimize electron induced reduction of the oxides.

### References

1. A.J. Window, A. Hentz, D.C. Sheppard, G.S. Parkinson, H. Niehus, D. Ahlbrendt, T.C.Q. Noakes, P. Bailey, D.P. Woodruff, *Phys. Rev. Lett* **107**, 016105 (2011).
2. J. Seifert, E. Meyer, H. Winter, H. Kuhlenbeck, *Surf. Sci.* **606**, L41 (2012).
3. S.Y. Quek, M.M. Biener, J. Biener, C.M. Friend, E. Kaxiras, *Surf. Sci.* **577**, L71 (2005).
4. [http://www.icts.hkbu.edu.hk/surfstructinfo/SurfStrucInfo\\_files/leed/leedpack.html](http://www.icts.hkbu.edu.hk/surfstructinfo/SurfStrucInfo_files/leed/leedpack.html)

## CO Oxidation on Au Cluster on Biphase Fe<sub>2</sub>O<sub>3</sub>/Pt(111)

H. Qiu<sup>a</sup>, E. Bauer<sup>b</sup>, V. Staemmler<sup>c</sup>, H. Kuhlenbeck, and H.-J. Freund

Fe<sub>2</sub>O<sub>3</sub> has many technically relevant applications. One class of applications is related to catalysis which was the topic triggering this study. We have investigated the activation of gold clusters on biphase Fe<sub>2</sub>O<sub>3</sub> on Pt(111) for CO oxidation, employing HREELS (vibrational and electronic excitations), PES and TDS. It could be shown that biphase Fe<sub>2</sub>O<sub>3</sub> can be slightly reduced by annealing at 790 K. With a combination of highly surface-sensitive methods and methods which are less sensitive to the surface it could be shown that the reduction takes place below the surface. LEED and water adsorption experiments show that the structure of the surface and the surface defect density are not affected by the reduction process.

Gold clusters on non-reduced biphase Fe<sub>2</sub>O<sub>3</sub> are not active for CO oxidation. CO binds only weakly ( $T_{\text{des}} < 200$  K) to the system and desorbs without reaction. If gold is deposited on reduced biphase Fe<sub>2</sub>O<sub>3</sub>, then dosing of some 100 L of CO leads to a more strongly bound CO species, which is oxidized towards CO<sub>2</sub> at 370 K via consumption of oxygen from the iron oxide substrate. This CO species does not form if there are no gold clusters on the surface and the experimental data indicate that the molecules bind to reduced iron oxide sites.

The activation of the system apparently occurs through an interaction of the gold clusters with the reduced states below the surface. One may speculate about an exchange of charge which activates the perimeters of the clusters such that CO can reduce the oxide.

<sup>a</sup> Technical Institute of Physics & Chemistry, Chinese Academy of Sciences, Xinjiang, China

<sup>b</sup> Lehrstuhl für Theoretische Chemie, Ruhr-Universität Bochum, Bochum, Germany

<sup>c</sup> Department of Physics, Arizona State University, Tempe, USA

## CO Oxidation over Ultra-Thin Films of Transition Metal Oxides

Y. Martynova, B.H. Liu, Q. Pan, M. McBriarty, I.M.N. Groot, S. Shaikhutdinov, and H.-J. Freund

A continuously growing body of experimental and theoretical results indicates that ultrathin oxide films may exhibit interesting catalytic properties in their own right, which may not be observed on thicker films or respective single crystal surfaces. For example, we have recently demonstrated that a thin FeO(111) film grown on Pt(111) is active for CO oxidation in the mbar pressure range at low temperatures where Pt(111) itself is essentially inert<sup>1</sup>.

In continuation of these studies, we have examined here catalytic properties of different ultrathin films of transition metal oxides using the CO oxidation reaction at low temperatures and near-atmospheric pressures as a benchmark. The systems included ultra-thin films of Fe, Mn, Zn, and Ru<sup>2-5</sup>. The observed structure-reactivity relationships suggest that oxygen binding energy in the films plays the decisive role for the CO oxidation reaction under these conditions. The more weakly bound surface oxygen species, the higher the reaction rate.

Although closed ZnO films showed the lowest activity among the films studied, the films only partially covered a Pt(111) support showed by a factor of 5-7 higher reaction rates. Such an enhancement is rationalized in terms of the reactions occurring at the oxide/metal boundary.

In addition, we have performed comparative studies of CO oxidation over ZnO(0001) films supported by Pt(111), Ag(111) and Cu(111). The results allowed to formulate an adequate structural model for elucidating the reaction mechanism on the so called “inverse model catalysts” at technologically relevant conditions.

### References

1. Y. Sun, L. Giordano, J. Goniakowski, M. Lewandowski, Z.-H. Qin, C. Noguera, S. Shaikhutdinov, G. Pacchioni, H.-J. Freund, *Angew. Chem. Intern. Ed.* **49**, 4418 (2010).
2. Y. Martynova, S. Shaikhutdinov, H.-J. Freund, *ChemCatChem* **5**, 2162 (2013).
3. Y. Martynova, B. Yang, X. Yu, J.A. Boscoboinik, S. Shaikhutdinov, H.-J. Freund, *Catal. Lett.* **142**, 657 (2012).
4. Y. Martynova, B.H. Liu, M.E. McBriarty, I.M.N. Groot, M.J. Bedzyk, S. Shaikhutdinov, H.-J. Freund, *J. Catal.* **301**, 227 (2013).
5. Y. Martynova, M. Soldemo, J. Weissenrieder, S. Sachert, S. Polzin, W. Widdra, S. Shaikhutdinov, H.-J. Freund, *Catal. Lett.* DOI: 10.1007/s10562-013-1117-0 (2013).

## Towards Metal-Supported Ultrathin Films of Zeolites and Clays

J.A. Boscoboinik, X. Yu, B. Yang, E. Emmez, S. Shaikhutdinov, and H.-J. Freund

Well-ordered thin silica films are used as model systems for studying of chemical reactions occurring on surfaces of silicates. Recently, our group has reported the preparation of the so-called “bilayer” silica film on Ru(0001)<sup>1</sup>. Further studies revealed a structural complexity and diversity of the silica overlayers on metals. The experimental (LEED, XPS, IRAS, STM) results, complemented by DFT calculations<sup>2</sup>, provided compelling evidence for the formation of a single-layer network of corner-sharing [SiO<sub>4</sub>] tetrahedra, with a SiO<sub>2.5</sub> stoichiometric composition, on Mo(112) and Ru(0001) substrates. However, on Ru(0001) and Pt(111), it is possible to grow a bilayer SiO<sub>2</sub> film that is weakly bound to the metal surface. The results showed that the metal-oxygen bond strength plays the decisive role for the principal structure of the silica film<sup>3</sup>. Metals with high oxygen adsorption energy favor the formation of crystalline monolayer films. Noble metal supports primarily form bilayer SiO<sub>2</sub> sheets. The metals with intermediate energies may form either of the structures. In addition, in contrast to monolayer films, the bilayer films exist in both crystalline and amorphous forms. These two-dimensional silica films provide unique opportunities to directly visualize the atomic structure of vitreous silica.

Besides these well-defined silica films can be used as model supports for metal and oxide clusters, the results opened new challenge for synthesis and surface science studies of structure and reactivity of zeolite-like surfaces and clay minerals. Introduction of Al into the silicate framework allowed us for the first time to fabricate ultrathin aluminosilicate films which upon hydroxylation expose surface resembling that of highly acidic zeolites<sup>4</sup>. Doping a silicate film with Fe resulted in a layered (silica-iron oxide) structure that can be considered as a monolayer of Nontronite (the Fe-rich clay mineral)<sup>5</sup>.

### References

1. D. Löffler, J.J. Uhlrich, M. Baron, B. Yang, X. Yu, L. Lichtenstein, L. Heinke, C. Büchner, M. Heyde, S. Shaikhutdinov, H.-J. Freund, R. Włodarczyk, M. Sierka, J. Sauer, *Phys. Rev Lett.* **105**, 146104 (2010).
2. DFT calculations were performed by the group of J. Sauer at Humboldt University Berlin.
3. X. Yu, B. Yang, J.A. Boscoboinik, S. Shaikhutdinov, H.-J. Freund, *Appl. Phys. Lett.* **100**, 151608 (2012).
4. J.A. Boscoboinik, X. Yu, B. Yang, F.D. Fischer, R. Włodarczyk, M. Sierka, S. Shaikhutdinov, J. Sauer, H.-J. Freund, *Angew. Chem. Int. Ed.* **51**, 6005 (2012).
5. R. Włodarczyk, J. Sauer, X. Yu, J.A. Boscoboinik, B. Yang, S. Shaikhutdinov, H.-J. Freund, *JACS*, accepted (2013).

## Resolving the Structure of Glass

C. Büchner, L. Lichtenstein, S. Stuckenholtz, M. Heyde, and H.-J. Freund

SiO<sub>2</sub> in its vitreous form is commonly known as glass for every-day uses whereas the best known crystalline form - quartz - provides higher mechanical, thermal and chemical stability as well as piezoelectric properties. Despite its many applications, the atomic structure of vitreous or amorphous SiO<sub>2</sub> is not well understood.

A bilayer thin film of SiO<sub>2</sub> on a Ru(0001) support acts as a model system for vitreous and crystalline silicate structures. The ordered and unordered variety can be prepared in an atomically flat film in our UHV setup<sup>1</sup>. With a dual mode atomic force microscopy (AFM) and scanning tunneling microscopy (STM) sensor, we achieved atomic resolution and characterized both morphologies<sup>2</sup>. By using chemically sensitive tip contrasts, direct imaging of the silicon atoms or the oxygen atoms is achievable. Positions and building blocks can be assigned directly from real space images. The tetrahedrally coordinated Si atoms span a network of rings. In the crystalline domain, six-membered rings are the only building blocks, apart from domain boundaries. In the vitreous phase, different ring sizes occur, forming an appearance in perfect agreement to the sketches for Zachariasen's random network theory, postulated in 1932<sup>3</sup>. Pair correlation functions which can be gained from atomic position data, agree well with the corresponding literature data extracted from diffraction on bulk SiO<sub>2</sub>.

By resolving the transition region between an amorphous and a crystalline domain, we were able to directly show how the one smoothly transforms into the other without exhibiting over- or undercoordinated bonds<sup>4</sup>. We investigated the occurring rings sizes perpendicular across the transition region of highly resolved images. Starting from the crystalline phase, at the transition line five- and seven-membered rings mix into the network of six-membered rings, later the less thermodynamically favorable ring sizes set in.

Our dual sensor, providing AFM and STM capabilities, allows us to investigate the mechanisms responsible for contrast formation of the SiO<sub>2</sub> bilayer. Constant height line scans in different distances yield a force map showing the scope of interactions from the attractive to the repulsive interaction regime<sup>5</sup>. In the repulsive force regime, a higher corrugation can be obtained than in the attractive regime at the same absolute value of interaction force. Investigations of this sort can be used to identify suitable parameters for constant height imaging, ultimately gaining complementary scanning probe microscopy information.

### References

1. L. Lichtenstein, C. Büchner, B. Yang, S. Shaikhutdinov, M. Heyde, M. Sierka, R. Włodarczyk, J. Sauer, H.-J. Freund, *Angew. Chem. Int. Ed.* **51**, 404 (2012).
2. L. Lichtenstein, M. Heyde, H.-J. Freund, *JPCC* **116**, 20426 (2012).
3. W.H. Zachariasen, *J.A. Chem. Soc.* **54**, 3841 (1932).
4. L. Lichtenstein, M. Heyde, H.-J. Freund, *Phys. Rev. Lett.* **109**, 106101 (2012).
5. L. Lichtenstein, C. Büchner, S. Stuckenholtz, M. Heyde, H.-J. Freund, *Appl. Phys. Lett.* **100**, 123105 (2012).

## Doping 2D Silicates Towards Aluminosilicates

C. Büchner, L. Lichtenstein, S. Stuckenholtz, G. Thielsch, M. Heyde, and H.-J. Freund

SiO<sub>2</sub> or silica is the main component of the earth's crust and find numerous applications in its crystalline and amorphous (or vitreous) varieties. Porous SiO<sub>2</sub> is employed as support material for catalytically active compounds in heterogeneous catalysis and thin SiO<sub>2</sub> layers are used in semiconductor devices for their insulating properties. In both cases, the atomic structure and its impact on the desired processes is not fully known.

A model system, consisting of a bilayer SiO<sub>2</sub> film on a Ru(0001) support crystal has been developed in our department. Vitreous and crystalline domains have been investigated with our dual mode atomic force microscopy (AFM) and scanning tunneling microscopy (STM) sensor (also see Poster CP 5). Ring size investigations have been carried out on the basis of real space image data. The formation of certain ring combinations can be predicted using a simple model based on statistical and geometrical considerations.

The porosity of this network was employed to adsorb metal atoms, thus creating a model catalyst. Single atoms, deposited at low temperatures, were found to prefer migration through the pores and bind at the substrate-oxide interface. While Pd atoms are able to penetrate either area in the SiO<sub>2</sub> film, selectivity for larger pores was observed for Au atoms, which only penetrated at domain boundaries or the vitreous phase<sup>1</sup>. DFT calculations contributed by our collaborators corroborate these findings.

By varying preparation conditions, Si sites in the film system can be exchanged for aluminum atoms. The resulting aluminosilicate networks are of special interest in catalysis, since they can exhibit catalytically active behavior, and the subgroup of Zeolites with highly regular pores is valued for medical, petrochemical and many other uses. We have studied how different amounts of Al dopant influence the film growth and the ring structures in the network system.

### References

1. W.E. Kaden, C. Büchner, L. Lichtenstein, S. Stuckenholtz, F. Ringleb, M. Heyde, M. Sterrer, H.-J. Freund, L. Giordano, G. Pachioni, C.J. Nelin, P.S. Bagus, under review.

## Oxygen Activation on Mo-Doped CaO Films

Y. Cui, M. Baldowski<sup>a</sup>, J. Sauer<sup>a</sup>, N. Nilius, and H.-J. Freund

Doping is a versatile approach to tailor the physical and chemical properties of oxide materials. The dopants provide new binding sites for molecules if located directly in the surface, but influence the adsorption behaviour also via charge transfer processes over larger distances. In this work, we use a Mo-doped CaO(001) film as model system for a doped oxide and explore its properties with scanning tunnelling microscopy and X-ray photoelectron spectroscopy.

Individual Mo dopants can be detected directly in the near-surface region of the oxide, as they produce characteristic ring features in STM topographic images. The rings come about due to a reversible charging / discharging of the Mo ions in the electric field of the STM tip<sup>1</sup>. Electronically, the dopants trigger a systematic upshift of the Fermi level with respect to the CaO conduction band. This shift manifests the electric activity of the Mo ions that have donor character and act as potential electron source in the lattice. Already small dopant quantities are sufficient to change the growth of gold from the usual 3D to a 2D regime when going from pristine to doped CaO<sup>2</sup>. The crossover of the Au particle shape is driven by an electron transfer from localized Mo 4d-states in the CaO band gap to the Au ad-species, followed by a substantial increase of the metal-oxide adhesion. In a similar manner, activation of oxygen molecules takes place upon adsorption on the doped CaO films<sup>3</sup>. We provide various experimental evidence that spontaneous charge transfer from the dopants leads to the formation of superoxo (O<sub>2</sub><sup>-</sup>) species with high propensity for dissociation on the surface. Co-adsorption of gold atoms and oxygen molecules results in a situation, in which both adsorbates compete for electrons from the Mo ions. Whereas at low O<sub>2</sub> partial pressure, the ad-gold is able to attract most of the excess charges and grows in a 2D fashion, oxygen becomes the dominant electron-trap at higher pressure and neutral 3D Au particles develop on the surface. DFT calculations reveal that Mo<sup>2+</sup> and Mo<sup>3+</sup> ions located in the first ten oxide layers are the relevant donors, while Mo<sup>4+</sup> and higher oxidized species in the lattice play only a minor role.

Our work demonstrates that insertion of donor-type impurity ions opens a powerful pathway for molecular activation even on the flat and defect-free surface of a wide-gap oxide, an idea that was picked up for powder samples as well<sup>4</sup>.

### References

1. Y. Cui, N. Nilius, H.-J. Freund, S. Prada, L. Giordano, G. Pacchioni, *Phys. Rev. B*, in press.
2. X. Shao, S. Prada, L. Giordano, G. Pacchioni, N. Nilius, H.-J. Freund, *Angew. Chem. Int. Ed.* **50**, 11525 (2011).
3. Y. Cui, N. Nilius, X. Shao, M. Baldowski, J. Sauer, H.-J. Freund, *Angew. Chem. Int. Ed.*, in press.
4. P. Schwach, M. Willinger, A. Trunschke, R. Schlögl, *Angew. Chem. Int. Ed.*, in press.

<sup>a</sup> Institut für Chemie, Humboldt-Universität zu Berlin, Unter den Linden 6, 10099 Berlin, Germany

## Ceria Thin Films: A Model System for Reducible Oxides

Y. Pan, J. Paier<sup>a</sup>, C. Penschke<sup>a</sup>, J. Sauer<sup>a</sup>, N. Nilius, and H.-J. Freund

The extraordinary performance of ceria as a support of catalyst relies on its ability to supply oxygen from its lattice when it's reduced. The reduction of ceria starts at the formation of oxygen vacancies at the surface. In order to understand this process and its impact on the supported metal aggregations at atomic level, we have been using low-temperature scanning tunneling microscopy and spectroscopy to study the CeO<sub>2</sub>(111) thin films supported on Ru(0001) substrates. The reduction of CeO<sub>2</sub>(111) is controlled by varying the pressure of O<sub>2</sub> and annealing temperatures during sample preparation. By this means we have successfully prepared the slightly reduced CeO<sub>2</sub>(111) films with mainly subsurface oxygen vacancy and heavily reduced CeO<sub>2</sub>(111) films which contain high concentration of surface oxygen vacancy.

We have deposited small amount of Au on the slightly reduced films at 15K. Two types of Au species are found on the surface<sup>1</sup>. The first one appears as isolated protrusion, while the second type always forms pairs of 8-10 Å distance and develops distinct Sombrero-shapes. The relative abundance of the two species sensitively depends on the reduction state of the surface, i.e. on the density of oxygen vacancies. According to DFT calculations, we assign the two species to Au atoms in two different charge states. While the simple protrusions correspond to a neutral Au that bind to the ideal, defect-free lattice, the paired species are negatively charged and decorate nearby subsurface oxygen-vacancies. The latter type pairs up, as each O-defect generates two Ce<sup>3+</sup> cations that are able to transfer one electron each to two surface Au atoms. The presence of Au pairs therefore provides direct evidence for charge-transfer processes between reduced Ce<sup>3+</sup> ions and electronegative Au species, but also indicates the typical separation of the two Ce<sup>3+</sup> associated to an O vacancy.

### References

1. Y. Pan, N. Nilius, H.-J. Freund, J. Paier, C. Penschke, J. Sauer, Phys. Rev. Lett., accepted.

<sup>a</sup> Humboldt-Universität zu Berlin, Unter den Linden 6, 10099 Berlin, Germany

## Impact of Molecular Adsorption on the Quantized Electronic Structure of Planar Au Clusters on MgO Thin Films

C. Stiehler, Y. Pan, W.-D. Schneider, P. Koskinen<sup>a</sup>, H. Häkkinen<sup>a</sup>,  
N. Nilius, and H.-J. Freund

Electron quantization is a fundamental phenomenon that accompanies the transition from bulk metals to single atoms. The associated opening of gaps at the Fermi level crucially affects various properties of the nanostructures, e.g. its electrical and optical behavior and its performance in catalytic reactions. By using low-temperature scanning tunneling microscopy and spectroscopy, we have investigated the electronic structure of differently shaped planar Au islands grown on MgO/Ag(001) thin films<sup>1,2</sup>.

The experiments were performed on islands with 50-200 atoms, covering the size range of the metal-insulator transition and ensuring the development of quantum well states (QWS) in the nano-gold. The symmetry and energy position of the QWS were mapped in a wide range around the Fermi level and analyzed with the help of a ‘particle-in-a-box’ model and a density-functional-tight-binding approach that accounts for structural disorder in the islands. From the nodal structure and energy position of the QWS, the dispersion relation of the Au electronic states was derived. A parabolic  $E-k$  dependence together with an effective electron mass of  $0.2m_e$  indicated that all QWS emerged from hybridization of the 6sp electronic states in the Au atoms, a conclusion that is in line with the calculations. Based on a statistically relevant number of single-cluster experiments, we derived general conclusions on the size of the HOMO-LUMO gap in the supported Au clusters. We found that not only the atom count is a relevant parameter, but the cluster geometry needs to be considered as well.

In order to investigate the interplay between the quantized electronic structure in the nano-gold and the presence of adsorbates, we have attached small quantities of isophorone ( $C_9H_{14}O$ ) to the surface. We observed preferential adsorption of the molecules at the cluster perimeter and a distinct influence on its electronic structure. The molecular adsorption induced an overall downshift of the Au QWS, indicative for the transfer of charge from the particle electronic system to the adsorbates. Simultaneously, new edge states occurred due to the molecule-gold interaction along the perimeter. Our results allowed us to draw general conclusions on the coupling between unsaturated ketons and noble-metal clusters over non-reducible oxide supports.

### References

1. X. Lin, N. Nilius, H.-J. Freund, M. Walter, P. Frondeliun, H. Honkola, H. Häkkinen, PRL **102**, 206801 (2009).
2. C. Stiehler, Y. Pan, W.-D. Schneider, P. Koskinen, H. Häkkinen, N. Nilius, H.-J. Freund, PRB, in press.

<sup>a</sup> Departments of Physics and Chemistry, Nanoscience Center, University of Jyväskylä, Finland

## A UHV Compatible W Band EPR Spectrometer for the Characterization of Paramagnetic Surface Species

D. Cornu, J. Rucker, W. Hänsel-Ziegler, T. Risse, and H.-J. Freund

### *Introduction*

EPR spectroscopy has proven to be a valuable tool for the characterization of paramagnetic centers at single crystal surfaces such as point defects or metal atoms. Up until now these experiments were performed at X-band (10 GHz). The experiments at X-band sometimes suffer from a lack in spectroscopic resolution as well as intrinsic problems with respect to the implementation of modern pulse spectroscopic techniques. Changing the operating frequency by a factor of 10 (W-band, 94 GHz) would resolve the resolution issues and would provide the prospect to go beyond continuous wave spectroscopy. For the characterization of single crystalline surfaces by EPR at W-band a commercially available spectrometer was integrated into a UHV setup comprising additionally STM, IRAS, LEED, Auger, TPD as well as preparation facilities. This poster will focus on the latest development of the instrumentation and results obtained for paramagnetic defects on single crystalline MgO films.

### *Results*

The heart of the EPR implementation at 94 GHz is a semiconfocal Fabry-Perot resonator consisting of a concave mirror attached to the microwave bridge and a planar mirror being the metal single crystal used as the substrate to grow the oxide films. A crucial point for the reliable measurement of submonolayer quantities of paramagnetic species is a stable and reproducible setup. To this end, the vacuum separation, which was first attempted by a thin quartz window, is a key problem. Therefore, the resonator has been redesigned now using a tiny sapphire windows glued into the coupling hole of the resonator. The coupling of the microwaves is achieved by an antenna made of 60  $\mu\text{m}$  Au wire, which is glued into holes in the sapphire window. This change of the resonator design has improved the reproducibility of the measurements tremendously, such that the signal to background level for two measurements where the sample has been transferred out of the EPR chamber is such that submonolayer quantities are easy to be measured. This design was tested on MgO films grown on Ag(001) single crystal surfaces. Even though we were not yet successful to observe paramagnetic surface centers yet, we see the formation of paramagnetic centers in the bulk of the film. For the first time it was possible to discriminate different signals arising after electron bombardment. These centers can be compared to results obtained by X-band EPR. The W-band EPR signals allow to identify at least three different paramagnetic centers, which are capable to explain the asymmetric line shape observed at X-band.

## Auger Parameter Analysis Applied to Oxide-Supported Metal Atoms and Particles

W. E. Kaden, Y. Fujimori, M. Sterrer, and H.-J. Freund

X-ray photoelectron spectroscopy (XPS) is often used to monitor the “chemical-state” of atoms in the near-surface region of various materials. When using this technique to probe the electronic structure of oxide-supported model-catalysts, interpretation of the results is complicated by the convolution of both initial- and final-state effects, which combine to yield the observable peak binding energy shifts relative to calibration samples. To help disentangle the different contributions, we have made use of Auger parameter analysis for different sample systems.

In the first case<sup>1</sup> we show that isolated Pd and Au atoms present at the bilayer SiO<sub>2</sub>/Ru(0001) interface give rise to negative core-level initial-state shifts, and that these shifts relate to the change in hybridization, rather than the charging, of the surface-bound atoms relative to those in bulk samples.

In the second case<sup>2</sup>, we make use of the Auger parameter to accurately track the changes in the chemical-state of MgO-supported Pd particles as a function of reaction with OH groups to form H<sub>2</sub>. From this, we have been able to correlate the onset of H<sub>2</sub> production with a partial oxidation of the Pd particles, which would not be possible using core-level shifts alone. This helps elaborate upon similar reaction mechanisms proposed previously by others to explain the increased durability of other metals over hydroxylated metal-oxide samples.

### References

1. W.E. Kaden, C. Büchner, L. Lichtenstein, S. Stuckenholz, F. Ringleb, M. Heyde, M. Sterrer, H.-J. Freund, L. Giodano, G. Pacchioni, C.J. Nelin, P.S. Bagus, PRB, submitted.
2. Y. Fujimori, W.E. Kaden, M.A. Brown, B. Roldan Cuenya, M. Sterrer, H.-J. Freund, *Angew. Chem. Int. Ed.*, submitted.

## Surface Science Investigations into Catalyst Preparation

R.M. Dowler, F. Ringleb, M. Sterrer, and H.-J. Freund

We have previously introduced, using Pd on Fe<sub>3</sub>O<sub>4</sub>(111) as a model system, a surface science approach to catalyst preparation that utilizes thin, single-crystalline oxide films as substrates for studying processes such as the adsorption of catalyst precursors from aqueous solutions and the formation of metal nanoparticles during the decomposition of the precursors, during wet-chemical based catalyst preparation procedures. In our recent studies, we have studied the bonding of Pd precursors to the Fe<sub>3</sub>O<sub>4</sub>(111) substrate in more detail and extended this approach also to other sample systems (Au-Fe<sub>3</sub>O<sub>4</sub>(111) and Pd-MgO(100)).

The interaction between aqueous Pd precursors (obtained from PdCl<sub>2</sub>) with Fe<sub>3</sub>O<sub>4</sub>(111) has been investigated for Pd adsorption from a strongly acidic or strongly alkaline precursor solution. By controlled rinsing experiments using either water or blank solutions we were able to reveal the differences in bonding strength and solubility of the adsorbed precursors, their respeciation upon rinsing, and the effect of residual chlorine on the support surface. The latter point is particularly important and it could be shown using STM that the formation of highly dispersed Pd particles requires complete removal of chlorine by water rinsing. Along the same line, we have studied the preparation of Fe<sub>3</sub>O<sub>4</sub>(111)-supported Au particles from strongly alkaline Au<sup>3+</sup> precursor solution, following a preparation procedure introduced by Masatake Haruta to obtain highly active Au catalysts. Our studies on Au-Fe<sub>3</sub>O<sub>4</sub>(111) represent the first successful realization of the preparation of highly dispersed Au nanoparticles on a single-crystalline substrate using Haruta's deposition-precipitation approach.

In addition to Fe<sub>3</sub>O<sub>4</sub>(111), we used MgO(100) thin films as substrate for the preparation of supported Pd particles to investigate the influence of support dissolution during catalyst preparation. Our studies show that the interaction of the Pd precursor with MgO during the period of maximum MgO dissolution rate leads to a stabilization of oxidized Pd species, possibly by incorporation of Pd<sup>2+</sup> in the MgO matrix during the fast MgO dissolution and re-precipitation events. These studies also revealed the strong influence of residual carbon, which was found to enhance the thermal decomposition of Pd precursors.

## Heats of Adsorption and Surface Reaction for CO and O<sub>2</sub> on Pd Nanoparticles by Single Crystal Adsorption Microcalorimetry

M. Peter, S. Adamovski, J.M. Flores-Camacho, J.-H. Fischer-Wolfarth, K.-H. Dostert, C.P. O'Brien, S. Schaueremann, and H.-J. Freund

Establishing the correlation between the energetics of adsorbate-surface interaction and the structural properties of a catalyst is an important fundamental issue and an essential prerequisite for understanding the realistic catalytic processes.

In this project, the particle size dependence of the oxygen adsorption energy on well-defined Pd nanoparticles ranging from 220 to 4800 atoms per particle and on an extended Pd(111) single crystal surface was investigated in a direct calorimetric study<sup>1</sup>. Two microscopic structural parameters were identified to critically control the oxygen binding energy on Pd nanoparticles: the local configuration of the adsorption site and the particle size. The change of the local adsorption environment from a three-fold hollow position on extended Pd (111) single crystal to an edge site of Pd nanoparticles results in a strong increase of oxygen binding energy by about 70 kJ·mol<sup>-1</sup>. The preferential adsorption site of oxygen atoms was investigated spectroscopically by IRAS, using CO as a probe molecule for different adsorption sites, and was found to be at the edges/corners of the Pd clusters. The unexpectedly strong binding energy of oxygen at the particles edges exceeds all literature values of oxygen adsorption energies at stepped single crystal surfaces. On the other hand, if the local configuration of the adsorption site is kept constant (O adsorption at the edges/corners of Pd nanoparticles), the reduction of the cluster size leads to a pronounced decrease of oxygen binding energy from 275 kJ·mol<sup>-1</sup> observed on the large clusters to 205 kJ·mol<sup>-1</sup> measured for the smallest investigated nanoparticles<sup>2</sup>. This latter trend coincides with the particle size dependence of CO adsorption energy on Pd particles obtained earlier. The decreasing adsorption energy observed in our studies with decreasing particle size both for CO and oxygen adsorption is indicative of the general nature of this phenomenon, which might be connected to the theoretically predicted weakening of chemisorptive interaction due to the contraction of the lattice parameter of the Pd cluster. The effects, which both of these structural parameters exhibit on the oxygen adsorption energy, result in counteracting trends – the increase of the binding strength due to adsorption at the low-coordinated surface sites, and the decrease of the adsorption energy due to reduced particle dimensions. In total, the oxygen binding energy turns out to be a convolution of these two trends resulting in a non-monotonous dependence of the oxygen adsorption energy on particle size.

### References

1. J.-H. Fischer-Wolfarth, J.A. Farmer, J.M. Flores-Camacho, A. Genest, I.V. Yudanov, N. Rösch, C.T. Campbell, S. Schaueremann, H.-J. Freund, *Phys. Rev. B* **81**, 241416(R) (2010).
2. M. Peter, J.M. Flores Camacho, S. Adamovski, L.K. Ono, K.-H. Dostert, C.P. O'Brien, B. Roldan Cuenya, S. Schaueremann, H.-J. Freund, *Angew. Chem. Int. Ed.* **52**, 5175 (2013).

## Chemoselective Partial Hydrogenation of Multi-Unsaturated Hydrocarbons over Pd/Fe<sub>3</sub>O<sub>4</sub>/Pt(111) Model Catalysts

K.-H. Dostert, C.P. O'Brien, W. Ludwig, A. Savara, S. Schauer mann, and H.-J. Freund

In this project, detailed kinetic investigations on the complex multi-pathway surface reaction are performed using a combination of pulsed multi-molecular beam techniques with IRAS. The focus of our current research lies on finding the structure-reactivity relationships with the particular emphasis on selectivity and on the elucidation of the reaction mechanism in partial selective hydrogenation of  $\alpha,\beta$ -unsaturated ketones, such as isophorone and acrolein. Pd nanoparticles supported on well-defined model Fe<sub>3</sub>O<sub>4</sub>/Pt(111) oxide film and Pd(111) are used as model surfaces in these studies.

Particularly, it was found that selectivity in partial hydrogenation of acrolein strongly depends on the nature of the catalytic surface and its chemical composition under the reaction conditions. Thus, selective hydrogenation of acrolein to an unsaturated alcohol was observed to proceed on Pd(111) while hydrogenation of the C=C bond resulting in saturated ketone was found to be favored over 6 nm-sized supported Pd nanoparticle. By employing IRAS detection of the surface reaction intermediates with a simultaneous detection of the gas phase product, we were able to directly correlate the product formation with a particular hydrocarbon surface intermediate formed in course of the reaction. Current IRAS investigations point to a crucial role of spectator species, which are formed via initial acrolein decomposition at the early stages of reaction, in governing the selectivity in partial hydrogenation. Our ongoing research is focussed on identifying the key microscopic features governing the selectivity of these processes.

## Reverse Transformation of Fe<sub>3</sub>O<sub>4</sub> into Fe<sub>2</sub>O<sub>3</sub>

F. Genuzio, A. Sala, Th. Schmidt, and H.-J. Freund

Fe<sub>3</sub>O<sub>4</sub> and  $\alpha$ -Fe<sub>2</sub>O<sub>3</sub>, the most common and stable iron oxides phases, are used in a variety of technological applications, ranging from magnetic devices to heterogeneous catalysis<sup>1</sup>. The crystal structure, stoichiometry as well as the surface properties of these iron oxide films can be tailored by special preparation procedures<sup>2-3</sup>. These oxide films are used as a support for chemical active noble metal nano-particles which, in some particular cases, can be encapsulated due to their interaction with the support (SMSI). For instance, Pt nano-particles on Fe<sub>3</sub>O<sub>4</sub> are encapsulated by a FeO skin, which enhances the activity in CO oxidation under reaction conditions<sup>4</sup>. Significant properties (like nano-particle size, density and shape) can be controlled by preparation parameters like amount of deposited material, deposition and annealing temperature.

Our investigations were carried out with the SMART<sup>5-6</sup>, an energy-filtered and aberration corrected LEEM-PEEM microscope, operating at BESSY-II. The high acquisition rate allows *real time* and *in situ* observations of processes like growth, chemical reactions and phase transitions. Here, we studied the growth and the stability of Fe<sub>3</sub>O<sub>4</sub> and  $\alpha$ -Fe<sub>2</sub>O<sub>3</sub> thin films on a Pt(111) substrate, as well as their interaction with Pt nano-particles. We found preparation parameters to grow  $\alpha$ -Fe<sub>2</sub>O<sub>3</sub> films in UHV. Starting from a mixed phase film with domains of Fe<sub>3</sub>O<sub>4</sub> and  $\alpha$ -Fe<sub>2</sub>O<sub>3</sub>, we applied different recipes to transform reversely the two iron oxide structures into each other. As expected from the bulk phase diagram, the annealing in oxygen transforms Fe<sub>3</sub>O<sub>4</sub> into  $\alpha$ -Fe<sub>2</sub>O<sub>3</sub>, with an intermediate phase, compatible with the  $\gamma$ -Fe<sub>2</sub>O<sub>3</sub> structure. Unexpectedly, the annealing of a thin Fe<sub>3</sub>O<sub>4</sub> film on Pt(111) in UHV produces also the  $\alpha$ -Fe<sub>2</sub>O<sub>3</sub> structure, i.e. oxidation, because the Fe diffusion into the Pt bulk is faster than the oxygen desorption. For the reverse process –  $\alpha$ -Fe<sub>2</sub>O<sub>3</sub> reduces to Fe<sub>3</sub>O<sub>4</sub> – Fe was deposited onto the film and subsequently annealed in UHV. The influence of the deposition temperature and oxygen atmosphere on the formation of Pt nano-particles on these iron oxide supports were characterized combining LEEM/LEED with XPEEM.

### References

1. Rochelle M. Cornell, in: *The Iron Oxides - Structure, Properties, Reactions, Occurrences and Uses*, Wiley (2003).
2. W. Weiss and W. Ranke, *Prog. Surf. Sci.* **70**, 1 (2002).
3. A. Sala, H. Marchetto, Z.-H. Qin, S. Shaikhutdinov, Th. Schmidt, H.-J. Freund, *Phys. Rev. B* **86**, 155430 (2012).
4. Z.-H. Qin, M. Lewandowski, Y.-N. Sun, S. Shaikhutdinov, H.-J. Freund, *J. Phys. Chem. C* **112**, 10209–10213 (2008).
5. Th. Schmidt, H. Marchetto, P.L. Levesque, U. Groh, F. Maier, D. Preikszas, P. Hartel, R. Spehr, G. Lilienkamp, W. Engel, R. Fink, E. Bauer, H. Rose, E. Umbach, H.-J. Freund, *Ultramicroscopy* **110**, 1358–1361 (2010).
6. Th. Schmidt, A. Sala, H. Marchetto, E. Umbach, H.-J. Freund, *Ultramicroscopy* **126**, 23–32 (2013).

## SMART-II: An Aberration Corrected LEEM/PEEM with Space Charge Compensation and a New Type of Electrostatic Omega Filter

F. Genuzio, H. Marchetto, Th. Schmidt, and H.-J. Freund

The SMART (Spectro-Microscope with Aberration correction for many Relevant Techniques), built up within a collaboration<sup>1</sup> with the University Würzburg, combines electron spectroscopy with electron microscopy at high lateral and energy resolution to obtain spatially resolved information about the morphology, chemical distribution, work function and structural properties at nano-metric scale. The basic instrument is a Low Energy Electron Microscope (LEEM) and Photo-Emission Electron Microscope (PEEM) equipped with an imaging energy analyzer and an aberration corrector, compensating simultaneously for both spherical and chromatic aberrations. In LEEM, this leads to an outstanding lateral resolution of 2.6 nm<sup>2</sup> which is twice as good as for an uncompensated system. In energy filtered XPEEM we demonstrated a resolution of 18 nm<sup>3</sup>, the best value achieved with this kind of instrument. The clear difference between these two modes is due to space charge effects caused by the pulsed time structure of the exciting synchrotron light. Currently we are setting up a new instrument, called SMART-II, funded by the General Administration of the Max Planck Society. The aims of the new instrument are the improvement of lateral and energy resolution in XPEEM (5nm and 70 meV, respectively) and a routine operation with easy handling. Compared to the optical design of SMART-I, the SMART-II will use (a) intensity reducing apertures and slits to limit the space charge and (b) the magnetic  $\Omega$ -filter will be replaced by an electrostatic analogous instrument which allows to float the analyzer potential on the sample potential, leading to much higher electronic stability.

The new design implements field apertures and high pass filtering slits to cut away electrons outside the field of view and secondary electrons, i.e. electrons not needed for imaging but blurring the image by its charge. The new Omega filter is optimized for both, lateral and energy resolution better than 2 nm and 100 meV, respectively. The majority of the possible second order aberrations are already compensated by the intrinsic symmetry. Half of the residual aberrations can be fully corrected by multipoles; the effect of the others is reduced to values smaller than of the unavoidable third order aberrations by an adequate design for the deceleration-acceleration optics in combination with optimized pass energy.

### References

1. R. Fink, M.R. Weiß, E. Umbach, D. Preikszas, H. Rose, R. Spehr, P. Hartel, W. Engel, R. Degenhardt, H. Kuhlenbeck, R. Wichtendahl, W. Erlebach, K. Ihmann, R. Schlögl, H.-J. Freund, A.M. Bradshaw, G. Lilienkamp, Th. Schmidt, E. Bauer, G. Benner, *J. Electr. Spectrosc. Rel. Phen.* **84**, 231 (1997).
2. Th. Schmidt, H. Marchetto, P.L. Levesque, U. Groh, F. Maier, D. Preikszas, P. Hartel, R. Spehr, G. Lilienkamp, W. Engel, R. Fink, E. Bauer, H. Rose, E. Umbach, H.-J. Freund, *Ultramicroscopy* **110**, 1358 (2010).
3. Th. Schmidt, A. Sala, H. Marchetto, E. Umbach, H.-J. Freund, *Ultramicroscopy* **126**, 23–32 (2013).

## The Control System at the FHI FEL

H. Junkes, W. Schöllkopf, and M. Wesemann

A new mid-infrared FEL has been commissioned at the FHI. It will be used for spectroscopic investigations of molecules, clusters, nanoparticles and surfaces. The oscillator FEL is operated with 15 – 50 MeV electrons from a normal-conducting S-band linac equipped with a gridded thermionic gun and a chicane for controlled bunch compression. First lasing was observed on February 14<sup>th</sup>, 2012<sup>1</sup>.

The Experimental Physics and Industrial Control System (EPICS) software framework was chosen to build the control system for this facility. The industrial utility control system used at the FHI is integrated using BACnet/IP. Graphical operator and user interfaces are based on the Control System Studio (CSS) package.

The EPICS channel archiver, an electronic logbook, a web based monitoring tool, and a gateway complete the installation.

This poster presents design and implementation aspects of some crucial controls such as cavity stabilization, IR beam diagnostic, and the machine protection system.

### References

1. W. Schöllkopf *et al.*, First Lasing of the IR FEL at the Fritz-Haber-Institut, Berlin MOOB01, Proc. FEL2012, <http://accelconf.web.cern.ch/AccelConf/FEL2012>







## Department of Molecular Physics

### Poster List

- MP 1**     **IR<sup>2</sup>MS<sup>2</sup> Spectroscopy of the Protonated Water Clusters H<sup>+</sup>(H<sub>2</sub>O)<sub>5-10</sub>**  
Matias R. Fagiani, Nadja Heine, Mariana Rossi, Volker Blum, and  
Knut R. Asmis
- MP 2**     **Structure and Microhydration of Atmospherically-Relevant Clusters**  
Nadja Heine, Torsten Wende, Claudia Brieger, Tara I. Yacovitch,  
Daniel M. Neumark, and Knut R. Asmis
- MP 3**     **Vibrational Spectroscopy and Surface Chemistry of Gold Clusters –  
The Activation of Molecular Oxygen**  
Alex P. Woodham, Gerard Meijer, and André Fielicke
- MP 4**     **Structures of Metal Clusters from Far-Infrared Spectroscopy**  
Christian Kerpel, Marko Haertelt, Dan J. Harding, John Bowlan,  
Gerard Meijer, and André Fielicke
- MP 5**     **Protein Structure in the Gas Phase – The Influence of Side-Chain  
Microsolvation**  
Stephan Warnke, Gert von Helden, and Kevin Pagel
- MP 6**     **Embedding Mass-to-Charge Selected - Biomolecular Ions in Helium  
Droplets**  
Doo-Sik Ahn, Isabel Gonzalez-Florez, and Gert von Helden
- MP 7**     **Structural Analysis of Complex Carbohydrates using Ion Mobility-  
Mass Spectrometry**  
Johanna Hofmann, Waldemar Hoffmann, Weston B. Struwe,  
David J. Harvey, Pauline M. Rudd, and Kevin Pagel
- MP 8**     **Quantum Reflection and Diffraction of Helium Atoms, Dimers, and  
Trimers from Micro-Structured Surfaces**  
Bum Suk Zhao, Weiqing Zhang, and Wieland Schöllkopf
- MP 9**     **Shedding Far-Off Resonant Light on Polar Paramagnetic Molecules**  
Ketan Sharma and Bretislav Friedrich

- MP 10 Imaging Molecules on a Chip**  
Silvio Marx, David Adu Smith, Mark J. Abel, Thomas Zehentbauer, Gerard Meijer, and Gabriele Santambrogio
- MP 11 Driving Vibrational Transitions on a Chip**  
Silvio Marx, David Adu Smith, Mark J. Abel, Thomas Zehentbauer, Gerard Meijer, and Gabriele Santambrogio
- MP 12 Low Energy Collisions of Ortho- and Para-H<sub>2</sub> with Stark Decelerated OH Radicals**  
H. Christian Schewe, Xingan Wang, Moritz Kirste, Nicolas Vanhaecke, Quianli Ma, Jacek Klos, Millard H. Alexander, Paul J. Dagdigian, Liesbeth M. C. Janssen, Koos B. Gubbels, Gerrit C. Groenenboom, Ad van der Avoird, Kopin Liu, Sebastiaan Y. T. van de Meerakker, and Gerard Meijer
- MP 13 Magnetic Transition Dipole Moments in the OH A-X System**  
H. Christian Schewe, Nicolas Vanhaecke, Xingan Wang, Boris G. Sartakov, Robert W. Field, and Gerard Meijer
- MP 14 Advanced Switching Schemes in a Stark Decelerator**  
Dongdong Zhang, Nicolas Vanhaecke, and Gerard Meijer
- MP 15 The IR and THz FEL at the FHI: Current Status and Prospects**  
Wieland Schöllkopf, Sandy Gewinner, Wolfgang Erlebach, Georg Heyne, Heinz Junkes, Andreas Liedke, Gerard Meijer, Viktor Platschkowski, Patrick Schlecht, Gert von Helden, and Weiqing Zhang

## IR<sup>2</sup>MS<sup>2</sup> Spectroscopy of the Protonated Water Clusters H<sup>+</sup>(H<sub>2</sub>O)<sub>5-10</sub>

Matias R. Fagiani, Nadja Heine, Mariana Rossi<sup>a</sup>, Volker Blum<sup>b</sup>, and Knut R. Asmis<sup>c</sup>

Understanding how protons are hydrated remains an important and challenging research area. The anomalously high proton mobility of water, for example, can be explained by a periodic isomerization between the Eigen and Zundel binding motifs, H<sub>3</sub>O<sup>+</sup>(aq) and H<sub>5</sub>O<sub>2</sub><sup>+</sup>(aq), respectively, even though the detailed mechanism is considerably more complex and not completely understood<sup>1</sup>. These rapidly interconverting structures from the condensed phase can be stabilized, isolated and studied in the gas phase in the form of protonated water clusters.

Infrared photodissociation (IRPD) spectroscopy serves as a powerful tool for studying the structure of gas phase clusters. However, the contribution of multiple isomers to the IRPD spectrum can complicate the assignment. Here, we report results<sup>2</sup> on the isomer-selective infrared/infrared double resonance (IR<sup>2</sup>MS<sup>2</sup>) spectroscopy<sup>3</sup> of the protonated water clusters H<sup>+</sup>(H<sub>2</sub>O)<sub>n</sub>·H<sub>2</sub> with  $n = 5-10$ . IR<sup>2</sup>MS<sup>2</sup> spectra are measured in the spectral region of the free and hydrogen-bonded OH-stretching vibrations (2880-3850 cm<sup>-1</sup>) and assigned on the basis of a comparison to the results of electronic structure calculations.

For  $n = 5-7$  we find evidence for one, two and four isomers, respectively. In contrast, for the bigger clusters,  $n = 8-10$ , the IR<sup>2</sup>MS<sup>2</sup> spectra measured at different excitation wavelengths look nearly identical, suggesting either the presence of only a single isomer or dynamically interconverting species. For the protonated water hexamer, we demonstrate that combining the radiation from an IR free electron laser with that from a widely tunable table-top IR laser allows extending this technique across nearly the complete IR region (260-3900 cm<sup>-1</sup>)<sup>2</sup>. *Ab initio* molecular dynamics calculations qualitatively recover the IR spectra of the two isomers for  $n=6$  and allow attributing the increased width of IR bands associated with hydrogen-bonded moieties to anharmonicities rather than excited state lifetime broadening. Characteristic hydrogen-bond stretching bands are observed, for the first time, below 400 cm<sup>-1</sup>.

### References

1. C. Knight, G.A. Voth, *Acc. Chem. Res.* **45**, 101 (2011).
2. N. Heine, M.R. Fagiani, M. Rossi, T. Wende, G. Berden, V. Blum, K.R. Asmis, *J. Am. Chem. Soc.* **135**, 8266 (2013).
3. B.M. Elliot, R.A. Relph, J.R. Roscioli, J.C. Bopp, G.H. Gardenier, T.L. Guasco, M.A. Johnson, *J. Chem. Phys.* **129**, 094303 (2008).

<sup>a</sup> Present address: Physical and Theoretical Chemistry Lab., Oxford, UK

<sup>b</sup> Present address: MEMS Dept., Duke University, Durham, USA

<sup>c</sup> Visiting Professor at the Wilhelm-Ostwald-Institut, Universität Leipzig, Germany

## Structure and Microhydration of Atmospherically-Relevant Clusters

Nadja Heine, Torsten Wende<sup>a</sup>, Claudia Brieger<sup>b</sup>, Tara I. Yacovitch<sup>c</sup>,  
Daniel M. Neumark<sup>c,d</sup>, and Knut R. Asmis<sup>e</sup>

Inorganic acids, their conjugate base anions and water are abundant species in the atmosphere, where they play a critical role in aerosol formation. In the process of ion-induced nucleation negative ions serve as more effective nucleation sites than positive ions. Among the most abundant anions in the troposphere and stratosphere are nitrate ( $\text{NO}_3^-$ ) and bisulfate ( $\text{HSO}_4^-$ ), as well as mixed clusters of both species with and without water<sup>1</sup>.

In order to understand the early steps of aerosol nucleation and gain insight in the microscopic structure of the bulk, we use infrared multiple photon dissociation (IRMPD) spectroscopy<sup>2</sup> ( $550\text{-}1800\text{ cm}^{-1}$ ) in combination with electronic structure calculations as a structural probe for mass-selected nitrate/nitric acid/water-, sulfate/sulfuric acid/water- and mixed-clusters. Moreover, we focus on how the structure evolves with increasing microsolvation<sup>2,3,4</sup>. The key results of our studies are: (i) Hydrogen dinitrate contains very strong hydrogen bonds and an equally shared proton ( $\text{NO}_3^- \cdots \text{H}^+ \cdots \text{NO}_3^-$ ). This arrangement is not disrupted by addition of a single water molecule. Only additional solvation with either more water or acid molecules induces the asymmetric  $\text{NO}_3^- \cdots \text{HNO}_3$  motif. (ii)  $\text{HSO}_4^-(\text{H}_2\text{SO}_4)_m(\text{H}_2\text{O})_n$  clusters show a recurring triply hydrogen-bound configuration, which can be disrupted by the incorporation of water. (iii) Charge localization depends intimately on the size and composition of the clusters and cannot be reliably predicted from known gas phase acidities. We also studied the phenomena of "IRMPD transparent" bands by comparing the IRMPD spectra of the bare and messenger-tagged cluster anions.

### References

1. H. Heitmann, F. Arnold, *Nature* **306**, 747 (1983).
2. K.R. Asmis, D.M. Neumark, *Accts. Chem. Res.* **45**, 43-52 (2012).
3. T.I. Yacovitch, N. Heine, C. Brieger, T. Wende, C. Hock, D.M. Neumark, K.R. Asmis, *J. Chem. Phys.* **136**, 1 (2012).
4. T.I. Yacovitch, N. Heine, C. Brieger, T. Wende, C. Hock, D.M. Neumark, K.R. Asmis, *J. Chem. Phys. A* **117**, 7081 (2013).
5. N. Heine, T.I. Yacovitch, F. Schubert, C. Brieger, D.M. Neumark, K.R. Asmis, submitted.

<sup>a</sup> Present address: Physical and Theoretical Chemistry Laboratory, Oxford, UK

<sup>b</sup> Present address: Institut für Chemie, Freie Universität Berlin, Germany

<sup>c</sup> Department of Chemistry, University of California, Berkeley, USA

<sup>d</sup> Chemical Science Division, Lawrence Berkeley National Laboratory, Berkeley, USA

<sup>e</sup> Visiting Professor at the Wilhelm-Ostwald-Institut, Universität Leipzig, Germany

## Vibrational Spectroscopy and Surface Chemistry of Gold Clusters – The Activation of Molecular Oxygen

Alex P. Woodham<sup>a</sup>, Gerard Meijer<sup>b</sup>, and André Fielicke<sup>a</sup>

Gold nano-particles remain at the forefront of cluster research due to their unexpected catalytic properties, in stark contrast to the nobility of the bulk phase. This unexpected reactivity includes highly selective and low temperature oxidation reactions using molecular oxygen as a feedstock, many of which have great potential for industrially relevant transformations. Despite the potential of these systems questions still remain as to the origin of this reactivity in the nano-scale: how does the cluster structure relate to reactivity? What are the active species? And how does the gold cluster activate molecular oxygen? Vibrational spectroscopy of gas-phase clusters, both with and without reactive ligands, can provide insight into the cluster structure and behaviour of adsorbed species.

In these studies clusters are investigated size-selectively using infrared multiple photon dissociation spectroscopy. As this requires an intense and tunable (far-) IR source, the experiments are performed with the Free Electron Laser for Infrared eXperiments “FELIX” formerly at the FOM Institute for Plasmaphysics in Nieuwegen, the Netherlands. The wide tunability of this light source allows access to the characteristic vibrational modes of cluster-bound ligands in the mid-IR as well as internal vibrational modes of the metal clusters in the far-IR. Similar experiments will be possible in collaboration with the new FHI-FEL.

In order to better understand the structure-activity relationships of these gold clusters we have investigated the bare neutral clusters by far-IR spectroscopy. Recent molecular dynamics simulations performed by L. Ghiringhelli (FHI, Theory dept.) find that the finite temperature behaviour is essential for understanding the experimental spectra and emphasize the role of fluctuonality in gold clusters<sup>1</sup>. For the oxygen complexes we confirm the assumption that the size dependent reactivity of the anionic clusters is based on electron transfer and formation of superoxo ( $O_2^-$ ) moieties for the even-sized clusters whilst the odd-sized clusters are unreactive<sup>2</sup>. Surprisingly we also find the neutral clusters to bind  $O_2$ <sup>3</sup>. They show a reversed reactivity pattern with the odd-sized clusters forming the superoxo species, driven by a charge transfer and structural rearrangement of the gold cluster core. Lastly the cationic clusters, which were previously thought to be unreactive, are found to form three different oxygen charge states, i.e. superoxo (-1), physisorbed (0), and dioxygenyl (+1), even within a single cluster complex composition.

### References

1. L.M. Ghiringhelli, P. Gruene, J.T. Lyon, D.M. Rayner, G. Meijer, A. Fielicke, M. Scheffler, *New J. Phys.* **15**, 083003 (2013).
2. A.P. Woodham, G. Meijer, A. Fielicke, *Angew. Chem. Int. Ed.* **51**, 4444 (2012).
3. A.P. Woodham, G. Meijer, A. Fielicke, *J. Am. Chem. Soc.* **135**, 1727 (2013).

<sup>a</sup> Present address: Technische Universität Berlin, Germany

<sup>b</sup> Present address: Institute for Molecules and Materials, Radboud University Nijmegen, NL

## Structures of Metal Clusters from Far-Infrared Spectroscopy

Christian Kerpel, Marko Haertelt<sup>a</sup>, Dan J. Harding<sup>b</sup>, John Bowlan<sup>c</sup>, Gerard Meijer<sup>d</sup>,  
and André Fielicke<sup>e</sup>

In the recent years our group has established different variants of far-infrared spectroscopy as tools to unravel the structures of gas-phase metal clusters in different charge states, including neutral species. The experimental findings provide valuable reference data for the evaluation of quantum chemical methods, which still have difficulties with reliable prediction of cluster structures and their related properties from first principles. This is a particular problem for metals with partially filled d (transition metals) or f (lanthanides, actinides) shells, or for heavy elements, like gold, where relativistic effects are significant. The vibrational fundamentals of metal clusters are typically found below 400 cm<sup>-1</sup>, i.e. in the far-IR, where free electron lasers are the only intense and tunable laser sources. We investigate the clusters size-selectively in the gas phase and measure the spectra via multiple photon excitation using the Free Electron Laser for Infrared eXperiments (FELIX).

For obtaining vibrational spectra of metal clusters IR multiple photon dissociation (IR-MPD) of weakly bound messenger complexes is the most widely used technique to date. Recently we focussed on the investigation of platinum group metals, in particular platinum<sup>1</sup>, ruthenium, and iridium. While Pt clusters show polytetrahedral close-packed structures similar to many other transition metals, Ru and Ir appear to follow a cubic growth motif for small sizes. Such structures had been theoretically predicted before for these metals as in the case of Rh, but for the latter we have identified this to be an artefact of using GGA-DFT<sup>2</sup>. Further studies have focussed on lanthanide clusters, in particular of terbium. Density functional theory calculations using a 4f-in-core effective core potential (ECP) accurately reproduce the experimental far-IR spectra. From this, we conclude that the bonding in Tb clusters is through the interactions between the 5d and 6s electrons, and that the 4f electrons have only an indirect effect on the cluster structures<sup>3</sup>.

In collaboration with the group of Joost Bakker from the FELIX facility (now RU Nijmegen, NL) we have performed proof-of-principle studies to obtain far-IR spectra of anionic metal clusters using resonance enhanced multiple photon electron detachment (IR-REMPED)<sup>4</sup> and for neutral metal clusters using resonance enhanced multiple photon ionization (IR-REMPI). These experiments made use of the Free Electron Laser for IntraCavity Experiments (FELICE)<sup>5</sup>.

### References

1. D.J. Harding, C. Kerpel, D.M. Rayner, A. Fielicke, *J. Chem. Phys.* **136**, 211103 (2012).
2. D.J. Harding *et al.*, *J. Chem. Phys.* **132**, 011101 (2010).
3. J. Bowlan, D.J. Harding, J. Jalink, A. Kirilyuk, G. Meijer, A. Fielicke, *J. Chem. Phys.* **138**, 031102 (2013).
4. M. Haertelt *et al.*, *J. Phys. Chem. Lett.* **2**, 1720 (2011).
5. V.J.F. Lapoutre, M. Haertelt, G. Meijer, A. Fielicke, J.M. Bakker, *J. Chem. Phys.* **139**, 121101 (2013).

<sup>a</sup> Present address: Joint Attosecond Science Laboratory, NRC Canada, Ottawa, Canada

<sup>b</sup> Present address: Max-Planck-Institut für biophysikalische Chemie, Göttingen, Germany

<sup>c</sup> Present address: Los Alamos National Laboratory, USA

<sup>d</sup> Present address: Institute for Molecules and Materials, Radboud University Nijmegen, NL

<sup>e</sup> Present address: Technische Universität Berlin, Germany

## Protein Structure in the Gas Phase – The Influence of Side-Chain Microsolvation

Stephan Warnke, Gert von Helden, and Kevin Pagel

Today, the gentle electrospray ionization (ESI) technique is routinely applied to characterize peptides and proteins via mass spectrometry (MS). However, how much of a protein's structures is retained after ionization and transfer into the gas phase is still a subject of intense debate. In this context, it is widely accepted that the repulsion between equal charges is one of the major determinants for the protein's structure: low charge states typically adopt compact, native-like conformations, while high charge states tend to unfold into more extended structures. Intermediate charge states can show a multitude of coexisting conformations<sup>1</sup>. Here we show that not only the direct effect of Coulomb repulsions but also the much more subtle coordination of charged side chains onto the protein backbone can severely influence the conformation of proteins in the absence of solvent<sup>2</sup>.

In order to study the impact of side chain-backbone coordination on the structure of a gas-phase protein, we non-covalently attached different amounts of crown ether (18-crown-6) to the charged lysine side chains of the proteins cytochrome C and ubiquitin. The resulting complexes were analyzed via ion mobility mass spectrometry (IM-MS) using a commercially available traveling wave IM-MS instrument (Waters, Synapt G2-S). Absolute collision cross sections (CCSs) were determined using an in-house constructed drift tube IM-MS instrument that follows a design described elsewhere<sup>3</sup>.

Independent of the charge state, complexes with up to five crown ethers attached to the lysine side chains of the proteins can be observed at gentle ionization conditions. Ions of low as well as high charge states essentially retain their shape upon crown ether complexation. Intermediate charge states, however, undergo an unusually distinct compaction upon binding to the crown ether, which has not been observed previously. This rather counter-intuitive effect can be explained to occur predominantly as a result of two competing types of microsolvation. In the absence of crown ether, protonated side chains rapidly collapse onto the protein backbone where they coordinate to carbonyl groups that are otherwise involved in vital H-bonds. Once the side chain is solvated with crown ether, however, the structure-forming H-bonds are less affected and a more compact, native-like conformation is retained. In a more general context this implies that crown ethers can solvate gas-phase proteins in a similar way to water molecules in the condensed phase.

### References

1. K.B. Shelimov, D.E. Clemmer, R.R. Hudgins, M.F. Jarrold, *J. Am. Chem. Soc.* **119**, 2240-2248 (1997).
2. S. Warnke, G. von Helden, K. Pagel, *J. Am. Chem. Soc.* **135**, 1177-1180 (2013).
3. P.R. Kemper, N.F. Dupuis, M.T. Bowers, *Int. J. Mass Spectrom.* **287**, 46-57 (2009).

## Embedding Mass-to-Charge Selected – Biomolecular Ions in Helium Droplets

Doo-Sik Ahn, Isabel Gonzalez-Florez, and Gert von Helden

Helium droplets are an ideal matrix for the spectroscopic study of molecules as they are isothermal at 0.38 K, superfluid, only weakly interacting with the embedded species and transparent over a wide spectral range from the far IR to the deep UV<sup>1</sup>. Here, we report on the use of liquid helium droplets as nano-cryostats for the investigation of mass-to-charge selected biomolecular ions.

In the experiment<sup>2</sup>, the biological molecules are brought into the gas phase via electrospray ionization. They are mass-to-charge selected using a quadrupole mass spectrometer and then stored and accumulated in a linear ion trap. Helium droplets generated with a pulsed nozzle are allowed to traverse the trap and pick-up ions and since the kinetic energy of the droplets is larger than the longitudinal trapping potential, ion doped helium droplets can escape the trap. Further downstream, the charged droplets are investigated and detected.

In our experiment, we have successfully doped helium droplets with mass-to-charge selected ions ranging from single amino acids to proteins as large as Cytochrome C. We have characterized the size of the doped droplets, which range from tens of thousands to several million helium atoms<sup>3</sup> and depend on the nozzle temperature, the size of the captured ion, and the ion's charge state. Additionally, we have investigated the UV spectra of several biological ions doped inside helium droplets by monitoring ions that are ejected from the droplet after photon absorption. The measured electronic spectra of different molecules ranging from the amino acids tryptophan and tyrosine to larger species as the peptide gramicidin, both in its monomeric and dimeric form will be discussed.

In the near future, the experimental setup will be used in combination with the FHI free electron laser to measure IR spectra of biological molecules embedded in helium droplets and investigate its conformational landscape.

### References

1. J.P. Toennies, A.F. Vilesov, *Angew. Chem. Int. Ed.* **43**, 2622-2648 (2004).
2. F. Bierau, P. Kupser, G. Meijer, G. von Helden, *Phys. Rev. Lett.* **105**, 133402 (2010).
3. F. Filsinger, D.S. Ahn, G. Meijer, G. von Helden, *Phys. Chem. Chem. Phys.* **14**, 13370-13377 (2012).

## Structural Analysis of Complex Carbohydrates using Ion Mobility-Mass Spectrometry

Johanna Hofmann, Waldemar Hoffmann, Weston B. Struwe<sup>a</sup>, David J. Harvey<sup>b</sup>,  
Pauline M. Rudd<sup>a</sup>, and Kevin Pagel

Carbohydrates are of great importance for a variety of biological functions. They can, for example, be linked to proteins as post-translational modifications or exist as free oligosaccharides in complex biological matrices such as milk. Oligosaccharides consist of monosaccharide building blocks, which often exhibit an identical atomic composition and mass. Moreover, each building block has multiple reactive sites at which new glycosidic bonds can be formed. As a consequence a variety of structurally different isomers can be expected for the resulting oligomers. This, in combination with the fact that the stereochemistry can vary at each linkage, makes carbohydrates extraordinarily complex and difficult to analyze using established techniques.

Today, most of the approaches to analyze complex carbohydrates are based on mass spectrometry (MS). Due to their diversity, however, it is often not possible to distinguish isomers simply by measuring the mass. A promising route to overcome this limitation is to implement an additional separation step using ion mobility spectrometry (IMS). Here, the ions are guided by a weak electric field through a cell filled with inert neutral gas, where they are separated according to their collision cross section (CCS).

With the introduction of the first commercial available travelling wave IM-MS instruments in 2005 the technique became readily available to more biological focused scientists. However, due to the inhomogeneous electric field utilized to propel the ions, it is necessary to carefully calibrate these instruments with references of the same molecular identity as the analyte to estimate CCSs. For complex carbohydrates such a calibration framework did not exist so far. Recently, we reported a calibration protocol using native glycans which were released of commercially available glycoproteins using an easy to follow procedure<sup>1</sup>. Currently, we are developing this approach further using negatively charged glycans and carbohydrate based polymers as calibrants.

To improve the separation of isobaric carbohydrates we further investigated the impact of the ionization mode and the adduct ion on their gas-phase structure. These experiments revealed that protonated and deprotonated ions can differ considerably in their CCS, while their size remains virtually identical when they are coordinated to alkali ions. Applied to real life samples these results were used to separate isobaric milk sugars, which are indistinguishable using established techniques. Furthermore, we tested an approach to improve the separation capability of IMS in which differences in gas-phase stability of the investigated ions are used to discriminate certain components of a complex mixture during separation<sup>2</sup>.

In the future, we are aiming to develop carbohydrate IMS technologies further to the high throughput level. This includes an automation of the calibration procedure and workflow as well as the compilation of a comprehensive carbohydrate CCS database.

### References

1. K. Pagel, D.J. Harvey, *Anal. Chem.* **85**, 5138-5145 (2013).
2. W. Hoffman, J. Hofmann, K. Pagel, *J. Am. Soc. Mass Spectrom.*, in press.

<sup>a</sup> Oxford Glycobiology Institute, Oxford, UK

<sup>b</sup> National Institute for Bioprocessing Research and Training (NIBRT), Dublin, IE

## Quantum Reflection and Diffraction of Helium Atoms, Dimers, and Trimers from Micro-Structured Surfaces

Bum Suk Zhao<sup>a</sup>, Weiqing Zhang, and Wieland Schöllkopf

In this project we investigate scattering of helium atoms and small clusters from various micro-structured surfaces. For grazing incidence conditions we observe “*quantum reflection*” of atoms and clusters tens of nanometer above the actual surface. In a classical description of surface scattering the attractive atom-surface van der Waals interaction accelerates the particle towards the surface, thereby increasing the particle’s kinetic energy by the potential well depth. The particle then smashes into the repulsive branch of the potential, which effectively forms a hard-wall from where the particle is scattered back. For helium dimers and trimers scattering off a surface, this process will inevitably lead to break-up of the fragile bonds, because the binding energies of 100 neV and 10  $\mu$ eV, respectively, are orders of magnitude less than the  $\sim$ 10 meV surface-potential well depth. Therefore, our observation of non-destructive scattering of He<sub>2</sub> and He<sub>3</sub> from a reflection grating<sup>1</sup> cannot be understood within classical mechanics.

It can, however, be readily explained by quantum reflection at the attractive van der Waals potential branch. The latter represents a steep slope on a length scale set by the de Broglie wavelength of the incident particle. If the particle’s velocity towards the surface (i.e. its velocity component perpendicular to the surface) is sufficiently small, the de Broglie wavelength gets sufficiently large, and the steep slope, effectively, appears as a potential step. According to quantum mechanics a particle’s wave-function is reflected at a potential step with a non-vanishing probability which even approaches unity in the limit of zero velocity. In our experiment a minute velocity component perpendicular to the surface is achieved by grazing-incidence angles of  $\sim$ 1 mrad. As a result, dimers and trimers are, with some probability, reflected without getting exposed to the surface-induced bond-breaking forces of the potential-well region.

To observe quantum reflection of He<sub>2</sub> and He<sub>3</sub> we have been using a commercial plane-ruled blazed reflection grating. The grating is mounted in the conical diffraction configuration, where the grating grooves are nearly (within a small azimuth angle) parallel to the scattering plane. As a result, varying the azimuth angle and the incidence angle allows for an adjustment of both, the effective grating period and the effective blaze angle. We have demonstrated that adjusting these two parameters allows to increase the resolution and the diffraction-peak intensities of He<sub>2</sub> and He<sub>3</sub><sup>2</sup>. This has allowed us to observe emerging beam resonances, which we had previously seen for helium atom diffraction, for He<sub>2</sub> as well<sup>3</sup>. Given the unusual fragility and size of He<sub>2</sub> this is a surprising observation, because emerging beam resonances imply multiple surface scattering and the existence of an evanescent wave of helium dimers.

### References

1. B. S. Zhao, G. Meijer, W. Schöllkopf, *Science* **331**, 892 (2011).
2. B. S. Zhao, W. Zhang, W. Schöllkopf, *Mol. Phys.* **111**, 1772 (2013).
3. B. S. Zhao, W. Zhang, W. Schöllkopf, submitted.

<sup>a</sup> Present address: Ulsan National Institute of Science and Technology, Ulsan, Republic of Korea

## Shedding Far-Off Resonant Light on Polar Paramagnetic Molecules

Ketan Sharma and Bretislav Friedrich

Interactions with external electric, magnetic or optical fields provide the chief means to manipulate the rotational and translational motion of neutral gas-phase molecules. The pursuit of such means is a leading frontier of chemical/molecular physics. Among recent developments are new methods to control the orientation and/or alignment of molecules as well as methods to deflect and focus their translational motion and to achieve molecular trapping. The importance of orientation comes also to light in novel applications such as time-resolved photoelectron dynamics, diffraction-from-within, separation of photodissociation products, deracemization, high-order harmonic generation and orbital imaging, quantum simulation or quantum computing<sup>1</sup>. All methods to manipulate molecular rotation and translation via external fields rely on the ability to create directional states of molecules. This is because only in directional states are the molecular body-fixed multipole moments ‘available’ in the laboratory frame where they can be acted upon by space-fixed fields.

A far-off resonant optical field hybridizes the rotational states of an anisotropic molecule and aligns the axis of the molecule along the field’s polarization vector. The hybrid states occur as tunneling doublets of opposite parity whose splitting can be arbitrarily diminished by raising the intensity of the optical field. For polar molecules, such quasi-degenerate doublet states can be efficiently coupled either by the electric dipole interaction with a superimposed electrostatic field<sup>2</sup> or by the electric dipole-dipole interaction arising between a pair of polar molecules<sup>3</sup>. The dual-field combination gives rise to an amplification effect that occurs for any polar molecule, as only an anisotropic polarizability, along with a permanent dipole moment, is required. This is always available in polar molecules. Thus, for a number of molecules in their rotational ground state, a very weak static electric field can convert second-order alignment by a laser into a strong first-order orientation that projects up to 90% of the body-fixed dipole moment on the static field direction.

For molecules that are paramagnetic apart from being polar, a superimposed magnetic field causes a further parity-conserving hybridization of the molecule’s rotational states. Such hybridization doubles the number of the tunneling doublets by splitting states that differ in the sign of the projection of the angular momentum on the common direction of the optical, electric, and magnetic fields. The triple field-combination not only offers a high efficiency and flexibility in amplifying molecular orientation but is also of fundamental theoretical interest, as monodromy and quantum chaos lurk behind the combined-field effects<sup>4</sup>.

### References

1. J.H. Nielsen, H. Stapelfeldt, J. Küpper, B. Friedrich, J.J. Omiste, R. Gonzales-Ferez, *Phys. Rev. Lett.* **108**, 193001 (2013).
2. M. Härtelt, B. Friedrich, *J. Chem. Phys.* **128**, 224313 (2008).
3. M. Leshchko, B. Friedrich, *Mol. Phys.* **110**, 1873 (2012).
4. D.A. Sadovskii, B.I. Zhilinski, *Mol. Phys.* **104**, 2595 (2006).

## Imaging Molecules on a Chip

Silvio Marx, David Adu Smith, Mark J. Abel, Thomas Zehentbauer, Gerard Meijer<sup>a</sup>,  
and Gabriele Santambrogio

For physics, the atom chip and ion chip have been employed in fields as diverse as quantum computation, many-body non-equilibrium physics, and gravitational sensing. For chemistry, the lab-on-a-chip shrinks the pipettes, beakers and test tubes of a modern lab onto a microchip-sized substrate, with applications from the international space station to anti-terrorism. The molecule chip, however, is currently in its infancy, but promises a marriage between fundamental quantum physics and the richness of the chemical world. A particular advantage of using molecules instead of atoms on a chip is that they can be coupled to photons over a wider range of frequencies due to their rotational and vibrational degrees of freedom. Moreover, for chemists the molecule chip offers the prospect of extending the control of molecular concentrations and interactions to the level of single molecules with the accuracy in interaction energy reduced to the mK scale and below.

A major obstacle that has delayed the development of the molecule chip arises from the extreme richness of molecules' internal degrees of freedom. As molecules generally lack a closed two-level system, efficient laser cooling and detection using absorption or laser-induced fluorescence is in general not possible. In recent years, we have demonstrated that one can exploit the cooling provided by a supersonic expansion and load the chip with cold molecules directly extracted from a molecular beam<sup>1</sup>. Here we show on-chip molecule detection, adding the final fundamental component to the molecule chip. We use resonant-enhanced multi-photon ionization, which is quantum state selective, can be saturated with a few mJ/mm<sup>2</sup> of laser light for most molecules, is intrinsically background-free, and is of general applicability. While in the simplest implementation of our detection scheme one would simply count the ions, we take the further step of using ion optics to create a time-resolved spatial image of the molecules<sup>2</sup>.

We resolve the spatial structure of an array of microtraps on our chip and use this resolution to analyze the phase space distribution of the molecules. We subsequently show a sequence of time-resolved snapshots from a ballistic expansion, in a similar fashion as for the time-of-flight imaging of atomic ensembles on atom chips. Moreover, we use this new detection method to investigate the effect of phase space manipulation sequences applied to the trapped molecules. Among other things, we observe experimentally that the time scale on which a velocity cooling manipulation can take place is comparable with the trap frequency.

### References

1. S.A. Meek, H. Conrad, G. Meijer, *New J. Phys.* **11**, 055024 (2009).
2. S. Marx, D. Adu Smith, M.J. Abel, T. Zehentbauer, G. Meijer, G. Santambrogio, *Phys. Rev. Lett.* accepted (2013).

<sup>a</sup> Present address: Institute for Molecules and Materials, Radboud University Nijmegen, NL

## Driving Vibrational Transitions on a Chip

Silvio Marx, David Adu Smith, Mark J. Abel, Thomas Zehentbauer, Gerard Meijer<sup>a</sup>,  
and Gabriele Santambrogio

Many of the advantages of magnetic atom chips could also be realized with electric molecule chips: the miniaturization of field structures enables the creation of large field gradients, i.e. large forces and tight potential wells for polar molecules<sup>1</sup>. Molecules on a chip can be coupled to photons over a wider range of frequencies than atoms. Polar molecules have a dense set of rotational transitions in the sub-THz (mm-wave) region of the spectrum, the fundamental molecular vibrational transitions are in the mid-infrared, whereas their overtones and combination modes extend into the near-infrared range. Being able to induce a transition to another internal quantum state in the molecule is particularly interesting when the molecule remains trapped in the final state as well.

At the 16<sup>th</sup> meeting of the Fachbeirat, we showed that transitions between adjacent rotational levels within a given electronic and vibrational state can be induced above the surface of the molecule chip<sup>2</sup>. We now present new experiments demonstrating that vibrational transitions can also be induced in molecules on a chip, with the breakthrough here being that vibrational transitions can be pumped without having to switch off the traps (as is the case for rotational transitions). The system we use is the carbon monoxide molecule, prepared with a pulsed laser in a single rotational level ( $J = 1$ ) of its first electronically excited, metastable state ( $a^3\Pi_1, v = 0$ ). The  $v = 1 \leftarrow v = 0$  vibrational transitions are induced using pulsed IR radiation around 5.9  $\mu\text{m}$ . Molecules pumped into selected rotational levels of the vibrationally excited  $v = 1$  state are subsequently state-selectively detected through ionization using another pulsed laser system. Besides demonstrating that pulsed IR radiation can be coupled to molecules that are trapped less than 50 microns above the chip without damaging the chip, we show that we can accurately model the transitions in the inhomogeneous and rotating field of our microtraps and that we can address selectively a subset of molecules from our traps by choosing the appropriate polarization of the laser beam<sup>3</sup>.

In addition we will also present one of our future projects, a new type of chip-based ring decelerator. This is the product of a collaborative effort to tackle two main challenges: first, the physical realization of the 3d structure, which was overcome in collaboration with the Fraunhofer-Institut für Zuverlässigkeit und Mikrointegration in Berlin and the Halbleiterlabor der Max-Planck-Gesellschaft in München. The second challenge was the realization of the required high-voltage amplifier, which we built here at the FHI and for which we hired an electronic engineer. We now have a linear amplifier (1:600) with a bandwidth of 0 to 600 kHz, an output 1200 Vpp and a total harmonic distortion of -43dB.

### References

1. S.A. Meek, H. Conrad, G. Meijer, *Science* **324**, 1699 (2009).
2. G. Santambrogio, S.A. Meek, M.J. Abel, L.M. Duffy, G. Meijer, *Chem. Phys. Chem.* **12**, 1799 (2011).
3. M.J. Abel, S. Marx, G. Meijer, G. Santambrogio, *Mol. Phys.* **110**, 1829 (2012).

<sup>a</sup> Present address: Institute for Molecules and Materials, Radboud University Nijmegen, NL

## Low Energy Collisions of Ortho- and Para-H<sub>2</sub> with Stark Decelerated OH Radicals

H. Christian Schewe, Xingan Wang, Moritz Kirste, Nicolas Vanhaecke, Quianli Ma<sup>a</sup>,  
Jacek Klos<sup>b</sup>, Millard H. Alexander<sup>b</sup>, Paul J. Dagdigian<sup>a</sup>, Liesbeth M.C. Janssen<sup>c</sup>,  
Koos B. Gubbels<sup>c</sup>, Gerrit C. Groenenboom<sup>c</sup>, Ad van der Avoird<sup>c</sup>, Kopin Liu<sup>d</sup>,  
Sebastiaan Y.T. van de Meerakker<sup>e</sup>, and Gerard Meijer<sup>e</sup>

The crossed beam technique is a mature and important experimental method to investigate molecular interactions, which can lead to energy transfer or chemical reactions. The Stark deceleration technique yields control over both the internal and external degrees of freedom of polar molecules in a molecular beam. The combination of these techniques opens up comprehensive investigations of molecular scattering processes as a function of the collision energy with a high energy resolution<sup>1,2</sup>.

Results on inelastic scattering of ortho- or para-H<sub>2</sub> with Stark-decelerated OH( $X^2\Pi_{3/2}$ ,  $J=3/2, f$ ) at collision energies between 40-150 cm<sup>-1</sup> are presented. The main difference in the scattering process of ortho- and para-H<sub>2</sub> is seen in the relative cross sections, originating from the different multipole interactions involved. Special care is taken to determine the ratio of ortho- and para-H<sub>2</sub> molecules and their quantum state population in the experimentally achievable mixtures. Absolute cross sections of ortho-H<sub>2</sub> or para-H<sub>2</sub> colliding with OH are calculated and compared with our experimental data. In addition, very high energy resolution has been achieved in our crossed beam experiment, allowing us to observe sharp thresholds and resonance effects.

### References

1. J. Gilijamse *et al.*, *Science* **313**, 1617 (2006).
2. M. Kirste *et al.*, *Science* **338**, 1060 (2012).

<sup>a</sup> Department of Chemistry, The Johns Hopkins University, Baltimore, Maryland, USA

<sup>b</sup> Department of Chemistry and Biochemistry and Institute for Physical Science and Technology, University of Maryland, Baltimore, USA

<sup>c</sup> Institute of Theoretical Chemistry, Radboud University Nijmegen, NL

<sup>d</sup> Institute of Atomic and Molecular Sciences (IAMS), Academia Sinica, Taipei, TW

<sup>e</sup> Present address: Institute for Molecules and Materials, Radboud University Nijmegen, NL

## Magnetic Transition Dipole Moments in the OH A-X System

H. Christian Schewe, Nicolas Vanhaecke, Xingan Wang, Boris G. Sartakov<sup>a</sup>,  
Robert W. Field<sup>b</sup>, and Gerard Meijer<sup>c</sup>

The hydroxyl radical plays a central role in many fields of physics and chemistry. It is one of the most abundant radicals in the atmosphere, and one of the most extensively studied molecular species to date.

Magnetic dipole allowed transitions (M1) are orders of magnitude weaker than the corresponding electric dipole allowed transitions (E1). They are therefore usually neglected in quantitative measurements of quantum state populations (e.g. via laser induced fluorescence). Nevertheless, in experiments requiring very sensitive state-selective detection, this approximation could lead to significant misinterpretation of the data, as discussed in ref<sup>1</sup>. This is the case for instance in fully state-resolved collision experiments.

We investigate magnetic dipole allowed transitions in the A-X system of OH. We apply a low external static electric field, which slightly mixes parities and allows E1 transitions to contribute to the signal. This contribution is comparable to that of the M1 transitions. Therefore both types of transitions are detected in a single experimental protocol, which allows us to compare the magnetic transition dipole moment to the electric transition dipole moment with unprecedented accuracy<sup>2</sup>.

### References

1. M. Kirste, X. Wang, G. Meijer, K.B. Gubbels, A. van der Avoird *et al.*, *J. Chem. Phys.* **137**, 101102 (2012).
2. H. Ch. Schewe *et al.*, submitted.

<sup>a</sup> General Physics Institute RAS, Moscow, Russia

<sup>b</sup> Department of Chemistry, Massachusetts Institute of Technology, Cambridge, USA

<sup>c</sup> Present address: Institute for Molecules and Materials, Radboud University Nijmegen, NL

## Advanced Switching Schemes in a Stark Decelerator

Dongdong Zhang, Nicolas Vanhaecke, and Gerard Meijer<sup>a</sup>

Over the last two decades, several techniques have been developed and have demonstrated their ability to produce slow, cold molecular ensembles. Among them, Stark deceleration has become one of the most successful and versatile methods to study and use cold molecules<sup>1,2</sup>.

In this work we revisit the operation of the Stark decelerator and present a new, large class of switching schemes, which can be optimized at will, depending of the required properties of the decelerated beam<sup>3</sup>. We show that after optimization, these schemes substantially improve the efficiency of the decelerator at both low and high velocities, which are relevant for trapping experiments and collision experiments, respectively. Both experimental and simulation results show that these new modes of operation outperform the schemes which have hitherto been in use. These new modes of operation could potentially be extended to other deceleration techniques.

### References

1. H.L. Bethlem, G. Berden, G. Meijer, Phys. Rev. Lett. **83**, 1558 (1999).
2. S.Y.T. van de Meerakker, H.L. Bethlem, N. Vanhaecke, G. Meijer, Chem. Rev. **112**, 4828 (2012).
3. D. Zhang, N. Vanhaecke, G. Meijer, submitted.

<sup>a</sup> Present address: Institute for Molecules and Materials, Radboud University Nijmegen, NL

## The IR and THz FEL at the FHI: Current Status and Prospects

Wieland Schöllkopf, Sandy Gewinner, Wolfgang Erlebach, Georg Heyne, Heinz Junkes, Andreas Liedke, Gerard Meijer<sup>a</sup>, Viktor Platschkowski, Patrick Schlecht, Gert von Helden, and Weiqing Zhang<sup>b</sup>

The IR and THz free-electron laser at the FHI has been designed for applications in gas-phase spectroscopy of (bio-)molecules, clusters, and nano-particles, as well as in surface science<sup>1-3</sup>. To cover the wavelength range of interest from about 4 to 500  $\mu\text{m}$ , the system design includes a normal conducting S-band linac providing electrons of up to 50 MeV energy to either of two oscillator FEL's; one for the mid-infrared (MIR) and one for the far-infrared (FIR). The MIR FEL with a design wavelength range from 4 to almost 50  $\mu\text{m}$  has been commissioned and is operational. The FIR FEL has not yet been built. With its design wavelength range from  $\sim 40$  to  $\sim 500$   $\mu\text{m}$  it can cover the FIR and THz regime.

The electron accelerator consists of a thermionic gridded electron gun, a subharmonic buncher and two S-band (2.99 GHz) standing-wave copper structures. It was designed to meet challenging e-beam specifications, including a final energy adjustable in the range of 15 to 50 MeV, low longitudinal emittance ( $< 50$  keV-psec) and transverse emittance ( $< 20 \pi$  mm-mrad), at more than 200 pC bunch charge with a micro pulse repetition rate of 1 GHz and a macro pulse length of up to 15  $\mu\text{s}$ . Two isochronous achromatic 90-degree bends deliver the beam to the undulator and to a beam dump. The accelerator and electron-beam transport system was designed and installed by Advanced Energy Systems, Inc.

The MIR undulator (STI Optronics, Inc.) is of the hybrid-magnet type made with radiation resistant NdFeB magnets. With a period of 40 mm it covers the undulator  $K$ -parameter range from 0.5 to almost 1.6<sup>4</sup>. The 5.4-m-long MIR-FEL cavity (Bestec GmbH) is formed by two gold-coated concave copper mirrors with an active feedback length stabilization. First lasing of this system was achieved at a wavelength of 16  $\mu\text{m}$  with an electron energy of 28 MeV in 2012<sup>1</sup>, and in 2013 we have observed pulse energies as large as 130 mJ<sup>5</sup>. The first six IR user beam lines, transferring the FEL pulses by  $\sim 25$  m to the user setups in the experimental hall, have been completed. As of fall 2013 first experiments investigating transition-metal carbonyl clusters, aluminium oxide clusters and conformer-selected biomolecules in the gas phase as well as peptides embedded in superfluid helium nano-droplets have been carried out. In addition, characterizing the FEL-radiation (measurements of pulse energy, pulse lengths, spectral width, etc.) is ongoing.

### References

1. W. Schöllkopf *et al.*, MOOB01, Proceedings of the 34th FEL Conference 2012.
2. W. Schöllkopf *et al.*, TUPB30, Proceedings of the 33rd FEL Conference 2011.
3. H. Bluem *et al.*, WEOC04, Proceedings of the 34th FEL Conference 2012.
4. S.C. Gottschalk *et al.*, THPD13, Proceedings of the 34th FEL Conference 2012.
5. W. Schöllkopf *et al.*, WEPSO62, Proceedings of the 35th FEL Conference 2013.

<sup>a</sup> Present address: Institute for Molecules and Materials, Radboud University Nijmegen, NL

<sup>b</sup> Present address: Dalian Institute of Chemical Physics, Chinese Academy of Sciences, Dalian, China







## Department of Physical Chemistry

### Poster List

- PC 1**      **Voltage-dependent charge transport through single molecular wires**  
Matthias Koch and Leonhard Grill
- PC 2**      **On-surface polymerization: Catalytically active sites and hierarchical covalent linking**  
Alex Saywell, Leif Lafferentz, and Leonhard Grill
- PC 3**      **Precise control of intramolecular H-atom transfer reactions**  
Takashi Kumagai, Janina Ladenthin, Felix Hanke, Sylwester Gawinkowski, John Sharp, Konstantinos Kotsis, Jacek Waluk, Mats Persson, and Leonhard Grill
- PC 4**      **Towards local vibrational spectroscopy at the single molecule level: Development of UHV-TERS**  
Takashi Kumagai, Philip Schambach, Bruno Pettinger, and Martin Wolf
- PC 5**      **Understanding catalytic hydrocarbon conversion on Ru(0001)**  
R. Kramer Campen, Harald Kirsch, Xunhua Zhao, Sergey Levchenko, and Martin Wolf
- PC 6**      **Elementary processes in water/ $\alpha$ -Al<sub>2</sub>O<sub>3</sub>(0001) interaction: Dissociative adsorption and surface reconstruction**  
Harald Kirsch, Yujin Tong, Jonas Wirth, Peter Saalfrank, Martin Wolf, and R. Kramer Campen
- PC 7**      **Structure and dynamics of the non-hydrogen bonded free OH at the air/water interface**  
Yujin Tong, Cho-Shuen Hsieh, Mischa Bonn, Ana Vila Verde, and R. Kramer Campen
- PC 8**      **Single-molecule kinetic modelling of tryptophan synthase**  
Dimitri Loutchko and Alexander S. Mikhailov
- PC 9**      **Short- and long-term coverage dynamics during the electrooxidation of small organic molecules**  
Melke A. Nascimento, Raphael Nagao, Markus Eiswirth, and Hamilton Varela

- PC 10**     **Tuning the coupling of excess charges to polar environments**  
Daniel Wegkamp, Michael Meyer, Clemens Richter, Amilcare Iacomino, Alejandro Pérez Paz, Julia Stähler, Uwe Bovensiepen, Angel Rubio, and Martin Wolf
- PC 11**     **Electronic structure and ultrafast exciton formation dynamics at the ZnO(10-10) surface**  
Jan-Christoph Deinert, Daniel Wegkamp, Michael Meyer, Clemens Richter, Martin Wolf, and Julia Stähler
- PC 12**     **Electronic and structural dynamics across the insulator to metal transition in VO<sub>2</sub>**  
Laura Foglia, Simon Wall, Daniel Wegkamp, Julia Stähler, and Martin Wolf
- PC 13**     **Ultrafast spin dynamics launched by transport of optically excited spin-polarized hot carriers in epitaxial metallic multilayers**  
Alexey Melnikov, Alexandr Alekhin, Damian Bürstel, Detlef Diesing, Tim Wehling, Ivan Rungger, Maria Stamenova, Stefano Sanvito, and Uwe Bovensiepen
- PC 14**     **Ultrafast demagnetization of a ferrimagnet driven by selective phonon excitation**  
Sebastian Mährlein, Ilie Radu, Martin Wolf, and Tobias Kampfrath
- PC 15**     **Probing ultrafast charge carrier dynamics in topological insulators by terahertz spectroscopy**  
Lukas Braun, Gregor Mussler, Luca Perfetti, Martin Wolf, and Tobias Kampfrath
- PC 16**     **New schemes for the generation and application of terahertz electromagnetic pulses**  
Mohsen Sajadi, Martin Wolf, and Tobias Kampfrath
- PC 17**     **First experiments on lattice dynamics in solids using the FHI IR-FEL**  
Alexander Paarmann, Marc Herzog, and Martin Wolf
- PC 18**     **Time- and angle-resolved photoemission spectroscopy of charge and spin density wave materials**  
Claude Monney, Christopher Nicholson, Michele Puppini, Yunpei Deng, Laurenz Rettig, Uwe Bovensiepen, Robert Carley, Martin Weinelt, Ralph Ernstorfer, and Martin Wolf

**PC 19 High-repetition rate ultrashort XUV source for time-and angle-resolved photoemission and molecular orbital mapping**

Michele Puppin, Yunpei Deng, Niels Schröter, Claude Monney, Christopher Nicholson, Marcel Krenz, Oliver Prochnow, Jan Matyschok, Thomas Binhammer, Uwe Morgner, Martin Wolf, and Ralph Ernstorfer

**Max-Planck-Research-Group – Ralph Ernstorfer**

**Poster**

**PC 20 Femtosecond low-energy electron diffraction and imaging**

Melanie Müller, Sebastian Lüneburg, Alexander Paarmann, and Ralph Ernstorfer

**PC 21 Non-equilibrium structural dynamics and phase transitions in solids**

Lutz Waldecker, Simon Wall, Roman Bertoni, Elisabeth Bothschafter, Eeuwe Zijlstra, Martin Garcia, Alexander Paarmann, and Ralph Ernstorfer

**PC 22 Observation and control of electron motion in solids on the attosecond time scale**

Ralph Ernstorfer, Stefan Neppl, Agustin Schiffrin, Tim Paasch-Colberg, Peter Feulner, Reinhard Kienberger, and Ferenc Krausz



## Voltage-dependent charge transport through single molecular wires

Matthias Koch and Leonhard Grill

Charge transport through molecules is an important property that is relevant in processes in chemistry and nature. On the other hand, molecular wires should play a key role in future applications in molecular nanotechnology as they should transport the current between functional units. It is also known that the conductance needs to be measured in single molecules, as assemblies of molecules can behave differently. However, such measurements are very challenging as it is necessary to know the precise configuration of the junction between the electrodes for a detailed understanding.

Here, we have pulled single molecules from a surface by using the tip of a scanning tunneling microscope (STM), thus allowing to measure the conductance of a single molecular as a continuous function of its length and distance from the surface in real time<sup>1</sup>. The molecule can furthermore be characterized before and after the pulling process by STM imaging and spectroscopy. In this work, we have used our expertise in on-surface polymerization<sup>2</sup> for the formation of graphene nanoribbons on a Au(111) surface, following a recipe of Fasel and co-workers<sup>3</sup>. By pulling individual graphene nanoribbons off the surface with the STM tip, the current decay along the polymer, which is the key property for the characterization of charge transport, can be determined. This was done for various electron energies, thus for the first time correlating the conductance of individual molecules with their electronic structure<sup>4</sup>. It was found that the charge transport is most efficient if the electron energy matches either the HOMO or the LUMO level, which are both delocalized along the ribbon. The results are in very good agreement with theoretical calculations by Francisco Ample and Christian Joachim (IMRE institute, Singapore). In very extreme pulling configurations, even pseudo-ballistic transport is found where the electric current does not decay with the polymer length, as predicted by theory.

### References

1. L. Lafferentz, F. Ample, H. Yu, S. Hecht, C. Joachim, and L. Grill, *Science* **323**, 1193 (2009).
2. L. Grill, M. Dyer, L. Lafferentz, M. Persson, M.V. Peters, and S. Hecht, *Nature Nanotech.* **2**, 687 (2007).
3. J. Cai, P. Ruffieux, R. Jaafar, M. Bierl, T. Braun, S. Blankenburg, M. Muoth, A.P. Seitsonen, M. Saleh, X. Feng, K. Müller, and R. Fasel, *Nature* **466**, 470 (2010).
4. M. Koch, F. Ample, C. Joachim, and L. Grill, *Nature Nanotech.* **7**, 713 (2012).

## On-surface polymerization: Catalytically active sites and hierarchical covalent linking

Alex Saywell, Leif Lafferentz, and Leonhard Grill

The controlled assembly of molecules on surfaces is of general interest to understand intermolecular interactions that are key in many processes in nature. The confinement in two dimensions is in this regard advantageous as it allows direct imaging by scanning probe techniques. On the other hand, such structures might act as functional entities that are constructed in a “bottom-up” manner. While many supramolecular structures have been reported in the last two decades, stabilized by rather weak interactions, the covalent linking of molecules by on-surface polymerization<sup>1</sup> is advantageous as it provides more stable connections and the potential for efficient charge transport between the molecules.

A key question in the field of on-surface polymerization is the precise location of the molecular activation process, i.e. the dissociation of Br substituents from the molecular building blocks, on the surface. By comparing flat and stepped gold surfaces, the kink sites at the step edges can be precisely identified as the catalytically active sites because there is a high preference for activation for that side of the molecules that points towards these sites<sup>2</sup>. After heating the surface, the step edges cause polymers that run parallel over the surface, which is of interest for a pre-alignment in future polymerization processes.

On the other hand, the complexity of the molecular structures produced by on-surface polymerization is quite limited because all approaches so far relied on a single step process, thus resulting in very simple structures. Here we show how the on-surface polymerization method can be extended by introducing a hierarchical growth process that is based on a sequential activation of the molecular building blocks<sup>3</sup>. The molecular building blocks *trans*-Br<sub>2</sub>I<sub>2</sub>TPP molecules exhibit two types of halogen substituents that are dissociated from the molecular core at different temperatures, resulting in a programmed reactivity. Also copolymers could be formed by mixing two different building blocks and the resulting structure could not be formed in a conventional single-step linking process.

### References

1. L. Grill, M. Dyer, L. Lafferentz, M. Persson, M.V. Peters, and S. Hecht, *Nature Nanotech.* **2**, 687 (2007).
2. A. Saywell, J. Schwarz, S. Hecht, and L. Grill, *Angew. Chem. Int. Ed.* **51**, 5096 (2012).
3. L. Lafferentz, V. Eberhardt, C. Dri, C. Africh, G. Comelli, F. Esch, S. Hecht, and L. Grill, *Nature Chem.* **4**, 215 (2012).

## Precise control of intramolecular H-atom transfer reactions

Takashi Kumagai, Janina Ladenthin, Felix Hanke<sup>a</sup>, Sylwester Gawinkowski<sup>b</sup>, John Sharp<sup>a</sup>, Konstantinos Kotsis<sup>a</sup>, Jacek Waluk<sup>b</sup>, Mats Persson<sup>a</sup>, and Leonhard Grill

Molecular processes and functions are fundamental in nature and also play a key role for molecular devices in future nanotechnology. In condensed phase the atomic-scale environment of individual molecules is known to have a significant impact on the potential energy landscape of chemical processes. However, such influences are very challenging to examine at the level of individual molecules in experiments and the effects of nearby single atoms or molecules on chemical reactions have never been studied so far. We achieved the precise control of intramolecular hydrogen transfer reactions (i.e. tautomerization) in single porphycene molecules using low-temperature scanning tunneling microscopy (STM)<sup>1</sup>.

Single porphycene molecules adsorbed on a Cu(110) surface were imaged by STM at 5 K and found to have only *cis* configuration in which the inner H-atoms located on one side in the cavity. The *cis-cis* tautomerization is induced either by STM via inelastic electron tunneling process at 5 K or thermal activation at elevated temperatures. We found that the tautomerization can be precisely tuned up and down by placing a Cu adatom nearby a molecule. The adatom is controlled using the STM manipulation. The results demonstrate the high sensitivity of the tautomerization process not only to the presence but also to the exact position of individual adatoms with respect to the molecule. Furthermore, we extended our study to molecular assemblies where even the hydrogen arrangement in the cavity of a neighboring molecule influences the reaction, causing positive and negative cooperative effects. On the other hand, porphycene molecules have both of a thermodynamically stable *trans* and meta-stable *cis* configuration on a Cu(111) surface and the conversion from *trans* to *cis* configuration can be induced by electric field. We found that the conversion efficiency depends on the coverage of molecules and it becomes higher in lower coverages, suggesting that intermolecular interaction has a significant impact on the process. The backward process from *cis* to *trans* is rarely induced by electric field, while it can be switched back to *trans* by heating the surface up to about 30 K<sup>2</sup>. Our results highlight the importance of controlling the environment of molecules with atomic precision and demonstrate the potential to regulate a single-molecule function.

### References

1. T. Kumagai, F. Hanke, S. Gawinkowski, J. Sharp, K. Kotsis, J. Waluk, M. Persson, and L. Grill. Nature Chemistry (in press).
2. T. Kumagai, F. Hanke, S. Gawinkowski, J. Sharp, K. Kotsis, J. Waluk, M. Persson, and L. Grill, Phys. Rev. Lett. (in press).

<sup>a</sup> Surface Science Research Centre and Department of Chemistry, University of Liverpool, United Kingdom

<sup>b</sup> Institute of Physical Chemistry, Polish Academy of Sciences, Warszawa, Poland

## Towards local vibrational spectroscopy at the single molecule level: Development of UHV-TERS

Takashi Kumagai, Philip Schambach, Bruno Pettinger, and Martin Wolf

Simultaneous measurement of molecular vibration and local electric or geometric structure of adsorbates would provide fruitful insight into physical and chemical processes on surfaces. Tip-enhanced Raman spectroscopy (TERS) is a variant of surface-enhanced Raman spectroscopy and it is one of the promising techniques to probe simultaneously the adsorbate local vibrations and adsorption site. In TERS an STM tip is employed to generate a plasmonic field to enhance the Raman scattering of adsorbates as well as imaging their local structure with sub-molecular resolution. We have developed TERS for ultra-high vacuum (UHV) conditions to achieve a local spectroscopy and this approach bears a great potential for local characterization of adsorbates at the single-molecule level<sup>1,2</sup>.

Currently we extend our previous studies on C<sub>60</sub>/Au(111) to graphene nano-ribbon (GNR) on the Au(111) surface. GNR are an attractive material in nano-science and technology<sup>3</sup>. To realize the full potential of GNR, structural control at the atomic scale is required and the local defect and deformation of GNR is expected to have a significant impact on its electronic properties, which is of fundamental importance in device applications. The local structure and defect of GNR can be directly observed by low-temperature STM<sup>4</sup>, but the structural details still remain an open question. We will address this question with our home-built UHV-TERS system.

### References

1. B. Pettinger, P. Schambach, C.J. Villagómez, and N. Scott, *Annual Review of Physical Chemistry* **63**, 379-399 (2012).
2. R. Zhang, Y. Zhang, Z.C. Dong, S. Jiang, C. Zhang, L.G. Chen, L. Zhang, Y. Liao, J. Aizpurua, Y. Luo, J.L. Jang, and J.G. Hou, *Nature* **498**, 82 (2013).
3. J. Cai, P. Ruffieux, R. Jaafar, M. Bierl, T. Braun, S. Blankenburg, M. Muoth, A.P. Seitsonen, M. Saleh, X. Feng, K. Müller, and R. Fasel, *Nature* **466**, 470 (2013).
4. M. Koch, F. Ample, C. Joachim, and L. Grill, *Nature Nanotech.* **7**, 713 (2012).

## Understanding catalytic hydrocarbon conversion on Ru(0001)

R. Kramer Campen, Harald Kirsch, Xunhua Zhao, Sergey Levchenko, and Martin Wolf

Interaction of CH<sub>4</sub> and C<sub>2</sub>H<sub>4</sub> with a metal (oxide) surface may lead to the stepwise decomposition of these species and the formation of higher hydrocarbons. Understanding the details of these processes is critical to engineering desired chemistry: e.g. the oxidative coupling of CH<sub>4</sub> to form C<sub>x</sub>H<sub>y</sub> or the steam reforming of CH<sub>4</sub>. Here we characterize the interaction of CH<sub>4</sub> and C<sub>2</sub>H<sub>4</sub> with the Ru(0001) surface under UHV conditions using temperature programmed desorption and vibrational sum frequency spectroscopy as a function of surface temperature (100 – 500 K) and carbon coverage. To overcome the dissociation barrier of CH<sub>4</sub> on Ru(0001) we employ a molecular beam source with CH<sub>4</sub> seeded in He or H<sub>2</sub>. By probing the CH spectral response (2800 – 3100 cm<sup>-1</sup>) during the decomposition of both CH<sub>4</sub> and C<sub>2</sub>H<sub>4</sub> we track the relative stability of all one and two carbon, CH containing species as a function of sample temperature and, for CH<sub>4</sub> dosing, carrier gas.

We find that both the relative stabilities and rates of interconversion of the various hydrocarbon species present in this system vary strongly as a function of surface coverage and sample temperature. Intriguingly, we observe a dramatic change in reactivity above 350 K. Prior work has suggested that at this temperature Hydrogen recombinatively desorbs from Ru(0001). Consistent with this observation, electronic structure calculation in this study suggests, because C and H share a common adsorption site on Ru(0001), that above this threshold temperature both the relative stability and rates of interconversion of all one and two carbon containing species should, as we observe experimentally, dramatically differ. This change in hydrocarbon reactivity is clearly demonstrated by two examples. We have experimentally quantified the activation energy for the conversion of CH<sub>2</sub> to CH (after dosing by CH<sub>4</sub>) and found it to exceed prior computational results<sup>1</sup> (in the low coverage limit) by a factor of 5. Electronic structure calculations in this work quantitatively reproduce the experimentally measured activation energy for this process at the surface coverages of this experiment and show that the change in activation energy for this process is *highly* nonlinear with surface coverage. Secondly, we show that at < 0.3 monolayer of carbon CCH<sub>2</sub>/CCH species are stable up to 350 K while at > 0.6 monolayers this stability region extends to 500 K. Computation clarifies that this effect can be completely explained, as for CH<sub>2</sub> to CH conversion, by surface coverage effects.

### References

1. I. Ciobîcă, F. Freechard, R.A. van Santen, A.W. Kleyn, and J. Hafner, *J. Phys. Chem. B* **104**, 3364 (2000).

## Elementary processes in water/ $\alpha$ -Al<sub>2</sub>O<sub>3</sub>(0001) interaction: Dissociative adsorption and surface reconstruction

Harald Kirsch, Yujin Tong, Jonas Wirth<sup>a</sup>, Peter Saalfrank<sup>a</sup>,  
Martin Wolf, and R. Kramer Campen

Alumina surfaces are abundant in engineered systems and a useful model for more complicated, environmentally omnipresent aluminosilicate phases. Most properties of these surfaces – e.g. structure, reactivity and polarity – change dramatically on exposure to water. As a result Alumina/water interaction has been studied for decades. Despite this work, understanding of water interaction with even the simplest of surfaces (e.g.  $\alpha$ -Al<sub>2</sub>O<sub>3</sub>(0001)) has proven surprisingly elusive. For example, computation predicts 4-6 water adsorption sites on this surface, while experiment has suggested more than twenty<sup>1</sup>. In a similar vein, study of the  $\alpha$ -Al<sub>2</sub>O<sub>3</sub>(0001)/liquid water interface by different groups using interface specific spectroscopy has produced very different results<sup>2</sup>. We here wish, then, to gain insight into the elementary steps of single molecule water dissociative adsorption on  $\alpha$ -Al<sub>2</sub>O<sub>3</sub>(0001) and how such dissociative adsorption changes surface structure.

We probe the dissociative adsorption of water by first dosing the well defined  $\alpha$ -Al<sub>2</sub>O<sub>3</sub>(0001) surface in ultra high vacuum using a molecular beam source. Following preparation we characterize the spectral response of the frequency range corresponding to dissociated water molecules as a function of sample temperature. This data show five clear resonances whose relative frequencies and relative intensities as a function of experimental geometry are consistent with computation. This consistency strongly suggests that we have observed experimentally, for the first time, the water fragments resulting from the two theoretically predicted single molecule dissociative adsorption pathways. By tracking the thermal stabilities of these fragments, we provide severe constraints on kinetic models of surface water reactivity. In parallel, we have demonstrated that surface reconstruction accompanying this dissociative adsorption can be monitored by quantifying the evolution of the spectral response of  $\alpha$ -Al<sub>2</sub>O<sub>3</sub>(0001) surface phonon modes. To avoid sample perturbation by an incident electron beam, and because we are interested in tracking surface reconstruction in the presence of liquid water, we probe these modes through vibrational sum frequency spectroscopy. Symmetry analysis of our observed response and comparison of the data with calculated normal modes for the fully de- and hydroxylated  $\alpha$ -Al<sub>2</sub>O<sub>3</sub>(0001) surfaces clearly demonstrates our capacity to observe surface reconstruction.

### References

1. K.C. Hass, W.F. Schneider, A. Curioni, and W. Andreoni, *Science* **282**, 265 (1998); J. Wirth and P. Saalfrank, *J. Phys. Chem. C* **116**, 26829 (2013).
2. L. Zhang, C. Tian, G.A. Waychunas, and Y.R. Shen, *J. Am. Chem. Soc.* **130**, 7686 (2008); M. Flörsheimer, K. Kruse, R. Polly, A. Abdelmonem, B. Schimmelpfennig, R. Klenze, and T. Fanghänel, *Langmuir* **24**, 13434 (2008).

<sup>a</sup>Institute of Chemistry, University of Potsdam, 14476 Potsdam, Germany

## Structure and dynamics of the non-hydrogen bonded free OH at the air/water interface

Yujin Tong, Cho-Shuen Hsieh<sup>a</sup>, Mischa Bonn<sup>a</sup>, Ana Vila Verde<sup>b</sup>,  
and R. Kramer Campen

Air/Water interfaces are both ubiquitous in the environment and a useful model for hydrophobic solvation more generally. From a molecular point of view hydrophobic interfaces are most obviously distinguished from hydrophilic by the large population of water molecules with one non-hydrogen bonded (free) OH, apparent in both simulation and experiment. However recent, predominantly computational work, has made clear that rationalizing larger scale effects of hydrophobicity, e.g. the free energy of protein folding or of wetting extended surfaces, requires going beyond this static Ångström scale picture of interfacial water: ultrafast structural fluctuations underlie the thermodynamics of hydrophobic solvation<sup>1</sup>.

We have recently applied both experimental, i.e. time resolved interface specific vibrational spectroscopy, and computational approaches, i.e. all-atom classical fixed charge and polarizable molecular dynamics simulation, approaches to understand the dynamics of the free OH. Taken together this work suggests: (1) The free OH rotates 3x faster than hydrogen bonded OH groups either at the air/water interface or in bulk water<sup>2,3</sup>. (2) The free OH is structurally heterogeneous on picosecond timescales: free OH groups closer to the vapor have a different orientational distribution and persist longer before rotating down towards the liquid than free OH groups closer to bulk water<sup>2,3,4</sup>. (3) Relaxation of vibrationally excited free OH groups proceeds by a combination of energy transfer between the free and hydrogen bonded OH within a single water molecule (responsible for 2/3 of the relaxation) and structural relaxation in which the excited free OH rotates towards the liquid and forms a hydrogen bond (1/3). Both relaxation channels contribute to the linewidth observed in the time averaged vibrational spectrum<sup>5</sup>.

### References

1. D. Chandler, *Nature* **437**, 640 (2005).
2. C.-S. Hsieh, R.K. Campen, A.C. Vila Verde, P. Bolhuis, H.-K. Nienhuys, and M. Bonn, *Phys. Rev. Lett.* **107**, 11602 (2011).
3. A. Vila Verde, P. Bolhuis, and R.K. Campen, *J. Phys. Chem. B* **116**, 9467 (2012).
4. Y. Tong, A. Vila Verde, and R.K. Campen, *J. Phys. Chem. B* **117**, 11753 (2013).
5. C.-S. Hsieh, R.K. Campen, M. Okuno, E.H.G. Backus, Y. Nagata, and M. Bonn, *Proc. Nat. Acad. Sci. USA*, in press (2013).

<sup>a</sup> Max Planck Institute for Polymer Research, 55128 Mainz, Germany

<sup>b</sup> Max Planck Institute of Colloids and Interfaces, 14476 Potsdam, Germany

## Single-molecule kinetic modelling of tryptophan synthase

Dimitri Loutchko and Alexander S. Mikhailov

Tryptophan synthase is employed by all bacteria and yeasts to produce one of the important amino acids. Some of the substrates used in tryptophan synthesis are scarce in the cell and enhanced process efficiency is therefore essential. Moreover, an intermediate product of the reaction is poisonous and therefore its release and interference with other cellular reactions have to be prevented. The nature has solved the problem in an elegant way: The entire reaction, combining 15 separate steps, is implemented by a single enzyme molecule consisting of two subunits, each with its own catalytic center. Allosteric interactions between the two subunits lead to coordination of chemical processes that take place in both of them. Indole, the poisonous intermediate formed in one subunit, is channelled inside the protein to the second subunit where it is used for the final synthesis. This molecular catalyst is slow and its one turnover cycle takes about a second. Extensive experimental investigations of the protein have been performed by M.F. Dunn, University of California, Riverside, and by I. Schlichting, MPI for Molecular Medicine, Heidelberg. In their work<sup>1,2</sup>, tryptophan synthase was characterized as a *channeling machine* and an *allosteric molecular factory*, stressing the complexity of operation of this molecular machine and the synchronization of chemical events inside a biomolecule.

Here, we report the first theoretical single-molecule kinetic study of tryptophan synthase. The complex reaction scheme, implemented by a single molecule, was modelled by a Markov network and the reaction progress was treated as stochastic wandering on this network. The model was based on an experimentally determined set of molecular chemical states and on the measured transition rates between them. Stochastic simulations have allowed us to characterize fluctuations in the catalytic turnover cycles and to reveal the presence of strong kinetic correlations in the states of two subunits. The origins of enzyme efficiency have been analyzed. Proceeding from the study results, new single-molecule experiments with tryptophan synthase are proposed.

### References

1. T. Barends, M.F. Dunn, and I. Schlichting, *Curr. Opin. Chem. Biol.* **12**, 593 (2008).
2. M.F. Dunn, D. Nicks, and H. Ngo, *Trends Biochem. Sci.* **33**, 254 (2008).

## Short- and long-term coverage dynamics during the electrooxidation of small organic molecules

Melke A. Nascimento<sup>a</sup>, Raphael Nagao<sup>a</sup>, Markus Eiswirth, and Hamilton Varela<sup>a</sup>

Oscillatory kinetics is ubiquitous in electrochemical systems. In particular for the electrochemical oxidation of small organic molecules such as formic acid, methanol and ethanol on platinum, examples of non-linear kinetics are abundant. A common feature found in experimentally recorded time-series is the long-term surface poisoning that occurs concomitantly to the short-term oscillations and acts as a slowly evolving bifurcation parameter. We have investigated the experimental stabilization of slowly evolving time-series during the electro-oxidation of methanol<sup>1</sup> and formaldehyde<sup>2</sup> on platinum in acidic media. As the main result, we have assigned the long-term poisoning process to the surface oxidation, predominantly, the slow formation of sub-surface oxygen.

After uncovering the general mechanistic aspects underlying the short- and long-term dynamics, we have incorporated these processes in a generic model for this family of oscillators. The resulting model consists of four ordinary differential equations, which we investigate over a wide parameter range. Besides the conventional bifurcation analysis, the system was studied by means of high-resolution period and Lyapunov diagrams. It was observed that the bifurcation diagram changes considerably as the irreversible poisoning evolves, and the oscillatory region becomes smaller. The qualitative dynamics changes accordingly and the chaotic oscillations are dramatically suppressed. Nevertheless, periodic cascades are preserved in a confined region of the resistance vs. potential diagram. The results are generally discussed in terms of the dynamics of adsorbates as the catalyst surface slowly deactivates.

### References

1. R. Nagao, E. Sitta, and H. Varela, *J. Phys. Chem. C* **144**, 22262 (2010).
2. M.F. Cabral, R. Nagao, E. Sitta, M. Eiswirth, and H. Varela, *Phys. Chem. Chem. Phys.* **15**, 1437 (2013).
3. M.A. Nascimento, R. Nagao, M. Eiswirth, and H. Varela, in preparation.

<sup>a</sup>Institute of Chemistry of São Carlos, University of São Paulo, Brazil

## Tuning the coupling of excess charges to polar environments

Daniel Wegkamp, Michael Meyer, Clemens Richter, Amilcare Iacomino<sup>a</sup>, Alejandro Pérez Paz<sup>a</sup>, Julia Stähler, Uwe Bovensiepen<sup>b</sup>, Angel Rubio<sup>a</sup>, and Martin Wolf

Solvated electrons (excess electrons in polar environments) play a crucial role in a wide variety of scientific fields for example astrochemistry, atmospheric physics and radiation chemistry. The stabilization of such excess charges can enhance electron-induced chemical processes at the solvation site and, for example, increase radiation damage. Amorphous ice on single crystal metal surfaces has been used as a model system to investigate the dynamics of such solvation processes using femtosecond time-resolved two-photon-photoemission (2PPE) spectroscopy. In these experiments, photo-injection of electrons from the metal into the D<sub>2</sub>O conduction band is followed by ultrafast localization and solvation of the excess electrons<sup>1</sup>. The subsequent energetic stabilization of these solvated electrons due to nuclear rearrangements of the polar molecular environment is accompanied by an increasing degree of localization.

We investigate two limiting cases in terms of the amount of polar molecules surrounding the excess charge:

(1) Solvated electrons located at the ice/vacuum interface are effectively decoupled from the metal substrate by increasing the ice layer thickness above 20 bilayers (BL). The thereby trapped excess electrons exhibit remarkably long lifetimes on the order of tens of seconds. This long residence time allows the excess charge to interact strongly with its environment leading to a change of the surface dipole of the system. We directly probe the surface dipole change in our photoemission experiment and observe a work function increase of up to 1 eV<sup>2</sup>. Electron-enhanced chemical reactions at the surface involving the creation of OH<sup>-</sup> may explain our findings.

(2) Decreasing the D<sub>2</sub>O coverage to the sub-monolayer regime, an alkali pre-covered (low-coverage) Cu(111) substrate is exposed to small amounts of D<sub>2</sub>O resulting in the build-up of a hydration shell around the alkali atom/ion, which is reflected in a pronounced change of electron relaxation dynamics and work function of the system. In agreement with recent density functional theory (DFT) calculations this can be explained by water molecules surrounding the alkali atom with their hydrogen atoms pointing towards the surface and the resulting change of the surface dipole.

### References

1. J. Stähler, M. Meyer, U. Bovensiepen, and M. Wolf, *Chem. Soc. Rev.* **37**, 2180 (2008).
2. D. Wegkamp, M. Meyer, C. Richter, M. Wolf, and J. Stähler, *Appl. Phys Lett.* **103**, 151603 (2013).

<sup>a</sup>Nano-Bio Spectroscopy Group UPV/EHU, Centro de Física de Materiales, Donostia-San Sebastian, Spain

<sup>b</sup>Universität Duisburg-Essen, Fakultät für Physik, 47048 Duisburg, Germany

## Electronic structure and ultrafast exciton formation dynamics at the ZnO(10-10) surface

Jan-Christoph Deinert, Daniel Wegkamp, Michael Meyer, Clemens Richter, Martin Wolf, and Julia Stähler

Hybrid systems consisting of inorganic and organic semiconductor materials (HIOS) are promising candidates for future optoelectronic devices such as organic LEDs or photovoltaic cells. The basic principle of HIOS is the combination of transparent and yet electrically conductive inorganic semiconductors with optically active organic molecules.

Zinc oxide (ZnO) is a well-suited inorganic semiconductor due to its transparency in the visible regime (band gap of 3.4 eV), possible n-type conductivity and abundance. Notably, a deep understanding of its highly complex surface properties is not yet achieved. It is known, however, that atomic hydrogen adsorption leads to the formation of a 2D surface electron accumulation layer and thus a metal surface, featuring electron densities up to  $10^{13} \text{ cm}^{-2}$ <sup>1</sup>. This is confirmed by using photoelectron spectroscopy (PES) on the pristine and hydrogen-covered ZnO(10-10) surface, where we observe the emergence of occupied electronic states right below the Fermi energy. Simultaneously, the work function is reduced by up to  $\Delta\Phi = -0.6 \text{ eV}$ . Considerably stronger modifications of the work function can be achieved using pyridine ( $\text{C}_5\text{H}_5\text{N}$ ) as an adsorbate. Here, interface formation leads to a huge work function decrease of  $\Delta\Phi = -2.9 \text{ eV}$ , caused by a cooperative effect of the chemical bonding and the large molecular dipole moment<sup>2</sup>. Exploiting this effect may lead to a significant reduction of interfacial energy barriers and consequently a boost in device efficiency.

The understanding of elementary electronic processes at HIOS interfaces requires insight into the femto- to picosecond dynamics of excited charge carriers. To achieve this, we use time- and angle-resolved two-photon photoemission spectroscopy (2PPE). At the ZnO(10-10) surface, the excitation with a femtosecond laser pulse leads to a population of formerly unoccupied electronic states in the ZnO conduction band (CB). By probing the subsequent non-equilibrium electron distribution we observe energetic relaxation processes in the CB on two distinct timescales: femtoseconds for highly excited electrons and picoseconds for electrons near the CB bottom. However, the most prominent feature is an extremely long-lived signature attributed to excitons, i. e. electron-hole pairs, located few 10 meV below the Fermi energy. After formation on a timescale of few hundred femtoseconds, this surface excitonic feature exhibits a lifetime exceeding hundreds of picoseconds. With its binding energy of 200 meV with respect to the bulk CB minimum, the surface exciton supposedly has great impact on the charge carrier and energy transfer dynamics at inorganic/organic interfaces.

### References

1. K. Ozawa and K. Mase, *Phys. Rev. B* **83**, 1 (2011).
2. O.T. Hofmann, J.-C. Deinert, Y. Xu, P. Rinke, J. Stähler, M. Wolf, and M. Scheffler, *J. Chem. Phys.* (in press).

## Electronic and structural dynamics across the insulator to metal transition in VO<sub>2</sub>

Laura Foglia, Simon Wall, Daniel Wegkamp, Julia Stähler, and Martin Wolf

Vanadium dioxide is probably the most famous compound of the broad family of vanadium oxides. It undergoes a first order insulator to metal transition at 340 K. This transition is characterized by a simultaneous structural distortion and change of the electronic structure when going from the low temperature, monoclinic and insulating phase (M<sub>1</sub>) to the rutile metallic phase (R). Despite being one of the most widely studied phase transitions ever since it was discovered in 1959<sup>1</sup>, its nature is still under strong debate, focusing in particular on the competing role of electronic correlations and structural distortion. The possibility of driving the transition by photoexcitation of the M<sub>1</sub> phase, with an energy density threshold of  $\cong 7 \text{ mJ cm}^{-2}$ , allows applying time-resolved techniques to investigate the interplay between the subsystems.

We present a detailed study of the broadband transient reflectivity response of VO<sub>2</sub> in the visible across the transition. At all excitation regimes the probed dynamics show a strong wavelength dependence, with the longer wavelengths being more sensitive to the changes in the carrier distribution, and the shorter wavelengths to changes in the structure. Furthermore, below the transition threshold, the reflectivity transients are modulated by strong oscillations, due to the coherent excitation of the four lowest Raman active modes of the M<sub>1</sub> phase. This allows us to track the evolution of the different subsystems separately. Pump-probe experiments performed on the transient states, i.e. after a previous photoexcitation below and above threshold, demonstrate that the coherent excitations are lost on the time scale of the exciting pulse<sup>2</sup>, while a metallic-like response emerges only on the picosecond time scale<sup>3</sup>. These results suggest that the photoexcitation of charges is sufficient to change the symmetry of the lattice potential, in such a way that the phonon modes of the M<sub>1</sub> phase are no longer defined, and thus exerting a force that drives the system into the R phase. However, the temporal evolution of lattice and electronic subsystem does not occur concomitant, suggesting that the system, shortly after photoexcitation, is in a nonequilibrium state, with electronic properties different from either the M<sub>1</sub> or the R phase.

### References

1. F.J. Morin, Phys. Rev. Lett. **3**, 34 (1959).
2. S. Wall, D. Wegkamp, L. Foglia, K. Appavoo, J. Nag, R.F. Haglund Jr., J. Stähler, and M. Wolf, Nature Commun. **3**, 721 (2012).
3. S. Wall, L. Foglia, D. Wegkamp, K. Appavoo, J. Nag, R.F. Haglund Jr., J. Stähler, and M. Wolf, Phys. Rev. B **87**, 115126 (2013).

## Ultrafast spin dynamics launched by transport of optically excited spin-polarized hot carriers in epitaxial metallic multilayers

Alexey Melnikov, Alexandr Alekhin, Damian Bürstel, Detlef Diesing<sup>a</sup>, Tim Wehling<sup>b</sup>, Ivan Rungger<sup>c</sup>, Maria Stamenova<sup>c</sup>, Stefano Sanvito<sup>c</sup>, and Uwe Bovensiepen<sup>d</sup>

The ultrafast spin dynamics induced by a transport of spin polarized carriers is a hot topic, which is motivated by the fundamental interest in magnetic excitations and applications like spintronics and data storage. To achieve a microscopic understanding of the underlying elementary processes typically occurring on femtosecond time scales, a time domain approach that probes the spin dynamics induced by hot carriers (HC) has been developed. *Spin polarized* hot carrier transport through Au/Fe/MgO(001) structures has been demonstrated<sup>1</sup>: Hereby, the excitation of Fe layer by femtosecond (fs) pulses leads to the injection of HC into Au and their consequent superdiffusive transport towards the Au surface. This transport is defined by the HC transmission of Fe/Au interface<sup>2</sup> and HC ballistic velocities and lifetimes. In Fe, the ballistic propagation length of majority spin HC  $\lambda_{\text{Fe}}^{\uparrow} \gg \lambda_{\text{Fe}}^{\downarrow}$ , which leads to much more effective HC<sup>↑</sup> emission. However,  $\lambda_{\text{Au}}^{\uparrow} \ll \lambda_{\text{Au}}^{\downarrow}$ , and the transport in Au is ballistic (fast) for HC<sup>↓</sup> and diffusive (slow) for HC<sup>↑</sup>. This separation of HC<sup>↑</sup> and HC<sup>↓</sup> in Au<sup>1</sup> leads to a ballistic spin current pulse of about 30 fs duration<sup>2</sup>.

To proceed towards a new concept of metal-based elements for fs-spintronics, we investigate the spin dynamics in Fe/Au/Fe/MgO(001) pseudo-spin valves. The different thickness of the two Fe layers allows us to realize parallel (P) or anti-parallel (AP) orientation of magnetizations  $\mathbf{M}_{\text{E}}$  and  $\mathbf{M}_{\text{C}}$  in Fe layers serving as HC emitter and collector, respectively. We use interface-sensitive time-resolved magneto-induced second harmonic (SH) generation in a back-pump-front-probe scheme to detect transient HC density and magnetization at the Fe/Au and Fe/MgO interfaces of the collector. Since optical phases of the two SH contributions depend on interface properties (e.g. roughness), their magneto-induced components can interfere either constructively or destructively, which leads, respectively, to high or low SH magnetic contrast  $\rho^1$ . In the first case SH is sensitive to average transient  $\mathbf{M}_{\text{C}}$  at the two interfaces while in the second case it monitors variations of the difference between two interface magnetizations. Using a sample with small  $\rho$ , we show that HC transport leads to the demagnetization of Fe/Au interface, which occurs on the timescale of ballistic (~40 fs) or diffusive (~200 fs) HC transport for P or AP configurations, respectively. In the case of sample with large  $\rho$ , we demonstrate that the reversal of  $\mathbf{M}_{\text{E}}$  allows one to alternate between positive and negative variations of  $\mathbf{M}_{\text{C}}$  in P and AP configurations, respectively, on a 100 fs timescale, which is promising for future development of fs-spintronics.

### References

1. A. Melnikov *et al.*, Phys. Rev. Lett. **107**, 076601 (2011).
2. A. Melnikov *et al.*, Proc. of Ultrafast Magnetism Conf., Strasbourg, October 2013.

<sup>a</sup> Universität Duisburg-Essen, Fakultät für Chemie, 45117 Essen, Germany

<sup>b</sup> Universität Bremen, Institut für Theoretische Physik, 28359 Bremen, Germany

<sup>c</sup> School of Physics and CRANN, Trinity College Dublin, Ireland

<sup>d</sup> Universität Duisburg-Essen, Fakultät für Physik, 47048 Duisburg, Germany

## Ultrafast demagnetization of a ferrimagnet driven by selective phonon excitation

Sebastian Mährlein, Ilie Radu<sup>a</sup>, Martin Wolf, and Tobias Kampfrath

One of the central research topics in contemporary solid state physics deals with the question how fast the magnetization of a magnetically ordered system (such as a ferromagnet) can be quenched by an external perturbation. This question is significant from an application-related perspective (to speed up data storage in magnetic media) as well as from a fundamental scientific viewpoint. Most of the experiments to date (such as the pioneering study conducted more than 15 years ago<sup>1</sup> make use of a femtosecond laser pulse that promotes the electrons of a ferromagnet into a highly excited state. By sampling the pump-induced dynamics with a second time-delayed laser pulse, an ultrafast reduction of the magnetization is observed, that usually proceeds on a sub-picosecond scale. So far the mechanism of this ultrafast magnetization quenching is not yet fully understood, a situation that partially arises from the complex interplay of spin, electron, and lattice degrees of freedom.

Here, we make an effort to reduce the complexity of the laser-induced non-equilibrium state by leaving the electronic subsystem of the solid completely unexcited. For this purpose, we illuminate the insulating ferrimagnet  $\text{Y}_3\text{Fe}_5\text{O}_{12}$  (YIG) by an ultrashort THz pulse (duration 200fs, center photon energy 80meV, energy 15 $\mu\text{J}$ ), thereby selectively promoting optical phonon modes of the solid into a highly excited state. Throughout this process, no electronic degrees of freedom are excited as the energy of the YIG band gap (2.85eV) is  $\sim 30$  times larger than that of the pump photons. Following excitation, the instantaneous magnetization is monitored by means of the Faraday effect with a time resolution of 10fs. We observe a reduction of the magnetization by  $\sim 3\%$  with a time constant of 1.2ps, followed by a slow recovery on a time scale of roughly 1ns.

The ultrafast magnetization quenching observed is extremely surprising because YIG is actually well-known for its very long spin-lattice relaxation time of many nanoseconds as determined in ferromagnetic resonance (FMR) experiments<sup>2</sup>. We conclude that the interaction of the YIG spin system with optical phonons (as excited in our study) is much stronger than with acoustical phonons (as observed in FMR). We are currently developing a microscopic understanding of this new route toward ultrafast magnetization.

### References

1. E. Beaurepaire, J.-C. Merle, A. Daunois, and J.-Y. Bigot, Phys. Rev. Lett. **76**, 4250 (1996).
2. D.S. Hung, Y.P. Fu, S.F. Lee, Y.D. Yao, and F.B. Abdul Ahad, J. Appl. Phys. **107**, 09A503 (2010).

<sup>a</sup> Helmholtz-Zentrum Berlin (HZB), 12489 Berlin, Germany

## Probing ultrafast charge carrier dynamics in topological insulators by terahertz spectroscopy

Lukas Braun, Gregor Mussler<sup>a</sup>, Luca Perfetti<sup>b</sup>, Martin Wolf, and Tobias Kampfrath

Topological insulators (TIs) are a recently discovered class of matter that exhibit an insulating bulk but gapless (metallic) surface states protected by time-reversal symmetry. In this project, we aim to gain insight into the transport properties of the TI surface states and their coupling to the bulk. For this purpose, we make use of femtosecond laser pulses, either to (i) trigger ultrafast electron currents or to (ii) directly deposit energy exclusively into the subsystem of the surface electrons.

(i) Recent work<sup>1</sup> has indicated that excitation of TIs with circularly polarized light can induce DC spin-polarized electron currents along the TI surface. Since electrons moving through a solid typically undergo scattering on sub-picosecond time scales, it is highly desirable to generate and detect such photocurrents in an AC manner, with femtosecond time resolution. For this purpose, we excite n-doped Bi<sub>2</sub>Se<sub>3</sub> crystals with a laser pulse (10fs duration, 1.55eV center photon energy). The resulting photocurrent gives rise to the emission of a terahertz (THz) electromagnetic pulse whose transient electric field is detected by means of electro-optic sampling<sup>2</sup>. We observe extremely broadband THz emission covering the range from 1 to 30THz. The directional dependencies of the THz signal (with respect to pump helicity and sample azimuth) are consistent with DC photocurrent data<sup>1</sup>. In addition, by monitoring the THz emission of a freshly cleaved sample, we find strong indications that the photocurrent is generated in a surface layer with a thickness of the order of 1nm. We discuss the origin of the photocurrent and implications for the relaxation of photoexcited TI electrons.

(ii) In an attempt to directly and exclusively excite the electronic states at the TI surface, we irradiate Bi<sub>1-x</sub>Sb<sub>x</sub>Te thin films with intense THz pulses having a photon energy of ~0.1eV, which is sufficiently lower than TI bulk band gap (~0.17eV). The instantaneous change of sample conductance is mapped by an “ultrafast Ohm-meter”, that is, a time-delayed probe pulse covering the spectral region from 0.5 to 4THz. We discuss the disentangling of bulk and surface contributions and their ultrafast interaction following surface excitation.

### References

1. J.W. McIver, D. Hsieh, H. Steinberg, P. Jarillo-Herrero, and N. Gedik, *Nature Nanotech.* **7**, 96 (2012).
2. T. Kampfrath, M. Battiato, P. Maldonado, G. Eilers, J. Nötzold, S. Mährlein, V. Zbarsky, F. Freimuth, Y. Mokrousov, S. Blügel, M. Wolf, I. Radu, P.M. Oppeneer, and M. Münzenberg, *Nature Nanotech.* **8**, 256 (2013).

<sup>a</sup>Forschungszentrum Jülich GmbH, 52425 Jülich, Germany

<sup>b</sup>École Polytechnique, 91128 Palaiseau cedex, France

## New schemes for the generation and application of terahertz electromagnetic pulses

Mohsen Sajadi, Martin Wolf, and Tobias Kampfrath

Electromagnetic radiation in the terahertz (THz) frequency range is a powerful spectroscopic tool that provides resonant access to fundamental modes of matter, for example the motions of free electrons, the vibrations of crystal lattices, and the precessions of spins. As a consequence, THz waves have extensively been used to probe such resonances with high sensitivity. In addition, the latest developments of high-power THz sources even enable to control matter rather than just probing it<sup>1</sup>. All these applications require the generation, manipulation, and detection of tailored THz transients, and we discuss here our recent technological developments.

The accurate determination of optical constants is important to identify THz resonances of materials. Opaque samples require reflection-mode measurements that come along with severe technical issues: substituting the sample of interest for a reference sample will inevitably modify the THz-interferometric setup. Consequently, we developed a self-referencing method in which the sample response to both *p* and *s* polarized light is measured, without touching the sample<sup>2</sup>. This THz ellipsometry is currently applied to magnetic samples to quantify the effects of spin-orbit coupling at highest frequencies.

In the field of spintronics, the measurement of spin transport (so-called spin-polarized electron currents) is of central interest. We have developed a method that allows us to generate and measure such spin currents with THz bandwidths<sup>3</sup>. For this purpose, we make use of the inverse spin Hall effect that converts the spin current into a charge current, leading to the emission of a detectable THz electromagnetic transient.

In order to generate intense THz radiation, we have built several sources in which two optical pulses are mixed down to their difference frequency<sup>4</sup>. By implementing and gently modifying approaches of other groups, we are able to generate 200fs-pulses with a center frequency tunable between 15 and 50THz and peak electric fields reaching  $\sim 20\text{MV cm}^{-1}$ . For a center frequency between 1 and 2THz, we are able to generate 1-ps transients with peak fields of up to  $1\text{MV cm}^{-1}$ . These pulses are now being used to excite various resonances in condensed matter. For particularly long-lived resonances, we are currently developing a scheme that permits generation of intense narrowband THz pulses with a duration of several picoseconds and a center frequency tunable between 15 and 50THz.

### References

1. T. Kampfrath, K. Tanaka, and K.A. Nelson, *Nature Photon.* **7**, 680 (2013).
2. A. Rubano, L. Braun, M. Wolf, and T. Kampfrath, *Appl. Phys. Lett.* **101**, 081103 (2012).
3. T. Kampfrath, M. Battiato, P. Maldonado, G. Eilers, J. Nötzold, S. Mährlein, V. Zbarsky, F. Freimuth, Y. Mokrousov, S. Blügel, M. Wolf, I. Radu, P.M. Oppeneer, and M. Münzenberg, *Nature Nanotech.* **8**, 256 (2013).

## First experiments on lattice dynamics in solids using the FHI IR-FEL

Alexander Paarmann, Marc Herzog, and Martin Wolf

Vibrational spectroscopy is a powerful technique to investigate molecular and condensed phase systems, and to study their dynamics. The availability of intense and coherent free-electron laser sources in the infrared (IR) spectral region opens the door to many previously inaccessible experiments. In particular for solid state systems, resonant interactions between specific IR-active modes and various other degrees of freedom, e.g. the electronic states, the spins, and the lattice, are of tremendous interest, both for the understanding of the underlying physics as well as for progress in designing new, technologically relevant materials<sup>1,2</sup>.

Here, we report on the development of new experimental approaches for probing the dynamics in solids after intense, resonant IR excitation using the FHI IR-FEL. The combination of the spectral tuning capability of the spectrally narrow FEL light with the high FEL intensity enables studies of the resonance behavior of the linear and nonlinear sample response. The temporal pulse structure of the FEL output allows studying these effects also in the time domain. Hereby, ultrafast ps-dynamics corresponding to the FEL micropulse duration, as well as ns-dynamics due to accumulation effects between subsequent micro-pulses are of interest. However, resonant high power IR-excitation and the resulting transient heating of samples poses a severe technical challenge, but potentially also opens up a new and unexplored area of nonlinear dynamics.

In a first stage and parallel to the commissioning of the FEL, IR absorption experiments are currently set up for solid state samples, addressing also the effect of transient temperature rise induced by the FEL pulse train. Secondly, optical probes will be used to study the optical and magnetic response of the sample to IR excitation. In collaboration with the group of T. Kampfrath, we will investigate the ultrafast demagnetization in the insulating ferrimagnet Yttrium iron garnet (YIG) after resonant mid-IR excitation. The FEL experiments with tunable, narrowband excitation are complimentary to broadband mid-IR excitation from tabletop laser sources, and will shed light specifically on the mode selectivity of the demagnetization process. Using IR double pulse excitation we will study the ps-dynamics and nonlinearities in the magnetic response.

Future experiments will implement measurements of the transient electrical properties after IR excitation, to study possible mode selectivity in driving electronic phase transitions in correlated electron materials<sup>1</sup>. We also envision FEL-based experiments on nonlinear phonon interaction and propagation, as well as nonlinear heat transport in (nano)structured solids<sup>2</sup>, since the time scale and intensity regime of these phenomena very well match the characteristics of the FEL output.

### References

1. M. Rini, R. Tobey, N. Dean, J. Itatani, Y. Tomioka, Y. Tokura, R.W. Schoenlein, and A. Cavalleri, *Nature* **449**, 72 (2007).
2. C.W. Chang, D. Okawa, A. Majumdar, and A. Zettl, *Science* **314**, 1121 (2006).

## Time- and angle-resolved photoemission spectroscopy of charge and spin density wave materials

Claude Monney, Christopher Nicholson, Michele Puppini, Yunpei Deng, Laurenz Rettig<sup>a</sup>, Uwe Bovensiepen<sup>b</sup>, Robert Carley<sup>c</sup>, Martin Weinelt<sup>c</sup>, Ralph Ernstorfer, and Martin Wolf

Femtosecond time- and angle-resolved photoemission spectroscopy (trARPES) has been recently demonstrated as an exceptional tool to investigate the complex physics of correlated materials<sup>1</sup>. Such materials often display rich phase diagrams involving metal-insulator instabilities, unconventional superconductivity or cooperative ordering phenomena. These phenomena are a consequence of the intricate interplay of electronic, spin and lattice degrees of freedom, which can be elucidated by bringing the material out of equilibrium with an intense optical pump pulse and monitoring the return back to equilibrium with an appropriate time-domain probe. Time-resolved ARPES can directly probe the time evolution of the electronic structure with energy and momentum resolution and disentangle collective excitations through their influence on the quasiparticle band structure

We have investigated the charge density wave (CDW) system, rare-earth tri-tellurides ( $\text{RTe}_3$ ,  $\text{R}=\text{Te, Ho, Dy}$ ), with trARPES using a 6-eV laser source<sup>2</sup>. In particular, we have directly mapped the transient changes of the Fermi surface near the center of the Brillouin zone and the opening and closing of the CDW gap. However, the low kinetic energy of photoelectrons in 6 eV laser ARPES restrict the accessible k-space to the center of the Brillouin zone. By using high harmonic generation (HHG) of XUV laser pulses<sup>1</sup>, we can discard this limitation and extend trARPES to several Brillouin zones.

Recently we have studied as a prototypical spin density wave (SDW) system chromium films using HHG-based trARPES. An ultrafast melting of the SDW phase was revealed from the response of the related backfolded band. In addition, the thermalisation dynamics of photoexcited electrons could be obtained from the transient hot electron distribution. Furthermore, we will investigate the CDW material  $\text{TiSe}_2$  with HHG-based trARPES. The mechanism responsible for its CDW phase transition is heavily debated<sup>3</sup>. By conducting temperature-dependent trARPES measurements and employing long-energy excitation pulses we will elucidate the peculiar physics of this system.

### References

1. T. Rohwer *et al.*, Nature **471**, 490 (2011).
2. Laurenz Rettig, PhD Thesis, Freie Universität Berlin (2013).
3. C. Monney, G. Monney, H. Beck, and P. Aebi, Phys. Rev. B **85**, 235150 (2012).

<sup>a</sup> Paul Scherrer Institut, 5232 Villigen, Switzerland

<sup>b</sup> Universität Duisburg-Essen, 47048 Duisburg, Germany

<sup>c</sup> Freie Universität Berlin, 14195 Berlin, Germany

## High-repetition rate ultrashort XUV source for time- and angle-resolved photoemission and molecular orbital mapping

Michele Puppin, Yunpei Deng, Niels Schröter, Claude Monney, Christopher Nicholson, Marcel Krenz, Oliver Prochnow<sup>a</sup>, Jan Matyschok<sup>a,b</sup>, Thomas Binhammer<sup>a</sup>, Uwe Morgner<sup>b</sup>, Martin Wolf, and Ralph Ernstorfer

Angle-resolved photoelectron spectroscopy (ARPES) provides the most direct access to the electronic structure of solids. The static electronic structure can be studied with high resolution employing tunable and spectrally narrow extreme ultraviolet (XUV) light readily available from 3<sup>rd</sup> generation light sources. On the other hand, the investigation of ultrafast dynamical processes and transiently populated states requires femtosecond XUV pulses, which can be generated from intense near-infrared laser pulses by high-harmonic generation (HHG). Up to now, such light sources have been applied to time-resolved ARPES by employing Ti:sapphire laser systems, however, only at limited repetition rates (up to max. 10 kHz) and with rather inflexible laser parameters. We aim at bridging this technology gap by developing an XUV photon source for time-resolved ARPES providing high counting statistics and a flexible balance between temporal and spectral resolution optimized for the scientific question.

Our approach is based on an ytterbium-based hybrid fiber-Innoslab laser system pumping a two-stage optical parametric chirped-pulse amplifier (OPCPA) operating at 500 kHz repetition rate. This laser system provides >20 W average power of tunable visible and near-infrared pulses with flexible pulse duration and bandwidth for HHG. As the time-bandwidth product of the XUV light relates to the fundamental pulse parameters, this approach promises certain flexibility in the XUV pulse parameters. In particular, the energy and temporal resolution can be adjusted using the flexibility of the OPCPA.

This novel photon source will be employed for time-resolved ARPES studies of charge and spin density wave materials and electronic structure and dynamics in quasi-one dimensional systems, and for mapping charge densities of transiently populated molecular orbitals of ordered adsorbate layers at surfaces.

<sup>a</sup> VENTEON Laser Technologies GmbH, 30827 Garbsen, Germany

<sup>b</sup> Leibniz Universität Hannover, Institut für Quantenoptik, 30167 Hannover, Germany

## Femtosecond low-energy electron diffraction and imaging

Melanie Müller, Sebastian Lüneburg, Alexander Paarmann, and Ralph Ernstorfer

The recent development of femtosecond electron and x-ray diffraction and imaging techniques allows for the direct observation of structural dynamics in the course of photo-induced chemical or physical processes. These techniques provide atomic spatial and femtosecond temporal resolution<sup>1</sup> and have been predominantly applied to crystalline samples. Photo-induced structural dynamics are governed by the interplay of electronic and nuclear degrees of freedom, which depend on the dimensionality of the system. We aim for the investigation of ultrafast dynamics in low dimensional systems, e.g. two-dimensional materials, surfaces and nanostructures, which ask for a time-resolved technique with maximal scattering cross section. Expanding ultrafast electron diffraction to low electron energies in the sub-kV range will combine femtosecond temporal resolution with high surface sensitivity.

We developed a novel setup for femtosecond low-energy electron diffraction (fsLEED) and imaging in the energy range of 50 to 1000 eV based on a laser-triggered metal nanotip. Owing to the confined emission area due to field enhancement, nanotips are nearly ideal point sources delivering highly coherent ultrashort electron pulses. Besides using single electron pulses at high repetition rates in order to eliminate space charge effects, femtosecond time resolution is achieved by using a compact geometry with sub-mm propagation distances, which minimizes dispersive temporal broadening of the electron wave packets. The feasibility of this approach is supported by numerical simulations of the propagation of single electron wave packets photo-generated from a nanotip<sup>2</sup>.

The instrument is designed for two operation modes: lens-less point-projection imaging and fsLEED, the latter either in transmission or reflection geometry:

### Time-resolved low-energy point-projection microscopy

Due to their high sensitivity to weak fields, low-energy electrons are particularly suited for mapping transient electric fields and charge distributions in photo-excited nanostructures. Specifically, we investigate charge carrier separation upon above-bandgap excitation in axially doped InP nanowires by measuring local variations of the vacuum level using PPM.

### Femtosecond low-energy electron diffraction

In order to maintain the short propagation distances in fsLEED experiments, we developed a compact microlens coated directly onto the shaft of the nanotip to collimate the divergent electron beam without any optics between tip and sample<sup>3</sup>. We present first experimental data on transmission fsLEED of free-standing monolayer graphene using our compact approach.

## References

1. R.J.D. Miller *et al.*, Acta Cryst. **A66**, 137 (2010).
2. A. Paarmann *et al.*, J. Appl. Phys. **112**, 113109 (2012).
3. S. Lüneburg *et al.*, Appl. Phys. Lett. (in press).

## Non-equilibrium structural dynamics and phase transitions in solids

Lutz Waldecker, Simon Wall<sup>a</sup>, Roman Bertoni, Elisabeth Bothschafter<sup>b</sup>,  
Eeuwe Zijlstra<sup>c</sup>, Martin Garcia<sup>c</sup>, Alexander Paarmann, and Ralph Ernstorfer

Intense ultrashort laser pulses allow for the preparation of transient states of matter far from equilibrium between electrons and lattice. The optical and structural properties as well as the temporal evolution of such non-equilibrium states provide insight into the mutual dependence of electronic and atomic structure. In particular, non-thermal reaction pathways of photoinduced processes like phase transitions are of key interest.

We investigate optical and structural properties of non-equilibrium states with time-resolved optical spectroscopy and femtosecond electron diffraction, a technique combining temporal resolution on the hundred femtosecond scale with structural information on the atomic scale. Here, two types of phenomena are addressed: i) the effect of electron temperature and carrier relaxation dynamics on a lattice potential energy surface and ii) non-thermal phase transitions induced by irreversible photoexcitation.

i) We investigate the effect of carrier relaxation on the evolution of excited-state potential energy surfaces. Following the dynamics of the coherent  $A_{1g}$  optical phonon in  $\text{TiO}_2$  after above bandgap excitation using ultrashort ultraviolet pulses, a phase shift of the phonon oscillation compared to a purely displacive excitation is observed. The phase shift indicates a significant contribution to the displacive force driving the lattice vibration due to the rapid cooling of the initially hot electron-hole plasma. This interpretation is supported by non-equilibrium density functional theory calculations revealing a shift of the potential energy surface minimum along the reactive phonon mode upon both, the primary population transfer from O  $2p$  valence band to Ti  $3d$  conduction band states as well as the subsequent carrier relaxation to the respective band edges<sup>1</sup>.

ii) Phase change materials exhibit several stable and quasi-stable crystallographic states at room temperature with significantly different electrical and optical properties.  $\text{Ge}_2\text{Sb}_2\text{Te}_5$  (GST) is widely-used as an optical data-storage medium, where semimetallic crystalline and semiconducting amorphous phases are reversibly switched by light pulses on the nanosecond time scale. We investigate the photo-induced ultrafast optical and structural response of crystalline (fcc) and amorphous GST by single-shot optical spectroscopy and electron diffraction. After femtosecond optical excitation above the fluence threshold for inducing a permanent phase transition, the optical properties show an apparently instantaneous, persistent change towards the optical properties of the final state. As revealed by electron diffraction, this change occurs faster than the thermalization of electrons and lattice. We discuss nonthermal structural phase transitions and ultrafast changes in the orbital order as possible mechanism driving the immediate optical response.

### References

1. E.M. Bothschafter *et al.*, Phys. Rev. Lett. **110**, 067402 (2013).

<sup>a</sup> ICFO – The Institute of Photonic Sciences, Barcelona, Spain

<sup>b</sup> Physik Department, Technische Universität München, 85748 Garching, Germany

<sup>c</sup> Universität Kassel, Theoretische Physik, 34132 Kassel, Germany

## Observation and control of electron motion in solids on the attosecond time scale

Ralph Ernstorfer, Stefan Neopl<sup>a</sup>, Agustin Schiffrin<sup>b</sup>, Tim Paasch-Colberg<sup>b</sup>,  
Peter Feulner<sup>a</sup>, Reinhard Kienberger<sup>a,b</sup>, and Ferenc Krausz<sup>b</sup>

The theoretical treatment of electron propagation in crystals is based on the description of electrons as coherent superposition of stationary Bloch eigenstates, that is, as Bloch wave packets. Such wave packets are localized in the reciprocal space and their group velocity is described by the dispersion of the eigenvalues at the central  $\mathbf{k}$  vector of the wave packet. This ansatz from the early days of quantum mechanics constitutes one of the fundamental concepts in electronic structure theory, but its direct experimental verification by the observation of undisturbed Bloch wave packets in the time domain remains elusive as scattering effects in the crystal hamper free propagation over macroscopic length scales. Here, we demonstrate that a time-resolved view on the photoelectric effect, given it provides attosecond resolution, provides a quantitative test of this concept of quasi-classical Bloch wave packet propagation. In the experiment, a sub-femtosecond extreme ultraviolet (XUV) light pulses excite electrons in a tungsten crystal capped by an ultrathin metal film of variable thickness of up to 10 Å. Probing the relative attosecond escape dynamics of core electrons from substrate and adlayer reveals a free-electron-like propagation of electrons according to the Drude-Sommerfeld model, i.e., the classical limit of Bloch wave packet motion. In contrast, the temporal emission profile of valence electrons reveals a hybridization of wave functions across the buried metal-metal interface<sup>1</sup>.

In addition to observing Bloch wave packet motion, we demonstrate that ultrashort laser pulses also allow for inducing and manipulating collective electronic motion on the attosecond and few-fs time scale. For very short periods of time, electric fields exceeding 10 V/nm, i.e. fields significantly beyond the threshold for dc dielectric breakdown, can be applied to insulators. Employing 1.5-cycle near-infrared laser pulses, we demonstrate the generation of directly measurable photocurrents in unbiased metal-dielectric-metal nanogaps<sup>2</sup>. The magnitude and sign of these currents can be controlled with the carrier-envelope phase of the laser pulse, i.e. by the shape and symmetry of the laser electric field. Such currents can be switched on and off on sub-femtosecond timescales as evidenced by employing two cross-polarized and time-delayed pulses. The ultrafast field-controlled current generation in a dielectric nanostructure represents a first step towards the realization of optical-field-controlled electronics.

### References

1. S. Neopl *et al.*, Phys. Rev. Lett. **109**, 087401 (2012); S. Neopl *et al.*, in preparation.
2. A. Schiffrin *et al.*, Nature **493**, 70 (2013).

<sup>a</sup> Technische Universität München, Physik Department, 85748 Garching, Germany

<sup>b</sup> Max-Planck-Institut für Quantenoptik, 85748 Garching, Germany





## Theory Department

### Poster List

Recent work done in the *Theory Department* is displayed on 24 posters. For this book we selected 16 poster abstracts but kept the numbering of the full display.

All posters are displayed in building T and the **poster site** is given below (left column).

The superscript <sup>E</sup> marks work of A. Tkatchenko's ERC group.

*Poster Site*     *Poster Title and Authors*

#### New Concepts, Methods, and Techniques

- TH 1**     **Advanced Electronic Structure Approaches in FHI-Aims**  
Igor Ying Zhang, Xinguo Ren, Arvid Ihrig, Wael Chibani,  
Sergey Levchenko, Patrick Rinke, Volker Blum,  
and Matthias Scheffler
- TH<sup>E</sup> 2**     **Self-Consistent Density Functional with Non-Local van der Waals Interactions**  
Nicola Ferri, Robert A. DiStasio Jr., Alberto Ambrosetti, Roberto Car,  
Alexandre Tkatchenko, and Matthias Scheffler
- TH 3**     **Accurate Thermoelectric Transport Coefficients up to the Melting Point**  
Christian Carbogno, Karsten Rasim, Björn Bieniek, Rampi Ramprasad,  
and Matthias Scheffler
- TH 4**     **Exploring the *GW* Ground State - the Self-Consistent *GW* Approach Applied to Molecules**  
Fabio Caruso, Patrick Rinke, Xinguo Ren, Angel Rubio,  
and Matthias Scheffler
- TH 6**     **Correlated Light-Matter Interactions in Cavity QED**  
Johannes Flick, René Jestädt, Heiko Appel, and Angel Rubio
- TH 7**     **Electronic Decoherence in Molecules**  
Ignacio Franco, Heiko Appel, and Angel Rubio

### Surfaces, Adsorption, and Heterogeneous Catalysis

- TH 8**      **Graphene Engineering: Stability of Epitaxial Graphene and the Surface Reconstructions of 3C-SiC**  
Lydia Nemec, Florian Lazarevic, Volker Blum, Patrick Rinke, and Matthias Scheffler
- TH 11**     **Importance of Space-Charge Effects for the Concentration of Defects at Metal-Oxide Surfaces**  
Norina A. Richter, Sabrina Sicolo, Sergey V. Levchenko, Joachim Sauer, and Matthias Scheffler
- TH 12**     **Stability and Metastability of Clusters in a Reactive Atmosphere: Theoretical Evidence for Unexpected Stoichiometries of  $Mg_MO_x$**   
Saswata Bhattacharya, Sergey V. Levchenko, Luca M. Ghiringhelli, and Matthias Scheffler

### Defects in Bulk Semiconductors and Insulators

- TH 13**     **Ferroelastic Stabilization and Toughening of Doped Zirconia**  
Christian Carbogno, Carlos G. Levi, Chris G. Van de Walle, and Matthias Scheffler

### Biophysics

- TH 16**     **Evidence for a  $\beta$ -Peptide Equivalent of the  $\alpha$ -Helix**  
Franziska Schubert, Carsten Baldauf, Mariana Rossi, Stephan Warnke, Gert von Helden, Kevin Pagel, Volker Blum, and Matthias Scheffler
- TH 17**     **The Peptide-Water Interaction: Accurate Description from First Principles and Nuclear Quantum Effects**  
Mariana Rossi, Sucismita Chutia, Michele Ceriotti, David Manolopoulos, Volker Blum, and Matthias Scheffler

### Organic Materials and Interfaces

- TH 18**     **Space Charge Transfer in Inorganic/Organic Hybrids**  
Yong Xu, Oliver T. Hofmann, Nikolaj Moll, Patrick Rinke, and Matthias Scheffler
- TH<sup>E</sup> 20**    **Concerted Effects of Covalent Bonding and van der Waals Interactions in Organic/Metal Interfaces**  
Wei Liu, Victor G. Ruiz, Matthias Scheffler, and Alexandre Tkatchenko

**TH<sup>E</sup> 21**     **Reliable Modelling of Stabilities, Polymorphism, and Response Properties in Organic Materials**  
Anthony M. Reilly, Alberto Ambrosetti, and Alexandre Tkatchenko

**And more...**

**TH 24**     **Strengthening Gold-Gold Bonds by Complexing Gold Clusters with Noble Gases**  
Luca M. Ghiringhelli and Sergey V. Levchenko



## Advanced Electronic Structure Approaches in FHI-Aims

Igor Ying Zhang, Xinguo Ren<sup>(\*)</sup>, Arvid Ihrig, Wael Chibani, Sergey Levchenko,  
Patrick Rinke, Volker Blum<sup>(†)</sup>, and Matthias Scheffler

Advanced electronic-structure methods (AESM) ideally combine accuracy and tractability with transferability across different chemical environments and dimensionalities and overcome the shortcomings of traditional (semi) local density-functional theory (DFT). We here present significant new developments in the all-electron electronic structure code FHI-aims: 1) *Double-hybrid DFT* semi-empirically adds the second-order perturbation energy to a hybrid density functional, which provides both accurate covalent-bond and van der Waals interactions [1]. 2) *Renormalized second-order perturbation theory (rPT2)* [2], on the other hand, systematically combines the random-phase approximation (RPA), second-order screened exchange (SOSEX), and renormalized single excitations, which all contain infinite summations of diagrams. rPT2 presents a considerable overall improvement over the standard RPA approach [2]. The SOSEX irreducible self-energy correction also improves the related *GW* approach, which has been the method of choice for charged excitations. 3) *A self-consistent dynamical embedding scheme* treats the physically important part of a system with AESMs, whereas the rest of the periodic system is treated with computationally less demanding approaches in a self-consistent manner. The embedding is based on the concept of dynamical mean-field theory using Green's function techniques. The 4) *full configuration interaction* scheme within the quantum Monte Carlo framework delivers ultimate benchmarks for our AESMs [3]. The numerical efficiency of these methods is facilitated by 5) *numeric atom-centered orbital (NAO) valence correlation-consistent (VCC) basis sets* and 6) *the localized resolution of identity (RI-LVL)*. NAO basis sets are efficient, compact, and transferable, but the basis set convergence for AESMs is slow due to the difficulty in describing the electron-electron cusp in the Coulomb interaction. We have developed basis sets that combine the concept of VCC with the compactness of NAOs, enabling an efficient extrapolation of the valence-correlation energy to the complete-basis-set limit. RI-LVL, on the other hand, allows us to remove the expensive four-center integrals occurring for AESMs. In RI-LVL, a product of basis functions is expanded in a rigorously justified, systematically converging subset of auxiliary basis functions, that gives efficient memory usage and linear scaling with system size.

(\*) Present address: Key Laboratory of Quantum Information,  
University of Science and Technology of China, Hefei, China

(†) Present address: MEMS Department, Duke University, Durham, NC, USA

[1] I.Y. Zhang and X. Xu, Proc. Natl. Acad. Sci. USA **106**, 4963 (2009).

[2] X. Ren, P. Rinke, G.E. Scuseria, and M. Scheffler, Phys. Rev. B **88**, 035120 (2013).

[3] D. Cleland, G.H. Booth, and A. Alavi, J. Chem. Phys. **132**, 041103 (2010).

## Self-Consistent Density Functional with Non-Local van der Waals Interactions

Nicola Ferri, Robert A. DiStasio Jr.<sup>(\*)</sup>, Alberto Ambrosetti, Roberto Car<sup>(\*)</sup>,  
Alexandre Tkatchenko, and Matthias Scheffler

Van der Waals (vdW) interactions are significant for a wide variety of systems, from simple noble-gas dimers to complex hybrid organic/inorganic interfaces. The long-range vdW energy is a tiny fraction ( $\sim 0.001\%$ ) of the total energy, hence it is typically assumed that it has no visible influence on the electronic properties. Although the Langreth/Lundqvist vdW-DF functional includes the effect of non-local correlation energy on the electronic structure [1,2], the influence of “true” vdW interactions is difficult to assess since a significant part of vdW-DF energy arises from short distances.

Here, we present a fully self-consistent (SC) implementation of the Tkatchenko-Scheffler DFA+vdW functional [3], where DFA stands for an approximate semi-local exchange-correlation density functional. The analysis of SC effects for atomic and molecular dimers allows us to establish a link between Feynman’s view on vdW binding arising from purely electrostatic interactions between perturbed electron densities [4] with the more traditional electrodynamic model based on non-local fluctuations and employed in practical calculations.

The effect of DFA+vdW<sup>SC</sup> on electronic densities of molecular dimers is assessed, finding quantitative agreement with correlated densities obtained from “gold standard” coupled-cluster quantum-chemical calculations. In agreement with previous work [2], we find a very small overall contribution from self-consistency in the structure and stability of vdW-bound molecular complexes. However, non-local vdW interactions turn out to significantly affect electronic properties of coinage metal (111) surfaces, leading to an increase of up to 0.3 eV in their workfunction. Furthermore, vdW interactions are also found to visibly influence workfunctions and charge transfer in hybrid organic/metal systems.

<sup>(\*)</sup> Department of Chemistry, Princeton University, Princeton, NJ, USA

- [1] M. Dion *et al.*, Phys. Rev. Lett. **92**, 246401 (2004).
- [2] T. Thonhauser *et al.*, Phys. Rev. B **76**, 125112 (2007).
- [3] A. Tkatchenko and M. Scheffler, Phys. Rev. Lett. **102**, 073005 (2009).
- [4] R.P. Feynman, Phys. Rev. **56**, 340 (1939).

## Accurate Thermoelectric Transport Coefficients up to the Melting Point

Christian Carbogno, Karsten Rasim, Björn Bieniek,  
Rampi Ramprasad<sup>(\*)</sup>, and Matthias Scheffler

The need for a sustainable energy economy has revamped interest in the development of thermoelectric materials, which have the potential to recover significant amounts of otherwise wasted heat. Research along these lines requires an accurate theoretical assessment of the transport coefficients that determine the thermoelectric efficiency, i.e., the electrical conductivity  $\sigma$ , the Seebeck coefficient  $S$ , as well as the electronic and vibrational heat conductivities  $\kappa_{el}$  and  $\kappa_{vib}$ . To date, methods based on the Boltzmann transport equation (BTE) [1,2] are the most widespread approaches to estimate these quantities. At elevated temperatures, however, these techniques become inaccurate, since they rely on the validity of the harmonic approximation (and small perturbations thereof). In particular, the relevant scattering processes that stem from the phonon-phonon [2] and the electron-phonon [3] interaction are only accounted for to lowest order.

In this work, we overcome the severe limitations of the BTE by the newly developed/implemented *ab initio* Green-Kubo [4] and Kubo-Greenwood [5] approach, in which *all* transport coefficients are determined from the correlation functions of the heat and charge fluxes [5]. Thereby, electron-phonon and phonon-phonon scattering is accounted for to all orders by evaluating the electronic and vibrational contributions to these fluxes by first-principles molecular dynamics. We discuss the details of our implementation as well as future extensions to account for ionic transport and validate our approach by investigating insulators ( $\text{ZrO}_2$ ), metals (Al) as well as direct and indirect band gap semiconductors (Si, InP). First, our calculations reveal that higher-order anharmonic effects are extremely effective in lowering  $\kappa_{vib}$ . Second, the electron-phonon interaction leads to a thermal renormalization of the electronic structure that significantly affects  $\sigma$ ,  $S$ , and  $\kappa_{el}$  at elevated temperatures. Both these mechanisms can thus not be neglected in the simulation of thermoelectric materials. The presented techniques are the only parameter-free, truly first-principles options available to date that account for these effects and that hence allow an accurate assessment of the thermoelectric transport coefficients up to the melting point.

<sup>(\*)</sup> Present address: Institute of Materials Science, University of Connecticut, Storrs, CT, USA

- [1] T. Scheidemantel *et al.*, Phys. Rev. B **68**, 125210 (2003).
- [2] J. Garg, N. Bonini, B. Kozinsky, and N. Marzari, Phys. Rev. Lett. **106**, 045901 (2011).
- [3] P. Boulet *et al.*, Comp. Mater. Sci. **50**, 847 (2011).
- [4] R. Kubo, M. Yokota, and S. Nakajima, J. Phys. Soc. Japan **12**, 1203 (1957).
- [5] B. Holst, M. French, and R. Redmer, Phys. Rev. B **83**, 235120 (2011).

## Exploring the $GW$ Ground State – the Self-Consistent $GW$ Approach Applied to Molecules

Fabio Caruso, Patrick Rinke, Xinguo Ren<sup>(\*)</sup>, Angel Rubio<sup>(†)</sup>, and Matthias Scheffler

Many-body Green's function theory holds the promise of a universal electronic structure approach, because it provides both ground and excited state properties in a single framework. In this context, the  $GW$  approach has become the method of choice for the description of charged excitations in solids, and its application to molecules and nanosystems is steadily increasing. However, with few exceptions the ground state properties of  $GW$  have not been explored yet.

We have implemented a fully self-consistent  $GW$  scheme (sc- $GW$ ) – based on the iterative solution of the Dyson equation – in the all-electron code FHI-aims [1,2,3]. Unlike in the more common perturbative  $GW$  schemes ( $G_0W_0$ ), sc- $GW$  is independent from the reference state. This provides a well defined total energy, which we calculate by means of the Galitskii-Migdal formula. Our results for a diverse set of (organic) molecules show that the sc- $GW$  quasi-particle energies are in good agreement with experiment and more accurate than  $G_0W_0$  based on Hartree-Fock or density-functional theory (DFT) with local or semi-local exchange-correlation functionals [2,3]. To assess the sc- $GW$  ground state, we calculated bond lengths, binding energies, and vibrational frequencies for a set of diatomic molecules. The accuracy of sc- $GW$  is comparable to exact-exchange plus correlation in the random-phase approximation (EX+cRPA), which is, however, not as good as that of renormalized second-order perturbation theory (rPT2) [4]. Since EX+cRPA is an advanced DFT functional that is on the same quantum mechanical level as  $GW$ , we address the question if the DFT and the Green's function framework are in fact equal. Inspecting the dissociation curve of  $H_2$ , we find that sc- $GW$  and EX+cRPA are indeed very close around the equilibrium bond distance, but when it comes to bond breaking DFT outperforms Green's function theory [5]. Finally, for prototypical donor/acceptor molecules we demonstrate that sc- $GW$  – due to its synergetic description of ground- and excited-state properties – is a promising method for charge-transfer systems, in which the electron density depends on the relative alignment of the molecular orbitals of the donor and the acceptor.

<sup>(\*)</sup> Present address: Key Laboratory of Quantum Information, University of Science and Technology of China, Hefei, China

<sup>(†)</sup> Also at Centro de Fisica de Materiales, Universidad del Pais Vasco, San Sebastian, Spain

- [1] V. Blum *et al.*, *Comp. Phys. Comm.* **180**, 2175 (2009).
- [2] F. Caruso *et al.*, *Phys. Rev. B* **86**, 081102(R) (2012).
- [3] F. Caruso *et al.*, *Phys. Rev. B* **88**, 075105 (2013).
- [4] X. Ren, P. Rinke, G. Scuseria, and M. Scheffler, *Phys. Rev. B* **88**, 035120 (2013).
- [5] F. Caruso *et al.*, *Phys. Rev. Lett.* **110**, 146403 (2013).

## Correlated Light-Matter Interactions in Cavity QED

Johannes Flick, René Jestädt, Heiko Appel, and Angel Rubio<sup>(\*)</sup>

Many chemical reactions are mediated through the interaction between light and matter. Important examples include photosynthesis, the vision process, photo-chemical reactions, solar cells, and nanoplasmonics based on metamaterials. To better understand these complex processes, experimentalists in the field of cavity quantum electrodynamics (QED) have developed methods to study quantum systems at the single-photon interaction limit (Nobel prize 2012). Further recent developments in this field are Fabry-Perot resonators with optical high-quality (high-Q) factors, circuit QED [1] and optomechanics [2].

In the electronic structure community, the quantized nature of the electrons is usually (approximately) incorporated, whereas the electromagnetic field is mostly treated classically. In contrast, in quantum optics, matter is typically simplified to models with a few levels, while the quantized nature of light is fully explored. In this work, we aim at treating both, matter and light, on an equal quantized footing.

To incorporate arbitrary geometries and matter distributions, we reformulate Maxwell's equations, by using the Riemann-Silberstein vector into a matrix spinor representation similar to the Dirac equation. In the stationary limit, its eigenvalues and eigenmodes are the essential input for a quantized description of the electromagnetic field. Using this input, we present exact solutions for fully quantized prototype systems consisting of atoms or molecules placed in optical one-dimensional high-Q cavities and coupled to the quantized electromagnetic modes in the dipole or quadrupole coupling regime. We focus on spontaneous emission, atomic revivals, strong-coupling phenomena, dipole-dipole couplings including van-der-Waals interactions, and Förster resonance energy transfer (FRET), all beyond the rotating wave approximation. Further, we compare to a propagation of coupled Maxwell-Schrödinger systems, using the matrix spinor representation on a real-space grid.

This work has implications for a future development of a time-dependent density functional theory formulation of QED [3,4] and further allows to study modifications to the classical Maxwell's equations for correlated multi-photon configurations. In the future, both may be used for the new field of correlated spectroscopy [5].

<sup>(\*)</sup> Also at Centro de Fisica de Materiales, Universidad del Pais Vasco, San Sebastian, Spain

- [1] R.J. Schoelkopf and S.M. Girvin, *Nature* **451**, 664 (2008).
- [2] T.J. Kippenberg and K.J. Vahala, *Science* **321**, 1172 (2008).
- [3] M. Ruggenthaler, F. Mackenroth, and D. Bauer, *Phys. Rev. A* **84**, 042107 (2011).
- [4] I. Tolkatly, *Phys. Rev. Lett.* **110**, 233001 (2013).
- [5] O. Roslyak, C.A. Marx, and S. Mukamel, *Phys. Rev. A* **79**, 033832 (2009).

## Electronic Decoherence in Molecules

Ignacio Franco<sup>(\*)</sup>, Heiko Appel, and Angel Rubio<sup>(†)</sup>

Electronic decoherence in molecules is a basic feature of the time evolution that accompanies photoexcitation, passage through conical intersections, electron transfer, or any other dynamical process that creates electronic superposition states. Understanding electronic decoherence is central to our description of fundamental processes such as photosynthesis and vision, and is also vital in the development of approximation schemes to the full vibronic evolution of molecules.

Here we present three basic contributions toward the understanding of electronic decoherence in molecules: First, we introduce a hierarchy of measures of decoherence for many-electron systems that is based on the purity and the hierarchy of reduced electronic density matrices [1]. Usual measures of decoherence are of limited applicability in molecules because they are based on the many-body electronic density matrix and this quantity is generally not available. By contrast, the reduced purities introduced here can be used to characterize electronic decoherence in the common case when only reduced information about the electronic subsystem is available.

Second, using the reduced purities and related measures we investigate decoherence dynamics in a model molecular system: the Su-Schrieffer-Heeger model of trans-polyacetylene [1,2]. The decoherence is modeled by following the coupled dynamics of electronic and vibrational degrees of freedom explicitly albeit approximately in an Ehrenfest mixed quantum-classical approximation. The simulations reveal the basic structure expected for the decoherence dynamics in molecules, provide insights into the main mechanisms for coherence loss, and illustrate how the decoherence dynamics changes with system size and initial state. Last, in this context, we identify a long-lived coherent-like phenomenon termed VIBRET [3]. In it, via vibronic interactions, the decay of an electron in the manifold of  $\pi^*$ -states resonantly excites an electron in the manifold of  $\pi$  states, and vice versa, leading to oscillatory exchange of electronic population between two distinct electronic states that lives for up to tens of picoseconds. The oscillatory structure is reminiscent of quantum beating patterns and is suggestive of the presence of a long-lived molecular electronic coherence. Significantly, however, a detailed analysis of the electronic coherence properties through the reduced purities shows that the VIBRET arises from a purely incoherent process.

<sup>(\*)</sup> Present address: Department of Chemistry, University of Rochester, Rochester, NY, USA

<sup>(†)</sup> Also at Centro de Fisica de Materiales, Universidad del Pais Vasco, San Sebastian, Spain

[1] I. Franco and H. Appel, *J. Chem. Phys.* **139**, 094109 (2013).

[2] I. Franco and P. Brumer, *J. Chem. Phys.* **136**, 144501 (2012).

[3] I. Franco, A. Rubio, and P. Brumer, *New J. Phys.* **15**, 043004 (2013).

## Graphene Engineering: Stability of Epitaxial Graphene and the Surface Reconstructions of 3C-SiC

Lydia Nemeč, Florian Lazarević, Volker Blum<sup>(\*)</sup>, Patrick Rinke,  
and Matthias Scheffler

Graphene films grown by Si sublimation on SiC are promising material combinations for future graphene applications based on existing semiconductor technologies [1]. To refine the growth quality and the resulting electronic character, it is important to understand the atomic and electronic structure of the interface. However, electronic-structure calculations are a challenge since the unit cells observed in experiment are large, requiring thousand(s) of atoms for a converged slab treatment. In this work, we present first-principles thermodynamic predictions for graphene and its precursor phases on SiC in their experimentally observable unit cell.

We performed a density-functional theory study on the Si-side of the polar 3C-SiC(111) surface using the all-electron electronic structure code FHI-aims, including  $(6\sqrt{3} \times 6\sqrt{3})R30^\circ$  zero-layer graphene (ZLG), monolayer (MLG), bilayer (BLG), and three-layer graphene (3LG). The formation energies of different reconstructions are presented as functions of the chemical potential of C. This (i) reveals a C-rich chemical-potential range for which ZLG is stable, in agreement with experiment [2], and (ii) indicates an even more C-rich stability range for MLG [2]. Thus, the calculations suggest that, by tuning the chemical potential (in experiment, e.g., by varying the temperature and background pressure of C or Si reservoir gases) it should be possible to grow high quality interfaces and graphene phases on the Si side.

The experimental situation on the C face of SiC is very different. Although few-layer graphene films with promising electronic structure can be grown [3], growing monolayer graphene films is difficult. A phase mixture of different surface phases is observed when surface graphitization sets in. However, the atomic structure of some of the competing surface phases and of the SiC-graphene interface is unknown. In our calculations, we compare the surface energies of the known  $(2 \times 2)$  phase with several structural models of the  $(3 \times 3)$  phase proposed in the literature. This shows that all the previously suggested  $(3 \times 3)$  models are higher in energy than the known  $(2 \times 2)$  phase. We present a new model for the  $(3 \times 3)$  reconstruction. Its formation energy crosses that of the  $(2 \times 2)$  phase at the carbon rich limit of the chemical potential, explaining the observed phase mixture.

<sup>(\*)</sup> Present address: MEMS Department, Duke University, Durham, NC, USA

[1] C. Riedl *et al.*, Phys. Rev. Lett. **103**, 246804 (2009).

[2] L. Nemeč, P. Rinke, V. Blum, and M. Scheffler, Phys. Rev. Lett. **111**, 065502 (2013).

[3] C. Berger *et al.*, Int. J. of Nanotechnology **7**, 383 (2010).

## Importance of Space-Charge Effects for the Concentration of Defects at Metal-Oxide Surfaces

Norina A. Richter, Sabrina Sicolo<sup>(\*)</sup>, Sergey V. Levchenko,  
Joachim Sauer<sup>(\*)</sup>, and Matthias Scheffler

Doping, either intentional or unintentional, can affect the charge state, the concentration, and the distribution of defects in a material. However, the different mechanisms and relative significance of these effects have not been studied properly so far. Experiments measuring defect concentrations as a function of thermodynamic variables (temperature, pressure, doping) are scarce. On the other hand, previous theoretical approaches have aimed at a description of isolated defects, or, more recently, dopant-defect complexes. In this work, we consider the charge-carrier conductivity induced by doping as a thermodynamic factor influencing defect concentrations. Our results show that in addition to the local contributions to the free energy of defect formation, such as breaking or making of bonds and local lattice distortions, there can be a significant global contribution at realistic conditions due to the overall electrostatic energy of the system.

As a technologically relevant example, we study surface oxygen vacancies (F centers) in MgO, which is widely used as a catalyst or catalyst support. The standard methodology for calculating defect formation energies is extended to include the electrostatic free energy. Defect formation energies are determined using *ab initio* atomistic thermodynamics in combination with hybrid density-functional theory (DFT), with parameters of the exchange-correlation functional optimized according to a condition on DFT ionization energies. Formation energies for neutral defects are validated by coupled-cluster CCSD(T) calculations for embedded clusters. The virtual-crystal approximation [1] is used for a realistic modeling of doping. We find that at catalytically relevant conditions charge transfer between surface defects and bulk dopants leads to formation of a macroscopically extended space-charge region. The concentration of  $F_s^{2+}$  centers at the (100) terrace of *p*-type MgO can be as high as 1%, while  $F_s^+$  and  $F_s^0$  concentrations are negligible [2].

<sup>(\*)</sup> Institut für Chemie, Humboldt-Universität zu Berlin, Berlin, Germany

[1] L. Vegard, Z. Phys. **5**, 17 (1921); M. Scheffler, Physica B+C **146**, 176–186 (1987).

[2] N.A. Richter, S. Sicolo, S.V. Levchenko, J. Sauer, and M. Scheffler, Phys. Rev. Lett. **111**, 045502 (2013).

## Stability and Metastability of Clusters in a Reactive Atmosphere: Theoretical Evidence for Unexpected Stoichiometries of $\text{Mg}_M\text{O}_x$

Saswata Bhattacharya, Sergey V. Levchenko, Luca M. Ghiringhelli,  
and Matthias Scheffler

The quest for new materials demands the accurate description of *all* their (meta) stable structures under realistic conditions. In particular, in heterogeneous catalysis, materials function at finite temperature and in an atmosphere of reactive molecules at finite pressure. As a first step towards understanding the catalytic behavior of metal-oxide clusters, we study the  $(T, p)$  dependence of the composition, structure, and stability of the various isomers for each size  $M$  of  $\text{Mg}_M\text{O}_x$  clusters in an oxygen atmosphere. The calculations are performed via a massively parallel genetic algorithm in a cascade approach. With the term “cascade”, we identify a multistep procedure in which successive steps employ higher levels of theory, with each next level using information obtained at the lower level.

Our results [1] show that phase diagrams of  $\text{Mg}_M\text{O}_x$  clusters calculated via DFT with a hybrid exchange-correlation (xc) functional agree with the benchmark at the rPT2 level. Neither a force field as flexible as reaxFF [2] (whose range of validity is found to be quite narrow for the studied class of systems) nor DFT with semilocal xc functionals are sufficient for even a qualitative prediction of the phase diagrams of the studied cluster sizes. The failure of the semilocal functionals is explained by the underestimation of the energy cost for the electron delocalization over excess oxygen atoms due to the self-interaction error. In contrast to bulk MgO, an interplay of ionic (Mg-O) and covalent (O-O) bonding in small  $\text{Mg}_M\text{O}_x$  clusters ( $M \leq 5$ ) favors  $x > M$  at realistic  $T$  and  $p_{\text{O}_2}$  (e.g,  $T \leq 800$  K for  $p_{\text{O}_2} \sim 1$  atm). As a result of this interplay,  $\text{O}_2$  and  $\text{O}_3$  moieties appear as structural elements of the non-stoichiometric clusters. At the same  $(T, p_{\text{O}_2})$  conditions, for bigger clusters there is a competition/coexistence between stoichiometric ( $M = x$ ) and non-stoichiometric ( $x > M$ ) compositions. Non-stoichiometric  $\text{Mg}_M\text{O}_x$  clusters with  $x > M$  are found to be paramagnetic, due to the localization of the spin density at the  $\text{O}_2$  and  $\text{O}_3$  moieties. Stoichiometric clusters are all diamagnetic. At most of the sizes, we observe a peculiar  $(T, p_{\text{O}_2})$ -dependent paramagnetic to diamagnetic transition, suggesting the possibility of tuning magnetic properties by changing environmental conditions.

- [1] S. Bhattacharya, S.V. Levchenko, L.M. Ghiringhelli, and M. Scheffler, Phys. Rev. Lett. **111**, 135501 (2013).
- [2] A.C.T. van Duin, S. Dasgupta, F. Lorant, and W.A. Goddard III, J. Phys. Chem. A **105**, 9396 (2001).

## Ferroelastic Stabilization and Toughening of Doped Zirconia

Christian Carbogno, Carlos G. Levi<sup>(\*)</sup>, Chris G. Van de Walle<sup>(\*)</sup>,  
and Matthias Scheffler

Thermal barrier coatings (TBCs) are widely used to protect superalloys from extreme temperatures. They increase durability, enable higher operational temperatures, and hence improve the fuel efficiency in power and propulsion turbines [1]. Due to its low thermal conductivity, high phase stability, and remarkable toughness, yttria stabilized zirconia (YSZ) is presently the material of choice for TBCs – but only in a narrow compositional range ( $\sim 7\text{-}8$  mol-%  $\text{YO}_{1.5}$ ). On the one hand, the addition of yttria stabilizes the tetragonal (and cubic) phase by suppressing the disruptive monoclinic transformation active in pristine  $\text{ZrO}_2$ ; on the other hand, it degrades the toughness [1]. Conversely, co-doping YSZ with titania (TiYSZ) recently resulted in superior phase stability *and* toughness [2]. This is particularly surprising, since previous theoretical investigations had rationalized the stabilization mechanism in YSZ solely in terms of  $\text{F}^{2+}$  oxygen vacancies [3], which are introduced by aliovalent  $\text{Y}^{3+}$  doping, but not by isovalent  $\text{Ti}^{4+}$ .

We use density-functional theory to investigate the dynamics and the stability of the monoclinic, tetragonal, and cubic phases of pristine and doped  $\text{ZrO}_2$ . Our *generalized solid-state nudged elastic band* [4] and molecular dynamics calculations show that the minimum-energy path for the tetragonal-to-cubic phase transformation differs significantly from the path that has been discussed in the literature so far [3]. In particular, we show that the correct minimum-energy path involves *ferroelastic switches*, i.e., the realignment of the tetragonal distortions along a different cartesian direction. This finding thus sheds light on the atomistic mechanism that determines these *ferroelastic switches*, which are generally considered to be the primary toughening mechanism in these compounds [1]. Furthermore, we discuss how various (co-)dopants affect this minimum-energy path and the associated *ferroelastic switches* and are thereby able to explain both the stabilization of the tetragonal phase *and* the controversial reduction/increase of toughness found in YSZ and TiYSZ, respectively. Accordingly, our calculations reveal that cation (co-)doping is essential to understand and control the toughness and thus the longevity of TBCs.

<sup>(\*)</sup> Materials Department, UC Santa Barbara, Santa Barbara, CA, USA

- [1] A. Evans, D. Clarke, and C.G. Levi, J. Eur. Ceram. Soc. **28**, 1405 (2008).
- [2] T.A. Schaedler, O. Fabrichnaya, and C.G. Levi, J. Eur. Ceram. Soc. **28**, 2509 (2008).
- [3] S. Fabris, A.T. Paxton, and M.W. Finnis, Acta Materialia **50**, 5171 (2002).
- [4] D. Sheppard *et al.*, J. Chem. Phys. **136**, 074103 (2012).

## Evidence for a $\beta$ -Peptide Equivalent of the $\alpha$ -Helix

Franziska Schubert, Carsten Baldauf, Mariana Rossi<sup>(\*)</sup>, Stephan Warnke<sup>(†)</sup>,  
Gert von Helden<sup>(†)</sup>, Kevin Pagel<sup>(†)</sup>, Volker Blum<sup>(‡)</sup>, and Matthias Scheffler

Compared to the natural  $\alpha$ -peptides, the backbone of a  $\beta$ -peptide contains one additional methylene group per residue. Research of such non-natural peptides is driven by the aim to find secondary-structure elements analogous to the ones in natural peptides. Various helical structures have been identified in  $\beta$ -peptides already [1]. However, a safe identification of the most prominent helix type, the  $\alpha$ -helix, was still lacking despite hints from diffraction experiments on nylon-3 polymers [2].

We compare the structure space of  $\beta$ -peptides and  $\alpha$ -peptides with specific focus on helical conformations. The polyalanine-based peptide series Ac-Ala<sub>*n*</sub>-Lys(H<sup>+</sup>),  $n \simeq 6 - 19$ , has been designed to form  $\alpha$ -helices in the gas phase [3-5], i.e., an environment where experiment and our theoretical results can be compared on equal footing. We concentrate on a comparison between isolated Ac-Ala<sub>6</sub>-Lys(H<sup>+</sup>) versus its related  $\beta$ -peptide Ac- $\beta^2$ hAla<sub>6</sub>-Lys(H<sup>+</sup>). For this, we employ density-functional theory (DFT) with the PBE functional corrected for van der Waals interactions and compare our results to ion-mobility mass-spectrometry and infrared multiphoton dissociation measurements. Our conformational search for Ac- $\beta^2$ hAla<sub>6</sub>-Lys(H<sup>+</sup>) is based on replica-exchange molecular dynamics (REMD). First, a large conformational pool is generated by force-field (FF) REMD simulations (OPLS-AA), which is then refined locally by DFT-based REMD runs for the lowest-energy helical structures that yielded even lower-energy helical conformations.

Ac-Ala<sub>6</sub>-Lys(H<sup>+</sup>) is found to be mostly  $\alpha$ -helical at room temperature [5]. After sorting all 14,000 DFT structures for Ac- $\beta^2$ hAla<sub>6</sub>-Lys(H<sup>+</sup>) (energy window about 1.6 eV) into families according to their H-bond network, free energy corrections at 300 K are considered in the harmonic approximation. We find both helical and non-helical conformers in the low-energy regime. Notably, the helical conformations are stabilized by vibrational free energy. The combination of theory and experimental fingerprints identifies a helical structure with a hydrogen-bond pattern analogous to the  $\alpha$ -helix as the most likely structure candidate – we here provide the first evidence for a  $\beta$ -peptide equivalent of the  $\alpha$ -helix.

(\*) Present address: Chemistry Department, University of Oxford, Oxford, UK

(†) Department of Molecular Physics, Fritz Haber Institute, Berlin, Germany

(‡) Present address: MEMS Department, Duke University, Durham, NC, USA

[1] C. Baldauf and H.-J. Hofmann, *Helv. Chim. Acta* **95**, 2348 (2012).

[2] J.M. Fernandez-Santin *et al.*, *Macromolecules* **20**, 62 (1987).

[3] R. Hudgins, M. Ratner, and M. Jarrold, *J. Am. Chem. Soc.* **120**, 12974 (1999).

[4] M. Rossi *et al.*, *J. Phys. Chem. Lett.* **1**, 3465 (2010).

[5] M. Rossi, M. Scheffler, and V. Blum, *J. Phys. Chem. B* **117**, 5574 (2013).

## The Peptide-Water Interaction: Accurate Description from First Principles and Nuclear Quantum Effects

Mariana Rossi<sup>(\*)</sup>, Sucismita Chutia, Michele Ceriotti<sup>(†)</sup>, David Manolopoulos<sup>(‡)</sup>,  
Volker Blum<sup>(‡)</sup>, and Matthias Scheffler

The function and stability of polypeptides and proteins rely on a delicate balance of various types of interactions. These comprise intramolecular and intermolecular interactions of the peptide with its environment. We here identify the importance of energetic contributions coming from the electronic structure and present the first steps towards the inclusion of nuclear quantum effects (NQE). We investigate isolated and microsolvated peptides large enough to form secondary structure, and isolated water clusters. We use density-functional theory including van der Waals dispersion (vdW) effects, as implemented in the all electron code FHI-aims [1].

Previously, we have shown that for the Ac-Ala<sub>n</sub>-LysH<sup>+</sup>,  $n=4-8$  peptide series, an interplay of H-bonds, vdW interactions, and vibrational entropy act to stabilize helical motifs at finite temperatures [2]. We here study the conformational preferences and water binding sites of  $n=5$  (non-helical) and 8 (helical). From conformational searches involving relaxations of thousands of microsolvated conformers with the PBE+vdW functional, we find the low energy structure candidates. For both molecules, the most favorable single water adsorption sites break intramolecular H-bonds associated with the LysH<sup>+</sup> ammonium group, in contrast to earlier suggestions. Our Gibbs free energies and equilibrium constants for the adsorption reaction are in excellent agreement with experiments. We trace a drop in the adsorption propensity from  $n=5$  to  $n=8$  to subtle changes in zero-point and vibrational free energy [3], which point to a clear importance of NQE in these systems.

We thus present our efforts to capture NQE in large systems realistically. We first study protonated water hexamers where NQE favor open clusters already at low temperatures, and compare their IR spectra to low temperature, conformer-selective experimental data [4]. We also discuss improvements, based on recently published techniques [5], in path integral and analytical continuation methods to approximate real time correlation functions that can be treated using *ab initio* potentials.

<sup>(\*)</sup> Present address: Chemistry Department, University of Oxford, Oxford, UK

<sup>(†)</sup> Chemistry Department, University of Oxford, Oxford, UK

<sup>(‡)</sup> Present address: MEMS Department, Duke University, Durham, NC, USA

[1] V. Blum *et al.*, Comp. Phys. Comm. **180**, 2175 (2009), <http://aims.fhi-berlin.mpg.de>.

[2] M. Rossi, M. Scheffler, and V. Blum, J. Phys. Chem. B **117**, 5574 (2013).

[3] S. Chutia, M. Rossi, and V. Blum, J. Phys. Chem. B **116**, 14788 (2012).

[4] N. Heine *et al.*, J. Am. Phys. Soc. **135**, 8266 (2013).

[5] M. Ceriotti, M. Parrinello, T. Markland, and D. Manolopoulos, J. Chem. Phys. **133**, 124104 (2010).

## Space Charge Transfer in Inorganic/Organic Hybrids

Yong Xu, Oliver T. Hofmann, Nikolaj Moll<sup>(\*)</sup>, Patrick Rinke,  
and Matthias Scheffler

Hybrid inorganic/organic systems (HIOS) have opened up new opportunities for the development of (opto)electronic and photovoltaic devices due to their potential of achieving synergy by combining the best features of two distinct material classes. From a quantum mechanical first-principles point of view, this combination is particularly challenging, because hard materials with a preference for band transport come in contact with soft, often disordered and van-der-Waals-bonded matter with a prevalence for localized states and polaron formation. An aspect that has so far been overlooked, however, is the build-up of a space-charge region at the inorganic/organic interface and the influence it has on the interface properties, although space-charge layers are a common occurrence in inorganic semiconductors and insulators.

We here present a quantum mechanical first-principles approach that introduces excess charge in the unit cell by means of the virtual crystal approximation with fractionally charged nuclei [1] to simulate bulk doping and that includes the energy contribution of the space-charge layer explicitly. For the bulk terminated ZnO(000-1) surface covered with half a monolayer of hydrogen (2x1-H), we demonstrate that electrons from bulk dopants can stabilize deviations from this half monolayer coverage at low hydrogen pressures [2]. Ambient hydrogen background pressures are therefore more conducive than ultra high vacuum conditions to form the defect free 2x1-H surface, which would be a more controlled substrate in HIOS [2]. For the interface between ZnO(000-1) 2x1-H and monolayers of tetrafluoro-tetracyanoquinodimethane (F4TCNQ), a strong acceptor that is frequently used for interface modifications, we show that the adsorption energy and the charge transfer to the molecules depend strongly on the bulk dopant concentration. While the build-up of a space-charge layer is not unexpected, the magnitude of its effect is astounding: the adsorption energy of F4TCNQ changes by more than 2 eV and more than doubles from low to high doping. In the limit of low bulk doping concentrations, charge transfer becomes vanishingly small in agreement with photoemission data [3], while the F4TCNQ induced work function change remains unaffected and large. The bulk doping concentration and the associated build-up of a space-charge layer therefore provide an additional way to tune the interface properties in HIOS.

(\*) IBM Research – Zurich, Rüschlikon, Switzerland

[1] N.A. Richter, S. Siculo, S.V. Levchenko, J. Sauer, and M. Scheffler,  
Phys. Rev. Lett. **111**, 045502 (2013).

[2] N. Moll, Y. Xu, O.T. Hofmann, and P. Rinke, New J. Phys. **15**, 083009 (2013).

[3] R. Schlesinger *et al.*, Phys. Rev. B **87**, 155311 (2013).

## Concerted Effects of Covalent Bonding and van der Waals Interactions in Organic/Metal Interfaces

Wei Liu, Victor G. Ruiz, Matthias Scheffler, and Alexandre Tkatchenko

The adsorption of aromatic molecules at transition-metal surfaces is important for fundamental and applied surface science studies. These systems are also promising in numerous applications including light-emitting diodes, transistors, sensors, and solar cells [1]. The understanding of electronic properties of organic/metal interfaces requires an accurate method for the prediction of their structure and stability. However, reliable treatment of both weakly and strongly adsorbed systems is a challenge for density-functional theory (DFT), due to the well-known fact that the accurate description of van der Waals (vdW) interactions is a difficult task for commonly used functionals. Recently, several promising vdW-inclusive DFT methods have shown remarkable accuracy for intermolecular interactions. However, none of these approaches accounts for non-local (inhomogeneous) collective electron response in the vdW energy tail, an effect that is particularly important in metals.

We developed the so-called DFT+vdW<sup>surf</sup> method [2] to accurately model adsorbates on surfaces, by a synergetic linkage of the DFT+vdW method [3] for intermolecular interactions with the Lifshitz-Zaremba-Kohn theory for the dielectric screening within the substrate surface. This method is demonstrated to achieve *quantitative* accuracy for 9 molecules adsorbed on 8 metals (25 systems in total), leading to a performance of 0.1 Å in adsorption heights and 0.1 eV in binding energies with respect to state-of-the-art microcalorimetry experiments, and the revised interpretation of temperature-programmed desorption data by Campbell's group [4,5]. Using the DFT+vdW<sup>surf</sup> method also enables us to obtain new *qualitative* findings. For example, our calculations predict the existence of an incipient precursor state for benzene/Pt(111) in agreement with experiments [4,6]. Finally, to demonstrate the predictive power of the DFT+vdW<sup>surf</sup> method, we design a novel type of single-molecule push-button switch, by carefully controlling the stability and activation barrier between a chemically bound state and a physically bound state for benzene derivatives adsorbed on metal surfaces [7].

- [1] F.S. Tautz, Prog. Surf. Sci. **82**, 479 (2007).
- [2] V.G. Ruiz *et al.*, Phys. Rev. Lett. **108**, 146103 (2012).
- [3] A. Tkatchenko and M. Scheffler, Phys. Rev. Lett. **102**, 073005 (2009).
- [4] H. Ihm *et al.*, J. Phys. Chem. B **108**, 14627 (2004).
- [5] C.T. Campbell and J.R.V. Sellers, J. Am. Chem. Soc. **134**, 18109 (2012).
- [6] W. Liu *et al.*, Phys. Rev. B **86**, 245405 (2012).
- [7] W. Liu, S.N. Filimonov, J. Carrasco, and A. Tkatchenko, Nat. Commun., in press.

## Reliable Modelling of Stabilities, Polymorphism, and Response Properties in Organic Materials

Anthony M. Reilly, Alberto Ambrosetti, and Alexandre Tkatchenko

Organic materials are of great fundamental and applied importance, with numerous applications in pharmaceuticals, food science, electronics, sensing, and catalysis. A key challenge for theory has been the prediction of their stabilities, polymorphism, and response to external perturbations. In recent years, there has been substantial progress in the modeling of organic materials with semi-local approximations to density functional theory (DFT) coupled with pairwise descriptions of dispersion interactions [1]. However, the majority of studies neglect the contribution of many-body dispersion (MBD) and also the self-interaction error (SIE) present in widely used density functionals. As a result, many quantitative and even qualitative failures remain [2].

To categorically understand the importance of MBD contributions and SIE we have studied two databases of gas-phase and solid-state intermolecular interactions [3,4]. While pairwise dispersion methods perform remarkably well for simple dimers, they substantially overestimate molecular-crystal lattice energies. Correctly accounting for electrodynamic response and many-body energy contributions using the MBD method [5] yields substantial improvements. The application of a hybrid functional (PBE0) also gives noticeable improvements, particularly for hydrogen-bonded solids. Overall, the PBE0+MBD method is capable of reaching accuracies of a few kJ/mol for both crystalline and gaseous phases compared to high-level theoretical and experimental stabilities [3,4], giving a systematic method for modeling both gas-phase and condensed molecular materials.

The accuracy achieved by PBE0+MBD enables us to account for the correct polymorphic ordering of a number of challenging systems, such as glycine, for the first time [6]. However, the importance of dispersion goes far beyond energetic stabilities. Many response properties show even larger contributions from many-body dispersion interactions. In particular, we have studied the elastic properties of a series of molecular crystals, finding that MBD contributions can account for up to 25% of the elastic constants.

- [1] D.A. Bardwell *et al.*, *Acta Crystallogr. B* **67**, 535 (2011).
- [2] A. Otero-de-la-Roza and E.R. Johnson, *J. Chem. Phys.* **137**, 054103 (2012).
- [3] A.M. Reilly and A. Tkatchenko, *J. Phys. Chem. Lett.* **4**, 1028 (2013).
- [4] A.M. Reilly and A. Tkatchenko, *J. Chem. Phys.* **139**, 024705 (2013).
- [5] A. Tkatchenko, R.A. DiStasio Jr., R. Car, and M. Scheffler, *Phys. Rev. Lett.* **108**, 236402 (2012).
- [6] N. Marom *et al.*, *Angew. Chem, Int. Ed.* **52**, 6629 (2013).

## Strengthening Gold-Gold Bonds by Complexing Gold Clusters with Noble Gases

Luca M. Ghiringhelli and Sergey V. Levchenko

In the great majority of molecular systems that contain rare-gas (RG) atoms, the bonding with RG can be explained as mainly due to either van-der-Waals interaction or electrostatics. In the latter case, the RG atoms can be simply polarized by multipole moments of the attached fragment. The few compounds where this is *not* the case always present a puzzling and fascinating challenge for the physical understanding of the bonding. In this work, we study a practically important case of RG-involving compounds: *neutral*  $\text{Au}_N\cdot\text{RG}$  complexes, where both isolated fragments have zero charge and zero or very small electric dipole moment. Knowing the atomic and electronic structure of gold clusters is important for understanding their catalytic activity. Rare gases can be exploited as “messengers” in experiments where infrared spectroscopy in combination with theoretical analysis is used to determine the atomic structure of metal clusters in the gas phase. The atomic and electronic structure of the complexes is calculated using various methods, from density-functional theory with semi-local exchange-correlation functionals to coupled-cluster theory with single, double, and perturbative triple substitutions (CCSD(T)). Our theoretical analysis reveals a relatively strong bonding of RG atoms to very small Au clusters. For example, the binding energy of Kr to  $\text{Au}_2$  is 0.2 eV. Attaching Kr (as well as Ar and Xe) to  $\text{Au}_2$  results in the shortening of the Au-Au bond and the blue shift of the corresponding stretching vibrational mode. Similarly, adsorption of Kr to  $\text{Au}_3$  induces the shortening of *one* Au-Au bond and the blue shift of the corresponding stretching vibrational mode. These results are qualitatively independent of the level of theory employed. Finite-temperature vibrational spectra (i.e., including anharmonic effects) are calculated using *ab initio* molecular dynamics simulations. The calculated spectra for  $\text{Au}_3\cdot\text{Kr}$  are in good agreement with measured far-infrared multi-photon dissociation (FIR-MPD) spectra [1] ( $\text{Au}_2\cdot\text{Kr}$  is invisible to the experiment due to too high ionization potential).

Analysis of the electronic structure of the complexes reveals that the unusual bonding is due to the overlap of the  $4p$  orbitals of Kr with  $d$  orbitals of the gold clusters, which leads to the depletion of the electron density in the region between the gold atoms. This reduces the electron-electron repulsion between the gold atoms and effectively strengthens the Au-Au bonds.

[1] L.M. Ghiringhelli *et al.*, New J. Phys. **15**, 083003 (2013).





## Notes

